NBS SPECIAL PUBLICATION 400-70

U.S. DEPARTMENT OF COMMERCE / National Bureau of Standards

Semiconductor Measurement Technology:

The Use of Acoustic Emission to Determine the Integrity of Large Kovar Glass-Sealed Microelectronic Packages

NATIONAL BUREAU OF STANDARDS

The National Bureau of Standards[1] was established by an act of Congress on March 3, 1901. The Bureau's overall goal is to strengthen and advance the Nation's science and technology and facilitate their effective application for public benefit. To this end, the Bureau conducts research and provides: (1) a basis for the Nation's physical measurement system, (2) scientific and technological services for industry and government, (3) a technical basis for equity in trade, and (4) technical services to promote public safety. The Bureau's technical work is performed by the National Measurement Laboratory, the National Engineering Laboratory, and the Institute for Computer Sciences and Technology.

THE NATIONAL MEASUREMENT LABORATORY provides the national system of physical and chemical and materials measurement; coordinates the system with measurement systems of other nations and furnishes essential services leading to accurate and uniform physical and chemical measurement throughout the Nation's scientific community, industry, and commerce; conducts materials research leading to improved methods of measurement, standards, and data on the properties of materials needed by industry, commerce, educational institutions, and Government; provides advisory and research services to other Government agencies; develops, produces, and distributes Standard Reference Materials; and provides calibration services. The Laboratory consists of the following centers:

Absolute Physical Quantities[2] — Radiation Research — Chemical Physics — Analytical Chemistry — Materials Science

THE NATIONAL ENGINEERING LABORATORY provides technology and technical services to the public and private sectors to address national needs and to solve national problems; conducts research in engineering and applied science in support of these efforts; builds and maintains competence in the necessary disciplines required to carry out this research and technical service; develops engineering data and measurement capabilities; provides engineering measurement traceability services; develops test methods and proposes engineering standards and code changes; develops and proposes new engineering practices; and develops and improves mechanisms to transfer results of its research to the ultimate user. The Laboratory consists of the following centers:

Applied Mathematics — Electronics and Electrical Engineering[2] — Manufacturing Engineering — Building Technology — Fire Research — Chemical Engineering[2]

THE INSTITUTE FOR COMPUTER SCIENCES AND TECHNOLOGY conducts research and provides scientific and technical services to aid Federal agencies in the selection, acquisition, application, and use of computer technology to improve effectiveness and economy in Government operations in accordance with Public Law 89-306 (40 U.S.C. 759), relevant Executive Orders, and other directives; carries out this mission by managing the Federal Information Processing Standards Program, developing Federal ADP standards guidelines, and managing Federal participation in ADP voluntary standardization activities; provides scientific and technological advisory services and assistance to Federal agencies; and provides the technical foundation for computer-related policies of the Federal Government. The Institute consists of the following centers:

Programming Science and Technology — Computer Systems Engineering.

[1]Headquarters and Laboratories at Gaithersburg, MD, unless otherwise noted; mailing address Washington, DC 20234.
[2]Some divisions within the center are located at Boulder, CO 80303.

Semiconductor Measurement Technology:

The Use of Acoustic Emission to Determine the Integrity of Large Kovar Glass-Sealed Microelectronic Packages

George G. Harman

Semiconductor Devices and Circuits Division
National Bureau of Standards
Washington, DC 20234

Sponsored by
Naval Avionics Center
Indianapolis, IN 46218

U.S. DEPARTMENT OF COMMERCE, Malcolm Baldrige, Secretary
NATIONAL BUREAU OF STANDARDS, Ernest Ambler, Director

Issued May 1982

Library of Congress Catalog Card Number: 82-600528

National Bureau of Standards Special Publication 400-70
Nat. Bur. Stand. (U.S.), Spec. Publ. 400-70, 80 pages (May 1982)
CODEN: XNBSAV

U.S. GOVERNMENT PRINTING OFFICE
WASHINGTON: 1982

Table of Contents

List of Figures

Page

List of Tables

Semiconductor Measurement Technology:
The Use of Acoustic Emission to Determine the Integrity of Large Kovar Glass-Sealed Microelectronic Packages

by

George G. Harman
Semiconductor Devices and Circuits Division
National Bureau of Standards
Washington, DC 20234

Abstract

The general objective of this research was to develop tests to determine the integrity of large hybrid packages under various thermal and mechanical stresses that may be encountered during assembly, during installation in systems, or in operation. Several measurement techniques were investigated, but emphasis was placed on acoustic-emission test procedures. The accomplishments were: (1) The effects of avionics environmental vibration on the seals of hybrid packages mounted on printed-circuit (PC) boards were determined. A major conclusion of this section was that lead fatigue failure occurs before seal damage on packages from high quality lots. (2) A small acoustic-emission detector was developed that is sensitive to surface waves, but relatively insensitive to vibration-induced cable noise. (3) A high-temperature (125°C) open-package helium leak test method was successfully developed to observe marginal seal damage. (4) An acoustic-emission test for inspection of hybrid packages during high-temperature thermal shock was developed. (5) A study of possible damage to seals during thermocompression and thermosonic bonding, during lead forming, and during other assembly operations was carried out. A general conclusion of this study is that the glass-metal seals in packages from known high quality lots are very reliable even when subjected to high stresses. However, the seals from packages "screened as good" from reject or poor quality lots are subject to hermetic failure under moderate stresses. There is little correlation between visual inspection failures of glass seals and their hermeticity.

Key words: acoustic emission; hermeticity; hybrid microelectronics; hybrid packages; microelectronic packaging; thermal shock; vibration.

INTRODUCTION

The general objective of this study was to develop tests to determine the integrity of large hybrid packages subjected to various thermal and mechanical stresses that they may encounter during assembly or later during operation. Several measurement techniques were investigated, but emphasis was placed on acoustic-emission test procedures. A preliminary report on the work was published in June 1980 [1]. Parts of that report included here serve as background or necessary introduction to the final acoustic-emission evaluations.

Acoustic emission (AE) is generally defined as being a transient elastic wave or stress wave generated by the rapid release of energy within a material when that material undergoes fracture or deformation. The classic example of this has been known for years as "tin cry" where merely bending a piece of tin will result in an audible sound. In 1950, Kaiser made the first comprehensive study of the phenomena [2]. His name is associated with the generally irreversible nature of AE, in which little or no acoustic emission occurs until previously applied stress levels are exceeded. The emitted stress waves may have frequencies ranging from the audible into the megahertz region, but the maximum energy is usually concentrated in the mechanical resonance modes of the test specimen. Detection of these waves usually takes place with ceramic piezoelectric transducers that are acoustically coupled to the specimen; however, wide band optical and capacitive detection methods have also been used. Publications are available that give theory, equipment, and applications of AE to a variety of nonelectronic applications [3,4].

The various sources of acoustic emission that have been observed include: crack nucleation and propagation; twinning; grain boundary sliding; multiple dislocation slip; creation of multiple dislocations; solid-solid, solid-liquid, and liquid-solid phase transformations; and the Barkhausen effect (realignment of magnetic domains). Most microelectronic uses of AE are concerned with solid-liquid-solid phase transformations (as in welding or soldering) or with crack propagation (as when a weld or a glass seal breaks). However, recently there have been AE studies of dislocation propagation in gallium arsenide LEDs and in silicon wafers.

The wavelength of AE in the usual detection frequency range is typically on the order of a centimeter. In the case of nuclear pressure vessels and other large structures, this wavelength offers sufficient resolution for triangulation to determine the source location of the AE. However, for electronic-sized samples multiple internal reflections inevitably mask the position of the AE source, and one must infer this from the position of the applied stress that caused the emission. Investigators are usually constrained to attach a transducer, which may be larger than the specimen, in whatever manner is possible (such as using tapered acoustic waveguides), and work with whatever signal is received. Waveform signatures, of frequency and amplitude, are recorded and empirically correlated with appropriate mechanical stress tests (e.g., destructive bond pull tests) for interpretation. The interpretation of AE signals from typical electronics applications may never be amenable to clear mathematical solution.

Recently, acoustic emission has been used to evaluate electronic materials and assembly processes. The largest effort in this area took place at the Western Electric Engineering Research Center, Princeton, New Jersey [5]. The first published use of AE in electronics was by Vahaviolos [6]. He used AE to reveal substrate cracking during the thermocompression bonding of beam lead semiconductor devices to gold metallization on ceramic substrates. Saifi and Vahaviolos [7] have reported the use of AE for real-time nondestructive evaluation of laser spot welding of small polymer insulated wires to electronic terminal posts. Carlos and Jon [8] used AE to detect cracks in the ceramic casings of capacitors that resulted from the thermal shock of soldering. Cracks so generated could not be observed during visual inspection because the crack-susceptible area was covered with solder. Jon *et al.*

[9,10] have described the use of AE for the nondestructive evaluation of the quality of several types of complex-metallurgy resistance welds such as those used in welding leads to tantalum capacitors. Another evaluation of resistance welding quality by AE monitoring of small diameter nickel wire welding in electronic assemblies was carried out by Knollman and Weaver [11]. Ikoma *et al.* [12] have used acoustic-emission measurements to investigate the conditions that produce crystallographic damage in GaAs LEDs during thermocompression wire bonding. Harman [13] used AE for nondestructive evaluation of beam lead, flip-chip, TAB, and hybrid chip capacitor bonds.

PART A VIBRATION EXPERIMENTS*

A-1 The Effects of Avionics Environmental Vibration on the Seals of PC Board-Mounted Hybrid Packages

A-1.1 Introduction

There have been a number of studies in the past to determine the effects of vibration on printed circuit (PC) board-mounted components. These have dealt primarily with such electronic components as resistors, capacitors, and transistors. In all of these studies, metal fatigue of the leads resulting from printed circuit board vibration was assessed. No studies have been carried out to determine more subtle damage such as vibration-induced cracks that may be produced and propagated in the glass hermetic seals of hybrids or other susceptible components mounted on the circuit board. If the hermetic seals were damaged, eventually moisture would penetrate inside the packages, and active devices could suffer corrosion damage. This would not only lead to the destruction of an expensive hybrid, but more importantly, the entire electronic system might fail.

While lead fatigue is well understood and well characterized, the kinds of forces that are required to produce hermetic-seal damage in hybrids have never been determined. The flatpack† type of package is generally considered to be more susceptible to hermetic-seal damage under various conditions than the plug-in type of package. The vibration experiment included both types of packages and was designed to determine whether lead fatigue or hermetic seal integrity is the most sensitive to vibration. Hermetic damage is more difficult to assess than lead fatigue since electrical measurements of the device and visual observation of the seals are of limited use. Therefore, AE instrumentation was used during vibration experiments to detect glass cracking in real time, and final determination of seal damage was made after vibration with a helium leak detector at both room temperature and ~125°C.

Before actual vibration tests began, a review of the literature was conducted in order to avoid repeating any earlier experiments. This was done both in the NBS library and at the DoD Shock and Vibration Information Center. It was found that most of the relevant work on vibration of electronic components had been done a number of years ago and the investigations were limited fatigue damage. In only one recent paper was the possibility of cracked glass seals suggested [14], but without photographs or other supporting evidence. The most convenient and complete single reference to vibration effects on electronic systems is a book by Steinberg [15] which has a chapter on the vibration of PC boards and other chapters on the fatigue of wire leads in components. Steinberg has also written a series of articles in trade magazines [16-21], most of which appear to be derived from his book. Other relevant papers in the archival literature or presented in conferences [22-26] were also reviewed. In all of these references, the resonant frequency

---

* Results and conclusions of this work were presented at the 51st Shock and Vibration Symposium, San Diego, California, October 21-23, 1980.

† This is sometimes called a butterfly package.

calculations for PC boards were based on simplified equations and were limited to the lowest (the "natural") vibration mode, which is typically in the 100- to 300-Hz range. Since military vibration requirements extend to 2000 Hz, it was necessary to derive more complex equations to obtain correlations with actual vibration measurements and to be able to locate relatively benign component mounting positions on PC boards.

A-1.2 Theoretical Considerations

The vibration modes of a printed circuit board may be obtained if the board is modeled as a vibrating plate. Various equations for the vibration modes of plates and membranes having specified boundary conditions have been derived in the literature [27-30]. The most commonly used mathematical methods were set forth by Rayleigh [31]. The boundary conditions are the dominating factor in determining modal frequencies; different conditions can result in frequencies which differ by an order of magnitude.

The three boundary conditions appropriate to PC boards are "fixed," "supported," and "free." For the fixed conditions, sketched in figure 1, the board edges are firmly clamped such that the edge motion is zero and the tangent is also zero. The term "supported" (also referred to as "simply supported" or "freely supported") is a carryover from beam-bending theory where the ends of the beam are supported on knife edges. For a PC board, each edge is considered supported on top and bottom between two knife edges. In this case, motion at the edge supports is zero but the tangent is not constrained, as shown in figure 2.

at $y = 0$, $\frac{dy}{dx} = 0$

Figure 1. Sketch of "fixed" boundary conditions.

at $y = 0$, $\frac{dy}{dx} \neq 0$

Figure 2. Sketch of "supported" boundary conditions.

The resonant frequencies of fixed boards are significantly higher than those of supported ones because the fixed mount effectively reduces the length of board available for vibration. The free case will not be considered here since all PC boards used in avionics are clamped or supported in some manner. As stated earlier, previous analysis of PC board vibration was done with simplified equations which did not permit calculation of higher resonant modes. In the present work, general equations were derived using, as a basis, the models of Warburton [28] and Hearmon [30]. The dimensions used in the equations are identified in figure 3.

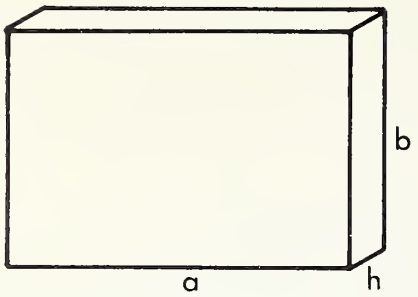

m = Number of nodes along dimension a.
n = Number of nodes along dimension b.
For fixed boundary conditions,
m = n = 2 for lowest mode.

Figure 3. Sketch identifying dimensions of a vibrating plate.

For the fixed (or clamped) edge board, the frequency equation is

$$f = \frac{1}{2\pi} \frac{Egh^2}{12\rho(1 - \sigma^2)} \left[\frac{\gamma^4}{a^4} + \frac{\varepsilon^4}{b^4} + \frac{2\gamma\varepsilon}{a^2b^2} (\gamma - 2)(\varepsilon - 2) \right]^{1/2}, \qquad (1)$$

where:

g = gravitational constant,
E = Young's modulus,
σ = Poisson's ratio,
ρ = board volume density = W/abh,
W = board weight,
$\gamma = (m - 1/2)\pi$, and
$\varepsilon = (n - 1/2)\pi$.

For the clamped board, the fundamental mode occurs for m = n = 2 (a node at each end of the board).

For the supported PC board, the frequency equation is

$$f = \frac{\pi}{2a^2} \frac{Egh^2}{12\rho(1 - \sigma^2)} \left[\gamma_1^4 + \frac{a^4 \varepsilon_1^2}{b^4} + \frac{2a^2 \gamma_1^2 \varepsilon_1^2}{b^2} \right]^{1/2}, \qquad (2)$$

where $\gamma_1 = m - 1$ and $\varepsilon_1 = n - 1$.

The sketches in figure 4 give pictorial examples of the first several vibration modes of boards having various a/b ratios. These were calculated for various boundary conditions as indicated.

To calculate the vibration modes to be expected in the first experiments (where boards that were fully copper clad on one side were used), the following values for E and ε are composites of the appropriate thicknesses of epoxy board and copper cladding (all in English units):*

* Dimensions and other values are generally given in English units since these are used exclusively in this field. Values of E and σ for epoxy boards are given in reference [15].

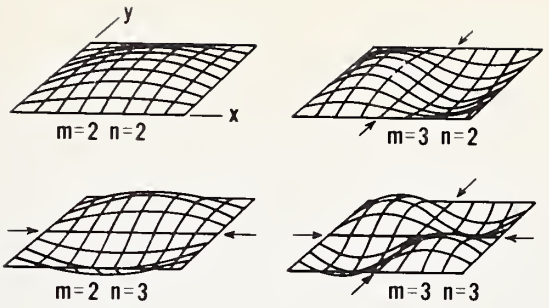

(a) The first four vibration modes of a simply supported plate. (From Morse [27].

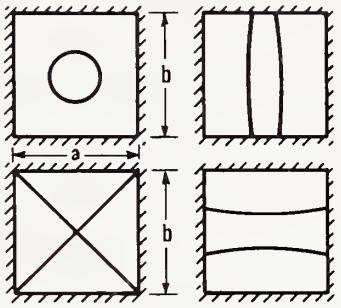

(b) Vibration patterns of a square plate with fixed edges.

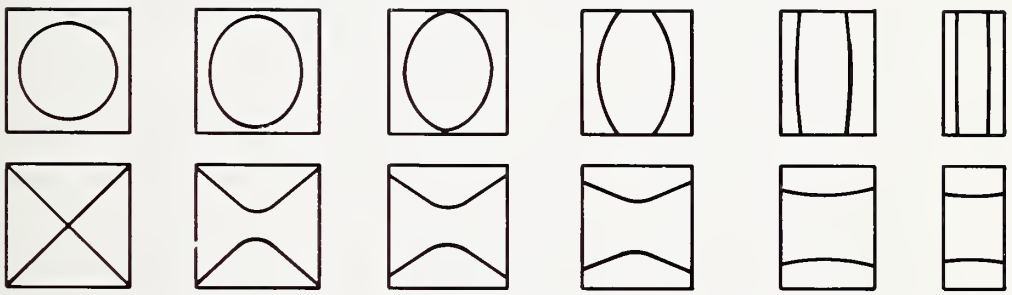

(c) The variation of the vibration pattern as the length-to-width ratio changes on a plate having free edges.

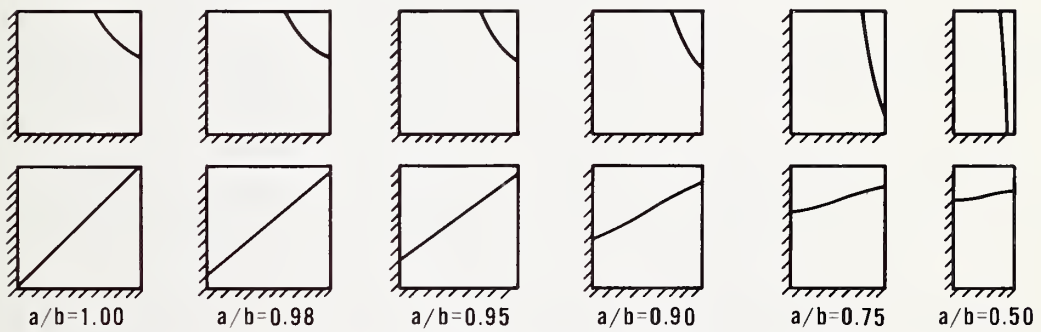

(d) The variation of the vibration patterns of a plate having two fixed and two free edges as the length-to-width ratio changes. These patterns also simulate the effect of nonuniform loading of a PC board. (From Warburton [28])

Figure 4. Pictorial examples of the first several vibration modes of rectangular boards.

$E = 2.8 \times 10^6$ psi,
$\sigma = 1.13$, and
$g = 385$ in./s^2.

The dimensions of the board were a = 8.2 in., b = 5.2 in., h = 0.062 in., and W = 0.21 lbs. The outside dimensions of the boards were typical of those used in avionics equipment (6 by 9 in.) reduced by the "fixed" clamp supports. The first several modal frequencies for fixed and supported edge boundary conditions are listed in table 1. The last column in the table gives the modal frequencies of a commonly used smaller board of the same thickness.

For comparison, if the constants appropriate to an epoxy board with no copper cladding ($E = 2 \times 10^6$ psi and $\sigma = 0.12$) were used, the modal frequencies would all be approximately 16 percent lower. Although some of the frequencies in table 1 may appear to be rather high, these were included because they may be excited by harmonics of lower frequency vibrations entering avionics equipment, as well as by "white" vibration transmitted from such sources as jet engines. Also, examination of eqs (1) and (2) shows that the modal frequencies of a uniformly loaded board decrease as the square root of the board's weight. Thus, since a board containing from 5 to 10 components (hybrids, capacitors, etc.) can easily weigh 2 to 4 times that of the unloaded board, the frequencies may be as little as 1/2 those calculated in table 1. It should be noted that all possible vibrational modes will not necessarily appear during actual PC board vibration.

Table 1. Calculated Modal Frequencies for Two PC Boards.

Modes		5.2 × 8.2 in. (W = 0.21)		4 × 6 in. (W = 0.118)
m	n	f_{fixed}	f_{supp}	f_{fixed}
2	2	330 Hz	170 Hz	570 Hz
3	2	495	320	885
2	3	820	540	1400
3	3	975	690	1685
4	2	775	570	1410
4	3	1235	935	2180
4	4	1960	1550	3400
3	4	1710	1300	2930

A-1.3 PC Board Layout Considerations

Sketches such as those shown in figure 4 may be used by the PC board layout engineer to minimize vibrational damage to attached components. Obviously, it would be desirable to solder components at nodes; however, a node for one vibration mode could be a maximum for another. Higher order modes usually produce lower vibration amplitudes and, even though the frequency is higher

(more excursions per second), result in less mechanical flexural damage to devices and their leads. Thus, only the four or five lowest order modes need to be considered with the lowest one being the most significant. Therefore, component lead placement should avoid straddling the maximum of the lowest order mode, which is across the shortest dimension of the PC board. Thus, generally, component placement in the center of the board should be avoided. It is preferred that the devices straddle a node of higher order modes along the length of that node (while avoiding the maxima of the lowest mode). One should especially avoid placement in positions where leads will experience torsional forces since torsion can more easily damage glass-metal seals than linear flexing. The designer should also be aware that a board asymmetrically loaded with components (e.g., having the weight concentrated at one end) will not vibrate in the symmetrical manner shown in figure 4c, but may more nearly approach modes shown in figure 4d. Thus, symmetrical loading is desirable, but if it is not possible, then various stiffeners or snubbers should be used [20,25,32] as compensation.

A-1.4 Experimental Measurements

A-1.4.1 The Equipment Setup and Preliminary Vibration Tests of PC Boards

The complete experimental setup consisted of a programmable frequency driver; an Unholtz-Dickie* vibration shaker and control unit Model 106 SP7; two accelerometers, one for the shaker head and a 1-gram weight unit to be attached to the board or hybrid; a double-pen recorder to simultaneously record both the shaker and the board's acceleration, as well as a special slip-synchronized strobe light to aid visual observation. A photograph of the overall experimental setup is given in figure 5.

In consultation with avionics equipment authorities, it was determined that a "fixed" mount for the PC boards best simulated mounts found in the avionics equipment of interest. An appropriate mount was designed and constructed for use in vibrating boards along two major axes. Design considerations were obtained from the literature [33,34] as well as from consultations with experts who have worked in the vibration field.

Several preliminary runs were made for calibration and equipment setup purposes. The equipment was programmed to follow curves required in MIL-E-5400R, such as is shown in figure 6, curve IIIa.

Figure 7 gives the resonant frequency plot of an unloaded copper-clad PC board with dimensions of 8.2 by 5.2 by 0.062 in. The resonant peaks approximate those calculated for the "fixed" board in table 1.

Frequencies obtained from the chart, along with the appropriate nodes, are shown in table 2.

---

* Certain commercial equipment, instruments, or materials are identified in this paper in order to adequately specify the experimental procedure. Such identification does not imply recommendation or endorsement by the National Bureau of Standards, nor does it imply that the materials or equipment identified are necessarily the best available for the purpose.

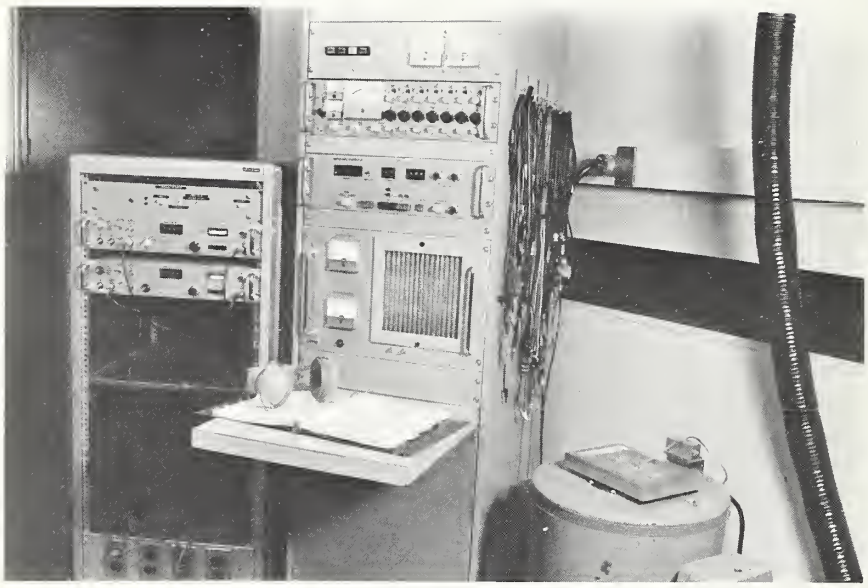

Figure 5. An overview of the vibration equipment. The PC board is shown in a fixed mount on top of the shaker which is in lower right of figure.

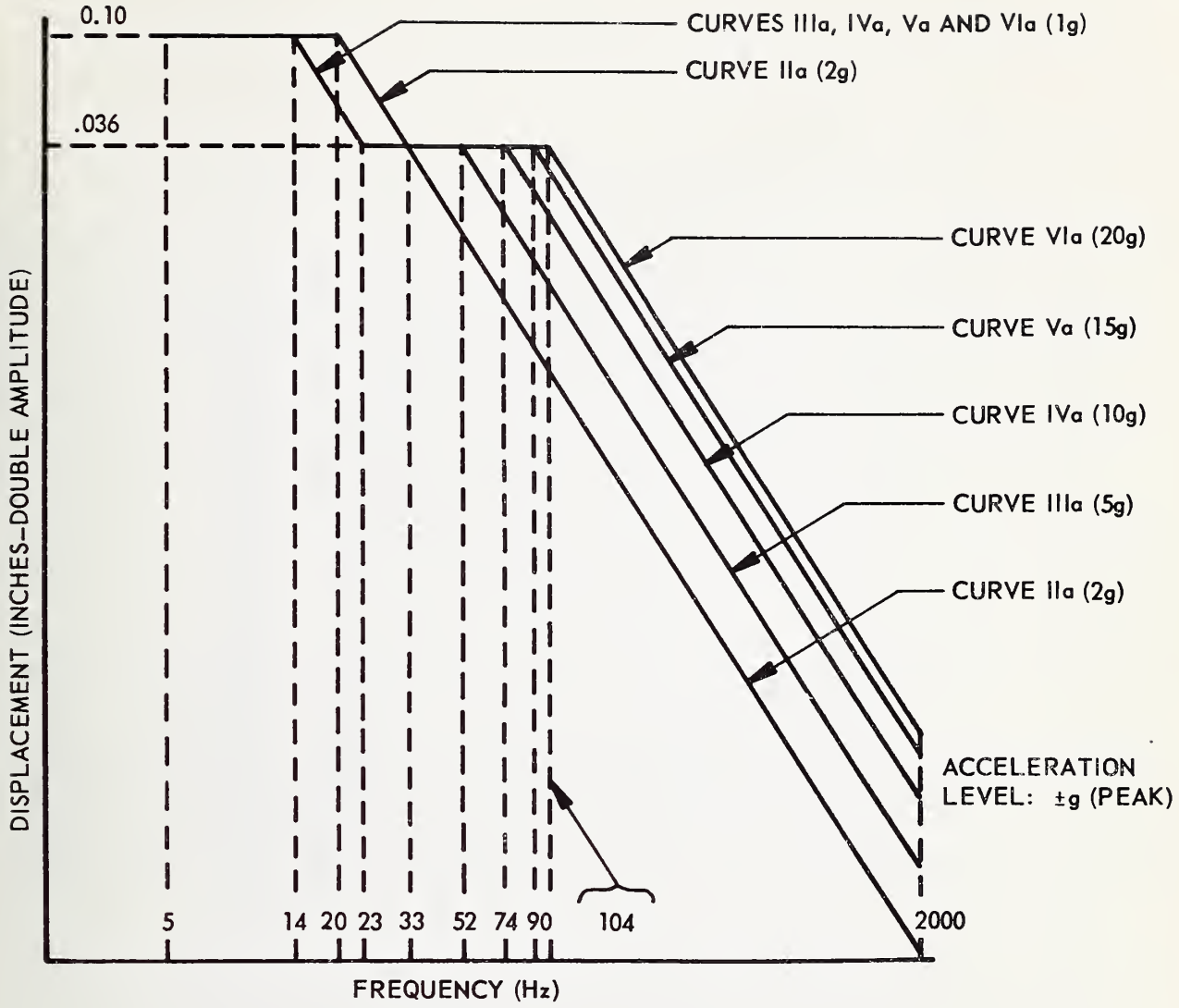

CURVE Ia (OF PREVIOUS ISSUES) – REPLACED BY CURVE IVa
CURVE IIa – EQUIPMENT DESIGNED FOR OPERATION ON ISOLATORS WITH ISOLATORS REMOVED
CURVE IIIa – EQUIPMENT MOUNTED IN FORWARD HALF OF FUSELAGE OR IN WING AREA WITH ENGINES AT REAR OF FUSELAGE
CURVE IVa – EQUIPMENT MOUNTED IN REAR HALF OF FUSELAGE OR IN WING AREA WITH WING OR FRONT MOUNTED ENGINES
CURVE Va – EQUIPMENT MOUNTED IN ENGINE COMPARTMENT OR ENGINE PYLON
CURVE VIa – EQUIPMENT MOUNTED DIRECTLY ON ENGINE

Figure 6. The sinusoidal vibration requirements for equipment designed for installation in jet airplanes (from MIL-E-5400R).

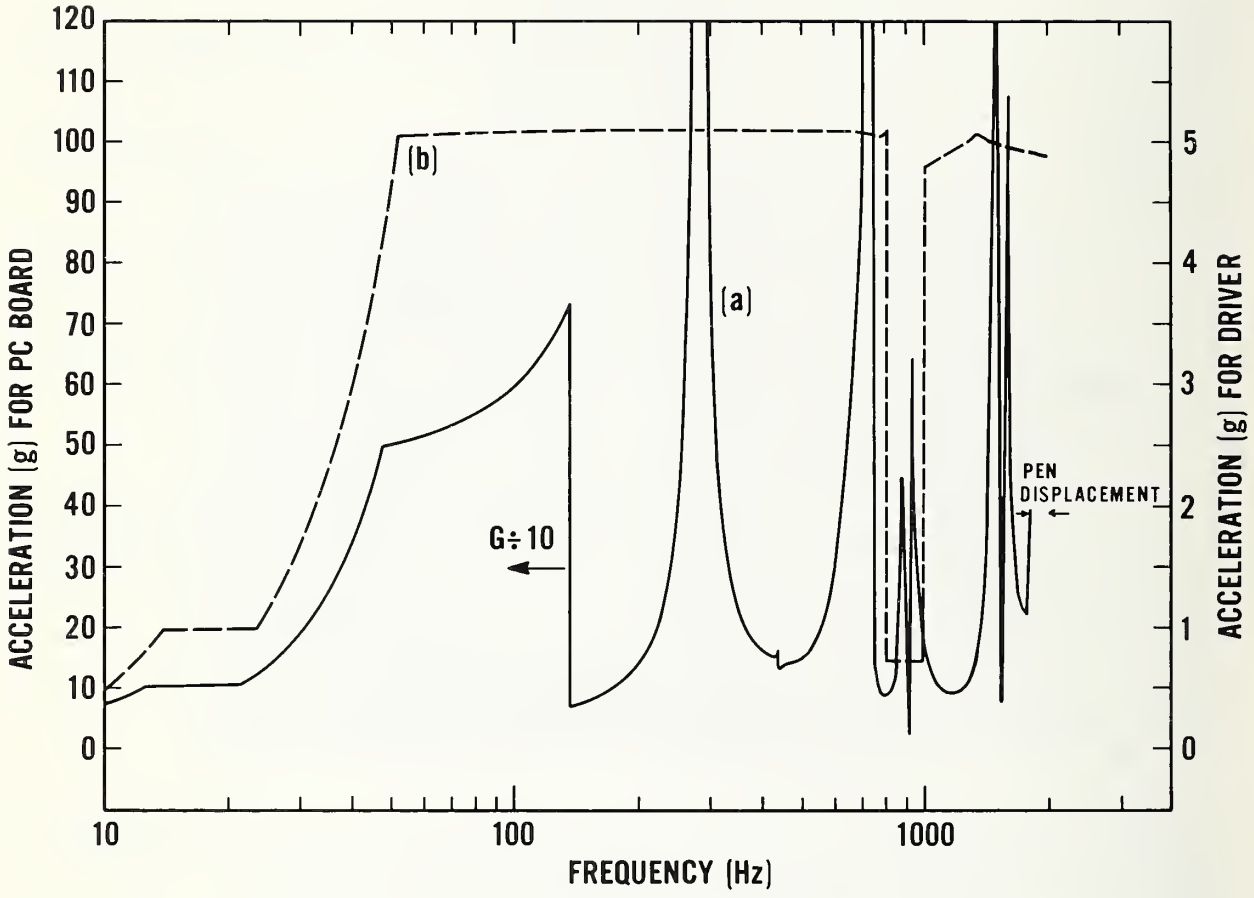

Figure 7. The resonant vibration peaks on a 20-min frequency sweep of an unloaded PC board (curve a). The recorder pen was displaced ∿1/8 in. to the left to prevent intercepting the calibrating pen that was recording the shaker drive (curve b). Saturation on the resonances is evident on three peaks.

Although the shaker drive was constant at 5 g, the accelerometer on the board recorded troughs of 10 g, which presumably resulted from overlapping resonances. Nevertheless, the board has an amplification factor (transmissibility) of >10 at some resonances. It is apparent from table 2 that there is excellent agreement with theory.

Table 2. Comparison Between Calculated and Measured Modal Frequencies for an Unloaded Board that was Copper Clad on One Side.

m	n	f_{meas}	f_{calc}	Comments
2	2	310 Hz	330 Hz	Peak > 100 g
3	2	480	495	Very small peak
2	3	800	820	Peak >100 g
3	3	960	975	Peak ≈ 80 g
5	2	1020	1160	Peak > 100 g
5	3	1640	1603	Peak near 100 g
3	4	1760	1710	Peak > 100 g

A-1.5 Preliminary Experiments on Vibration of PC Board-Mounted Hybrid Packages

In order to prepare flatpack hybrid packages for mounting on boards, it was necessary to bend and cut the leads. Package manufacturers recommend bending leads no closer than 0.10 in. from the package and they prefer a 0.15-in. spacing [35]. Subsequently, two lead bending-cutting jigs were designed and constructed. One bent the leads 0.07 in. and the other 0.15 in. from the edge of the package.

For this particular experiment, eight packages had their leads bent and cut, four on each jig. All showed a small degree of visually observable glass damage to two or three out of 30 leads, but this was much less than on prebent samples supplied from outside. Two high-quality packages, one with 0.07-in. and one with 0.15-in. leads, were soldered to unetched PC boards. This was facilitated by scribing a moat with a sharp knife in the copper cladding around the area to be soldered. The thermal conductivity away from the leads was thereby decreased, and soldering with a small iron was possible. The open packages were mounted side by side in the center of the board with the leads in the short direction of the board. This was intended to be the worse position for damage by excitation at the lowest mode. An accelerometer which weighs one gram was attached to the package with the shorter lead spacing.

The "fixed" nature of the board mount was verified by observation under slip-synchronized strobe light, as well as by observation of lycopodium powder patterns on the board after a preliminary run. Resonant amplitude acceleration peaks were measured both with the accelerometer and by the peak displacement method using a depth-gage micrometer mounted on a fixed nonresonant portion of the mount. The lowest resonant mode of the board with two

soldered-in hybrids was 280 Hz, which compares well with the calculated value of 308 Hz (including the weight of the packages, solder, and accelerometer). Had this weight been more evenly distributed, presumably the two frequencies would have been even closer.

During the test, several frequency sweeps were made from 10 Hz to 2 kHz; however, the programmed rate of frequency change was varied to allow longer observation with the strobe at the resonances and to make amplitude measurements. At several resonances, clear differential motion was observed between the packages, with the greatest motion occurring on the one having the longer leads. At one point, package rotation was observed, and at higher modes differential motion from one side of the package to the other was observed. After the third frequency sweep, different vibration noises were heard. It was concluded that some lead damage had been sustained, and the test was terminated. The damage was extensive both to the leads, by fatigue, and to the glass seals as observed under a microscope. Eighty percent of the leads on the package with longer lead spacing were damaged or broken, as is evident in the photomicrograph in figure 8. No leads were broken on the package with shorter leads, but some glass cracks were observed.*

The packages were then removed from the board for further observation of the damage and evaluated by the newly developed high-temperature leak test method, which is described in Part B of this report. The room temperature leak test showed both packages to have leak sizes less than 10^{-8} atm•cm^3/s helium. Tests at 125°C gave similar results, leak sizes less than 5×10^{-8} atm•cm^3/s helium, the test limit. The packages were put on a thermoelectric temperature cycling system and cycled 25 times from -55° to 125°C with a 7-min cycle time. They were retested, and again the package with shorter leads had a leak size less than 10^{-8} atm•cm^3/s helium at room temperature and 5×10^{-8} atm•cm^3/s helium at 125°C. However, the package with the longer leads, which had sustained considerable damage, showed a 10^{-7} atm•cm^3/s helium leak at one seal at room temperature and 10^{-7} atm•cm^3/s helium leaks at two seals (one was the room temperature leak) at 125°C. It should be noted, however, that a 10^{-7} leak is acceptable in Method 1014.2 of MIL-STD-883 [36] for packages of volume 2 cm^3 or greater. Thus, these packages cannot be considered to have failed hermetic tests even though 1/2 of the leads had been fatigued off.

The above preliminary work was performed on copper-clad boards to establish techniques, vibration amplitudes, and the accelerations required to induce visual glass seal damage and lead fatigue.

A-1.6 The Vibration Characteristics of Metallization-Patterned PC Boards with Soldered-In Hybrid Packages

When pattern-etched PC boards were available, a series of experiments were run on them in both loaded and unloaded condition with accelerometers attached to the boards and to the hybrids at various board positions. A typical board with three flatpack hybrids soldered into it is shown in figure 9.

* All further flatpack vibration tests in this study were carried out with the shorter (0.07-in.) bent leads which gave better fatigue resistance than the longer leads.

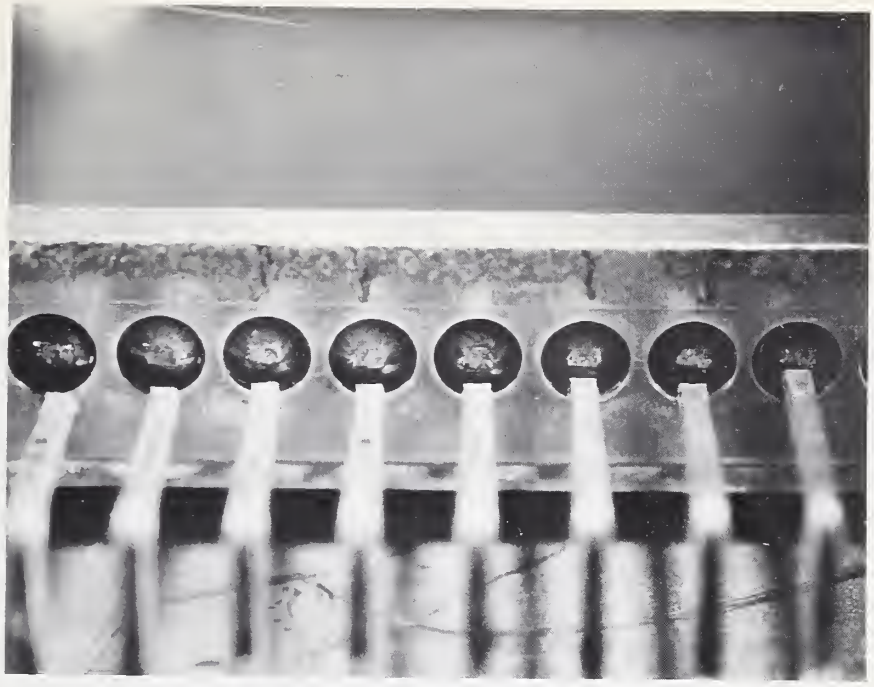

(a)

(b)

Figure 8. Photomicrographs of a 1-in. square hybrid package after vibration testing. (a) Leads fatigued off during vibration tests at the package seals, showing glass damage. (b) Leads fatigued off at the bends or at the solder joints.

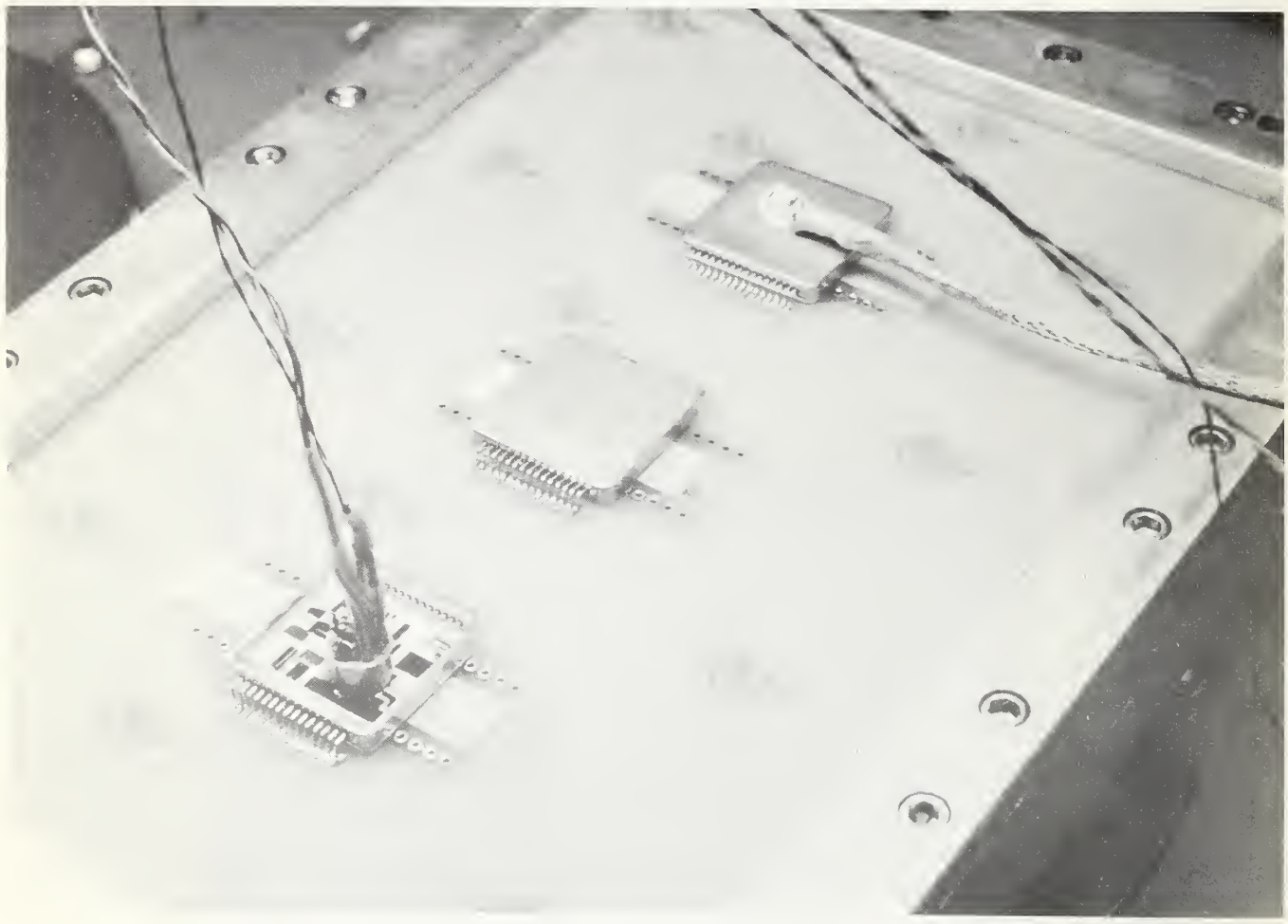

Figure 9. A closeup of the vibration mount and the printed circuit board with three flatpack hybrids soldered on it. The accelerometer that weighs only one gram is on the upper hybrid, and a TO-100 acoustic-emission detector (sec. A-2.1) is shown on the lower hybrid.

Figure 10 shows the acceleration *versus* frequency for two frequency sweeps made on an etched PC board that contained no hybrids and was only loaded with a 1-gram accelerometer placed in two different positions. The solid curve was obtained with the accelerometer in the center of the board on the position of the middle hybrid in the previous figure. The dotted curve is taken with the accelerometer placed on the side position of the board. The resonance peaks have quite different amplitudes depending on sensor placement. This is to be expected since the vibration amplitude varies considerably from point to point on the board when various vibration modes are excited. This particular board was driven with only 1.5-g constant acceleration. The transmissibility in the center of this board for the first or fundamental vibration mode is almost 100. It is even higher for some other modes. Differences between the various modal frequencies in figure 10 and those calculated in table 1 are attributed to changes in E, σ, and W resulting from patterning the copper film and introducing large numbers of plated-through solder-covered vias.

Figure 11 shows the vibration amplitudes (given as acceleration) as a function of frequency for a printed circuit board with one 15-gram plug-in-type hybrid package mounted in the center of the board. The solid curve represents data obtained with the accelerometer mounted in the hybrid. The dashed curve is a result of placing the accelerometer in an empty side position on the board. It is to be noted that in this position the unloaded board (fig. 10) showed a higher acceleration for the center placement; however, in this case the side placement results in a higher acceleration due to the loading in the center. An even greater change is observed in the second vibration mode in which the side accelerometer position shows a much higher acceleration than the center position.

Three plug-in-type hybrids were placed on the board and vibrated. The data are shown in figure 12. The solid curve represents the acceleration measured by placement of the accelerometer in the center hybrid position and the highest peak is the fundamental. The second solid curve peak is about half the amplitude of the first and successively higher frequency peaks are of lower amplitude. Thus, as is apparent from eq (1), the placement of several hybrids on the board loads the board and lowers the frequency and amplitude of each modal peak. The constant acceleration drive for this experiment was 3 g, twice as high as that of the unloaded board in figure 10. The dashed curve represents the placement of the accelerometer on one of the side hybrids. The situation is quite different from the center position, the fundamental is lower, and the second resonant peak is as high in amplitude as that measured in the solid curve.

A-1.7 Susceptibility of Plug-in-Type Packages to Fatigue Damage at High-g Levels

Preliminary experiments showed that all flatpack-type packages regardless of lead length would suffer some fatigue breakage of leads when subjected to resonant vibration in the order of 100 g for a period of 30 min. Therefore, it was decided to perform similar evaluations of the plug-in-type packages. The same PC board packages vibrated in figure 12 were further stressed at the 100-g level (center hybrid) at the fundamental resonant frequency (~250 Hz) for 1 hour. There was no apparent damage and so the experiment was continued

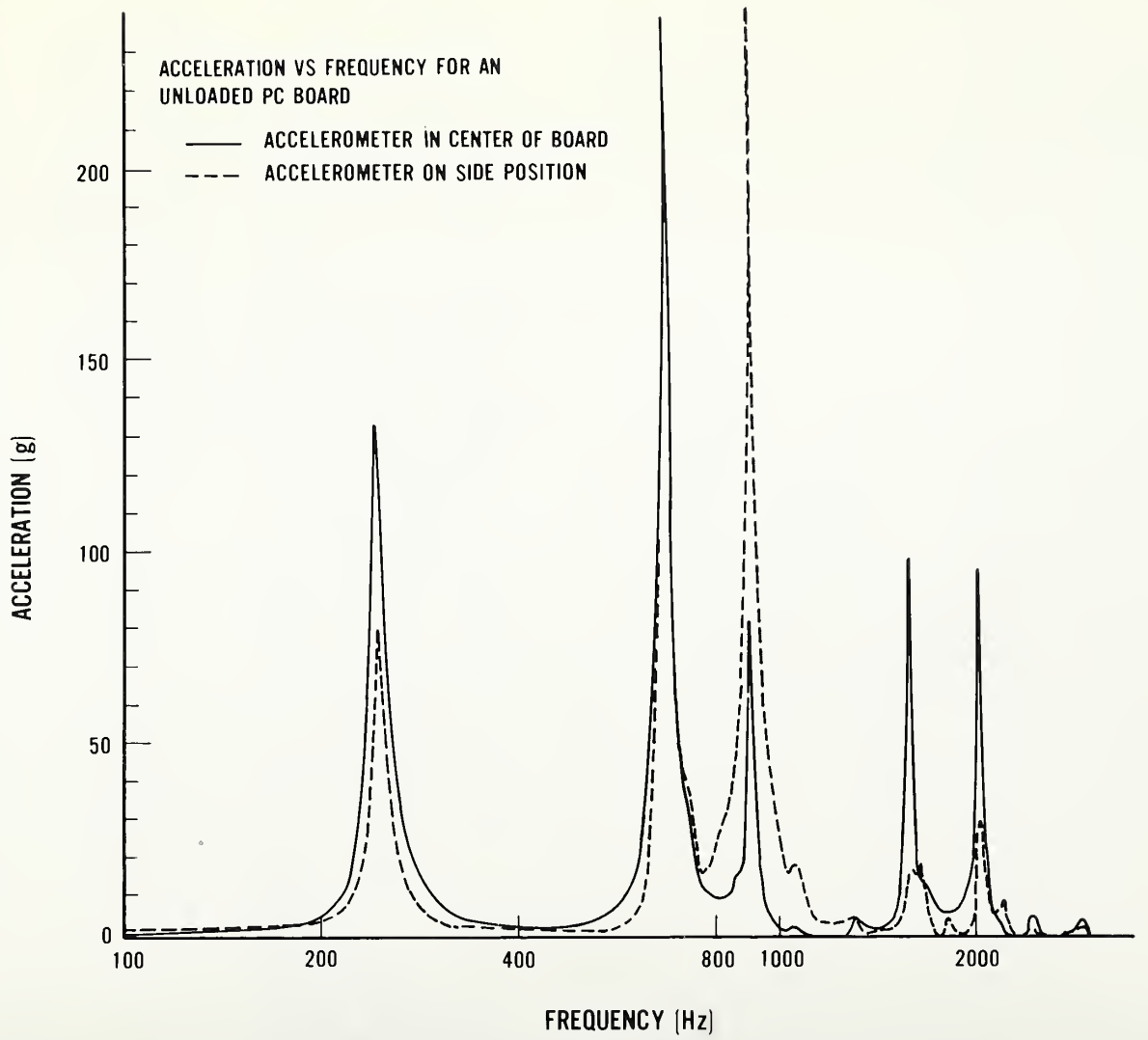

Figure 10. Acceleration *versus* frequency for an etched PC board similar to that in figure 9, but containing no hybrids. The acceleration drive to the board was 1.5 g across the entire spectrum.

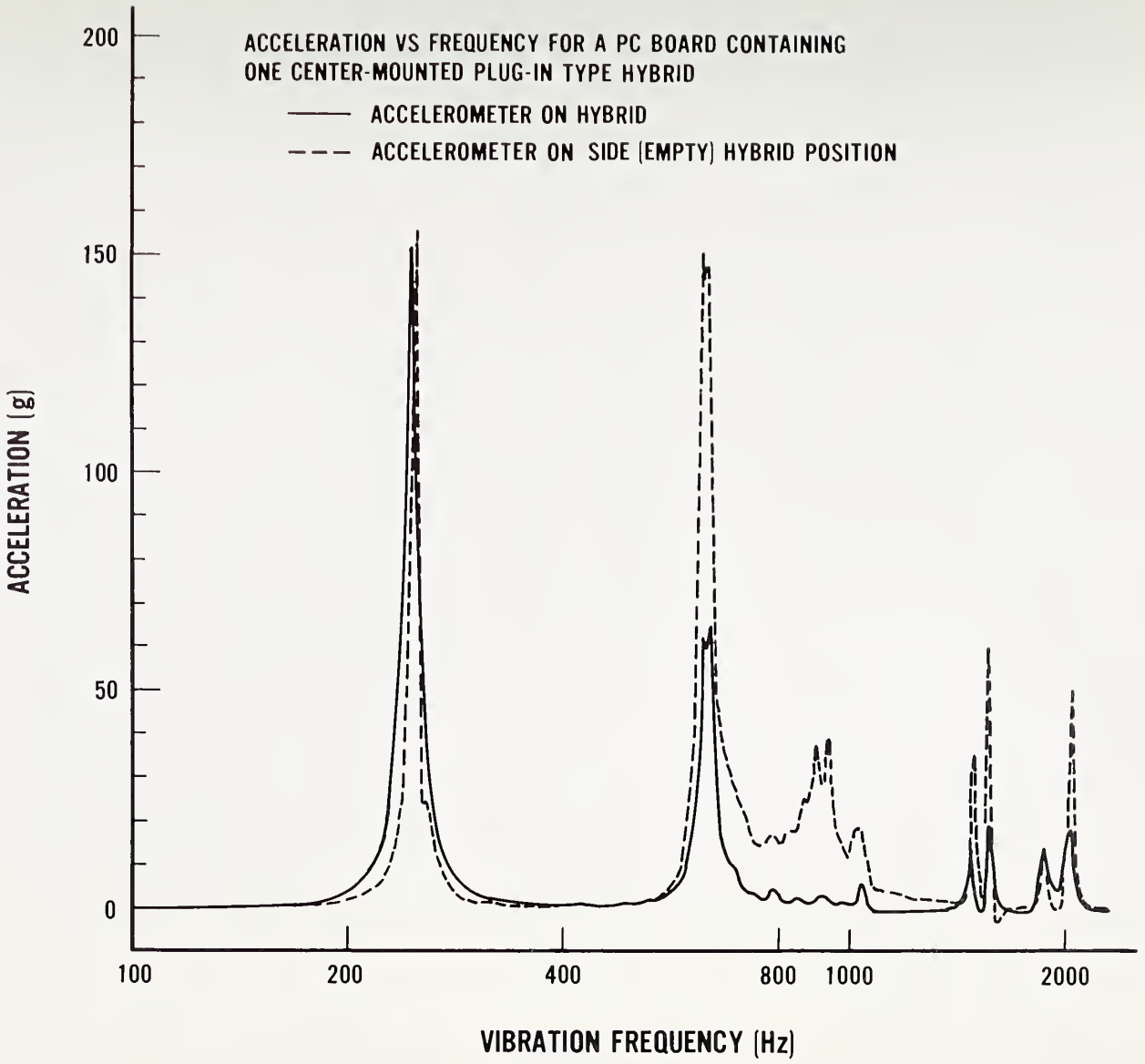

Figure 11. Acceleration *versus* frequency for a PC board similar to that in figure 9 except that it contains one center-mounted flatpack hybrid. The acceleration drive to the board was 2.0 g across the entire spectrum.

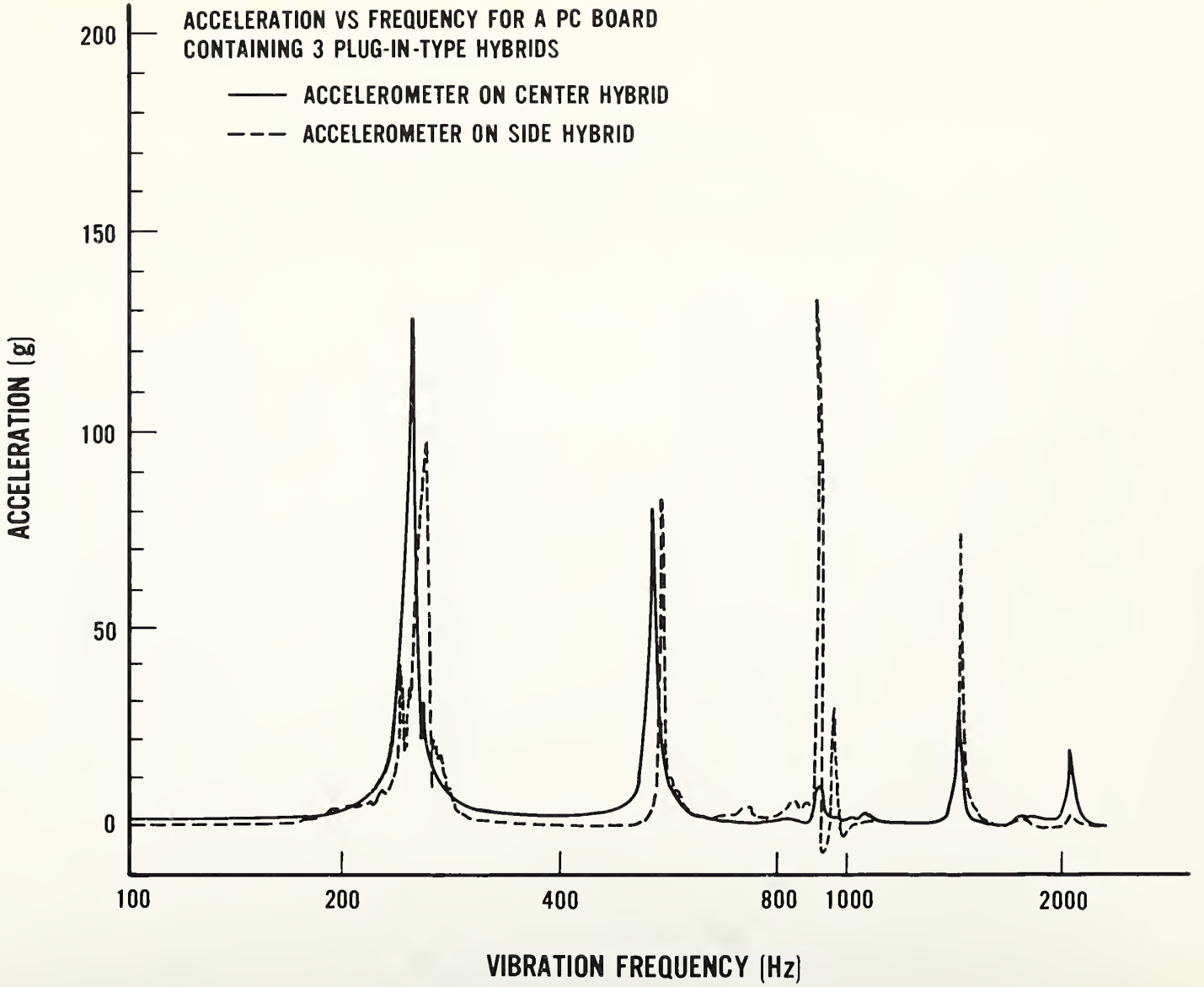

Figure 12. Acceleration *versus* frequency for a PC board similar to that shown in figure 9 except that three plug-in-type hybrids were mounted on the board. The acceleration drive for the board was 3.0 g across the spectrum.

at 450 g for 30 min longer. Observation with a strobe revealed that the hybrid packages acted as board stiffeners. The board moved only vertically (up-and-down) in the vicinity of the hybrids with no flexing occurring under them.

After these high-stress experiments, the hybrids were removed from the board. No visual seal damage was observed, and leak tests revealed no loss of hermeticity as a result of this extreme stress test. An additional stress test was performed at 450 g for 30 min with two plug-in-type hybrids on the board, one in the center and the other on one side to assess the results of asymmetrical board loading and possible torsional forces on the leads. Again, no damage occurred to the hybrids. However, the 1-gram accelerometer (rated for 1000 g) that was used to monitor the experiment was damaged due to its leads fatiguing and had to be repaired before other experiments could proceed.

Even though soldered-in, plug-in packages appear to be immune from vibration-induced damage, there is still a possibility that seal damage can result from thermal shock during soldering or desoldering to remove them from the board. For experimental purposes, open hybrids (as in fig. 10) should be leak tested on the board before and after vibration.

A-1.8 Long-Term Low-g Nonresonant Vibration Effects

Since low-g nonresonant vibration may occur in avionics environments, one test was run to assess fatigue and/or glass seal damage under low stress, extended time conditions. Four flatpack hybrid packages with short (0.070 in.) bent leads were soldered onto a prepared (etched) board (three symmetrically on top and one in the center on the bottom) and vibrated at 90 Hz for 20 h at the 10- to 15-g level. They were removed, visually inspected, and leak tested. No glass cracking was observed and no leaks at $>10^{-8}$ atm•cm^3/s were found.

A-1.9 Effect of Very High-g Forces on Flatpacks

Experiments were performed to determine whether seal damage in high-quality packages could be induced when the leads were fatigued off rapidly and violently at high-g levels. Two flatpack packages were soldered onto a PC board symmetrically, near the center, and vibrated at 200 to 300 g for several minutes until all of the leads of one package fatigued off and the package fell from the board. The other package remained on the board held by three or four (out of 30) leads. Figures 13a and 13b are scanning electron microscope (SEM) micrographs of two of the severely damaged but still hermetic seals! Figure 13c is included from an earlier vibration run at a lower stress level (~80 g for 10 min). All of the packages were tested for leaks at room temperature and at 125°C and found to be better than 10^{-7} atm•cm^3/s. An important conclusion of this experiment was that no correlation was observed between the visual appearance of the seal and leaks when high-quality packages were studied [37].

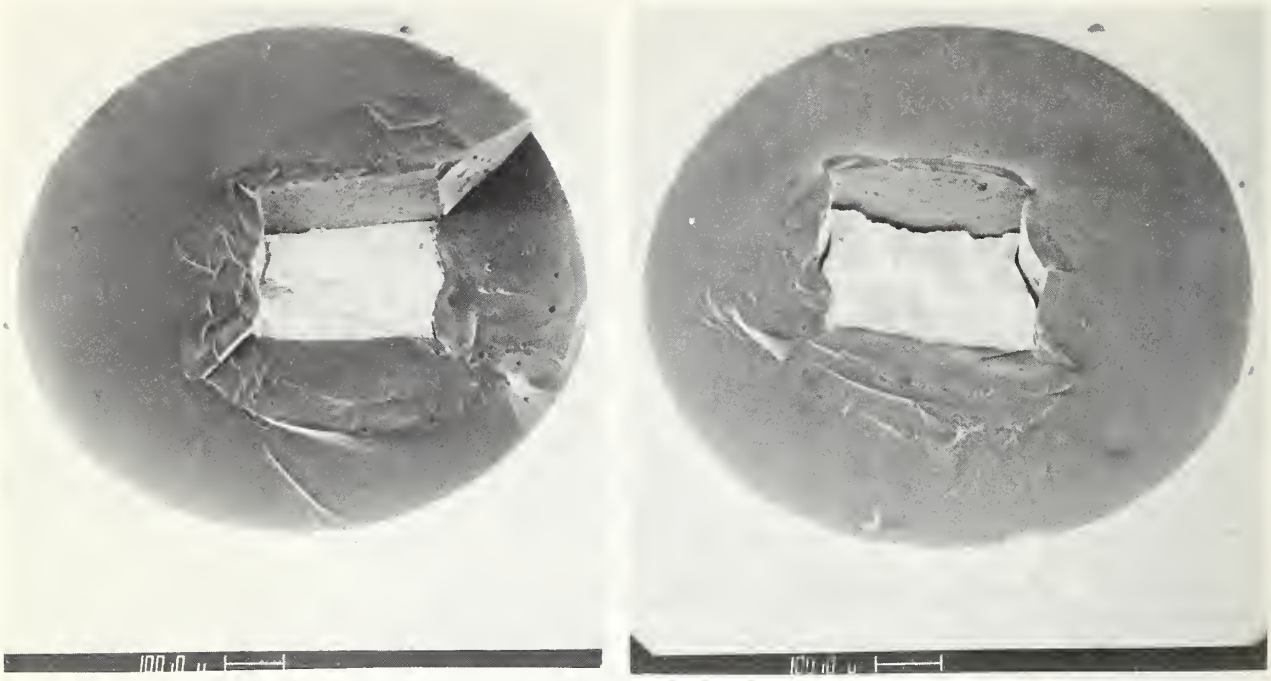

(a) (b)

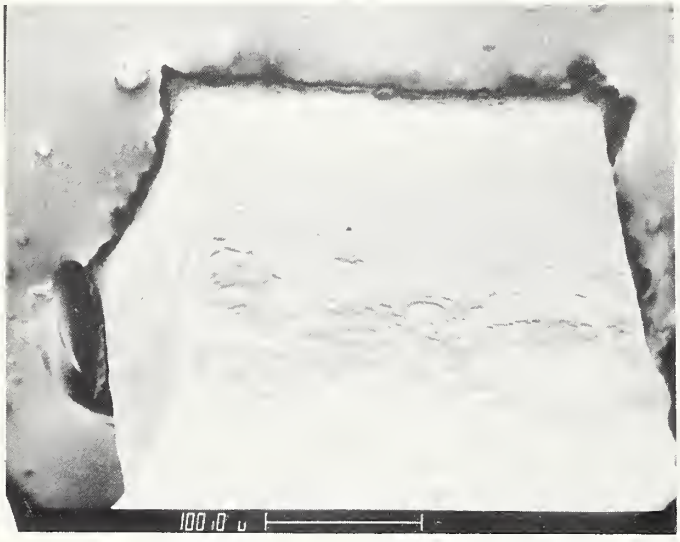

(c)

Figure 13. SEM photomicrographs of glass-metal seals in hybrid packages that have been vibrated. No hermetic damage occurred to the packages. (a) and (b) Seals from packages vibrated at 200 and 300 g at 250 Hz. (c) Seal and lead from a package vibrated at 80 g at 260 Hz. The small dots on the glass portion are foreign particles and not a part of the seal.

A-2 Acoustic-Emission Equipment and Techniques for Detecting Glass Seal Cracking During Vibration

A-2.1 Development of an Acoustic-Emission Detector for Use in Vibration Experiments

When acoustic-emission tests are used to establish the after-production integrity of microelectronic welds and seals, the sensor may be attached to a printed circuit board (thickness ~0.06 in.) or to an electronic package such as the casing of a hybrid microcircuit which may have wall thicknesses of only ~0.015 in. The AE wave detected in a test generally has a wavelength on the order of 0.4 in. and propagates along these thin materials as some form of surface wave such as Rayleigh and Lamb waves. Normal acoustic-emission detectors are relatively insensitive to these surface waves.

AE detectors are usually constructed with the piezoelectric transducer (PZT) element recessed into the case and with plastic extending to the surface for acoustic wave coupling. These sensors are typically designed to have maximum sensitivity in the direction of the thickness of the PZT disc. Thus, maximum sensitivity occurs for waves entering the detector normal to its surface rather than for a surface wave propagating along the base or top of a hybrid package. Acoustical wedges have been used to increase the sensitivity of AE detectors to surface waves. However, a disc-shaped PZT sensor lying flat on the surface is sensitive to surface waves propagating along its diameter, and the resonant frequency of the sensor to such waves is determined by the diameter rather than the thickness of the sensor. Also, the impedance of AE sensors is relatively high (~20 KΩ at resonance and higher off resonance), and the output for weak signals is low, in the order of microvolts. Some of the signal may be lost due to cable capacitance; in addition, shielded cable noise generated during PC board vibration tests may limit the maximum sensitivity of the detectors. In order to complete objectives of this study, it was necessary to develop an improved sensor to overcome the above limitations.

A detector-preamplifier having high sensitivity to surface waves was constructed as follows: AE sensors with diameters of about 0.25 in. were ultrasonically cut from larger diameter 1-MHz and 5-MHz PZT ceramic stock. Copper wires, PTFE-coated and 0.003 in. in diameter, were soldered to the silver-coated faces of the ceramic disc, and the element was bonded into the cap of a TO-100 IC package, which had a thin layer of polyimide in it as insulation. A 733 differential input-output operational amplifier chip was attached with insulating epoxy to the base of the TO-100 package and wire bonded so that it had a gain of 100. The chip was cleaned with fluorocarbon and DI water and then protected with a film of xylene-thinned silicone rubber. The bonding wires were protected from possible shorting by a film of photoresist. Photographs of the basic assembly steps are given in figure 14.

The completed AE detector-amplifiers weigh approximately 1.3 grams and, therefore, offer negligible damping when attached to hybrids undergoing vibration tests. All connections to the device, including signal leads, are unshielded twisted pairs in which vibration-induced noise is negligible at the relatively low output impedance of the 733 chip.

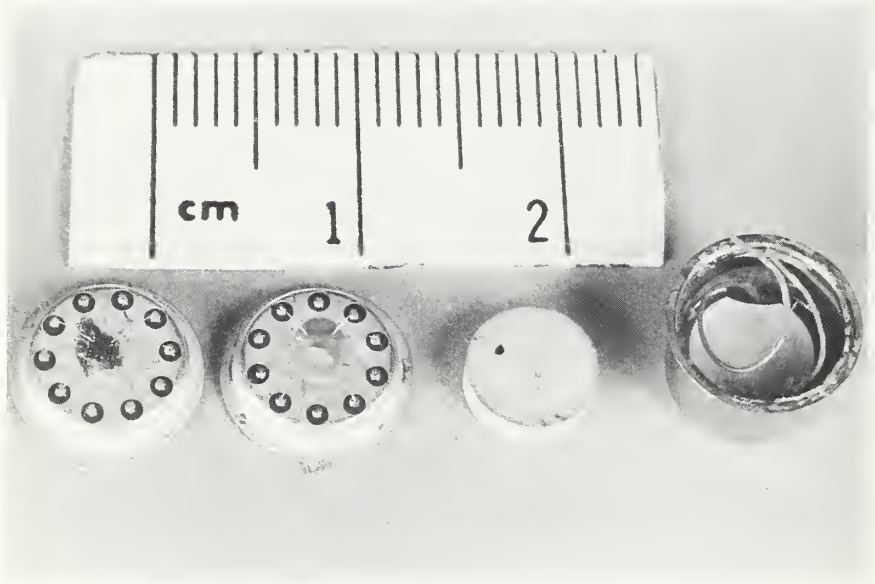

Figure 14. Steps in the assembly of the TO-100 acoustic-emission detector-preamplifier. From left to right, the μA-733 chip is die bonded and wire bonded; then a silicone rubber coating material is applied. Next, a PZT AE detector chip is shown. On the right it has leads attached and is held to the TO-100 cap with a polyimide adhesive. The leads are then ultrasonically attached to the package, the cap is welded on, and external power and signal leads are attached. (A closeup of a finished detector is shown in fig. 21.)

The amplitude *versus* frequency response for surface waves of several of these acoustic-emission detectors was determined by calibration at NBS.* Figure 15 is the amplitude *versus* frequency curve for one of the detector units that contains a 1-MHz PZT (in the thickness mode). Note that there are high response peaks at approximately 0.2, 0.4, and 0.7 MHz with only small peaks occurring around 1 MHz, the thickness mode response peak. The method of mounting enhances the response to surface waves traveling parallel to the diameter.

Figure 16 shows the amplitude *versus* frequency response of a detector whose PZT has a 5-MHz peak response when used in the normal or thickness mode. The diameter response mode is around 0.4 MHz. The amplitude at this frequency is considerably smaller than that of the first detector, but there are three clear peaks in the 0.35- to 0.4-MHz range. No other response of any significance is evident in the indicated frequency range. For comparison, figure 17 shows the frequency response of a high-quality acoustic-emission detector obtained from a commercial source. This has a peak at approximately 0.3 MHz. It was chosen to peak in the same frequency range as the other two detectors as well as having a high sensitivity as stated in the manufacturer's specifications. The commercial unit which contained no built-in 40-dB preamplifier was plotted on a different relative intensity scale from the two NBS detectors. The three curves (figs. 15, 16, and 17) are made equivalent if one multiplies the commercial detector response (fig. 17) by 1.35. This makes its peak magnitude approximately 3 on the scale of figures 15 and 16. The first detector is clearly far more sensitive in the 0.3-MHz range (in the order of six times) than the commercial unit. The second TO-100 detector has a peak sensitivity somewhat less than the commercial unit, but the response is much broader, in the 0.3- to 0.4-MHz range. Therefore, that TO-100 detector should be more sensitive to a typical acoustic-emission burst.

A-2.2 Determining AE Waveform Signatures in Order to Separate Glass Cracking From Metal Fatigue

The TO-100 detector whose calibration was given in figure 15 was chosen to determine the waveform signature of glass cracking. This detector was acoustically coupled to a hybrid flatpack containing 30 leads. To obtain an acoustic-emission signal of glass seal cracking, one of the leads was intentionally bent upward until the glass cracked. The acoustic-emission signal was fed into a transient recorder. This recorder was interfaced to a computer, which performed a fast Fourier transform (FFT) on the data. The data were analyzed in three separate parts: (a) the first third of the waveform that included the leading edge of the AE burst, (b) the middle portion, and finally (c) the remaining third. The wave form analysis was divided to determine any differences in the frequency output as a function of time. Figure 18a is the FFT of the leading edge of one of these glass-seal-crack acoustic-emission bursts. There are two high peaks, one near 0.2 MHz and one at about 0.4 MHz. There is also a moderate signal in the 0.6- to 0.7-MHz region. The amplitude of this latter signal was not corrected for the sensitivity characteristics of the detector. If it had been, the 0.7-MHz signal would be much larger.

* The calibrations were carried out in the Mechanical Production Metrology Division of NBS by F. R. Breckenridge.

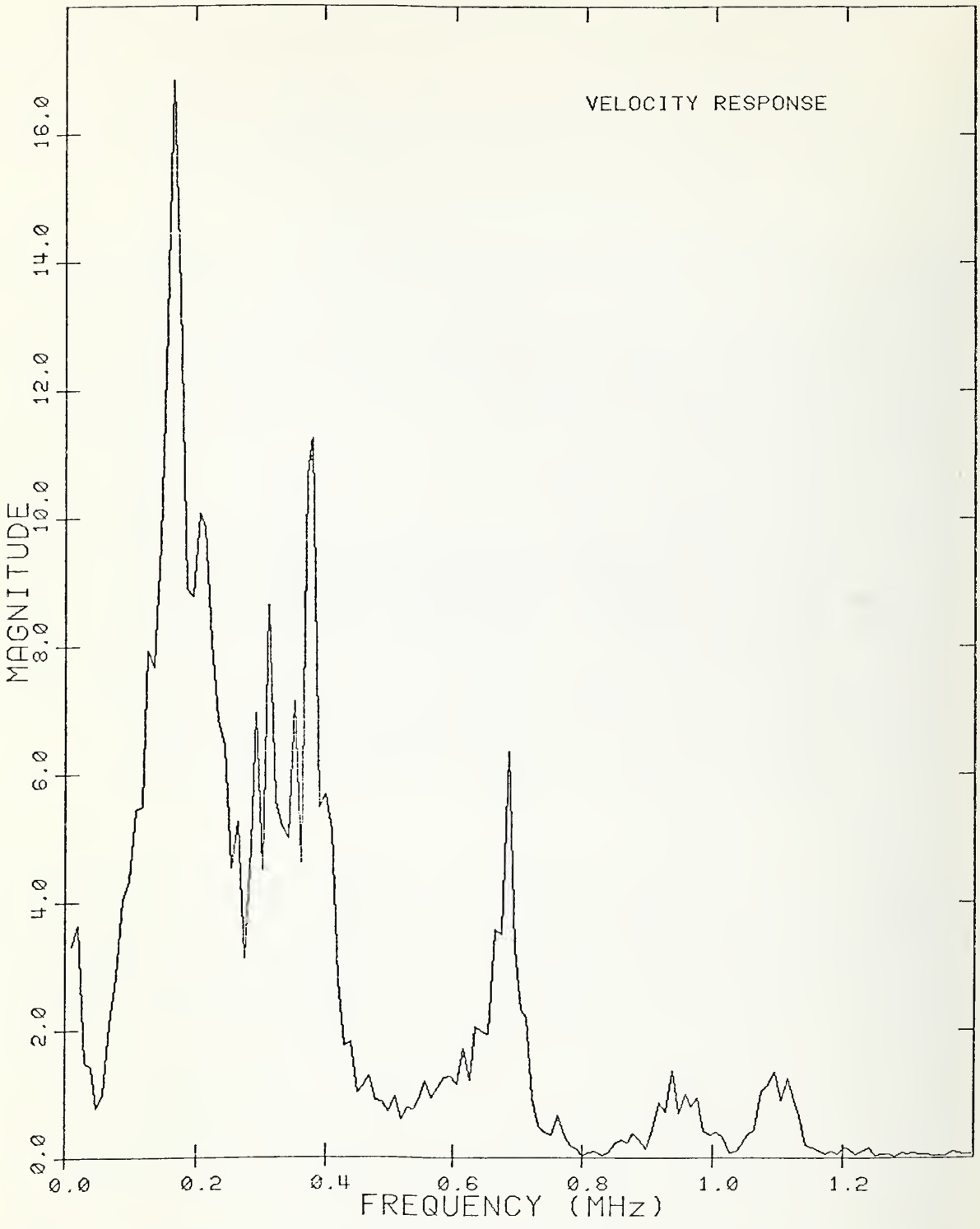

Figure 15. The frequency spectral response of a TO-100 acoustic-emission detector-preamplifier. (The PZT ceramic element used in this test was designed for a 1-MHz peak response.)

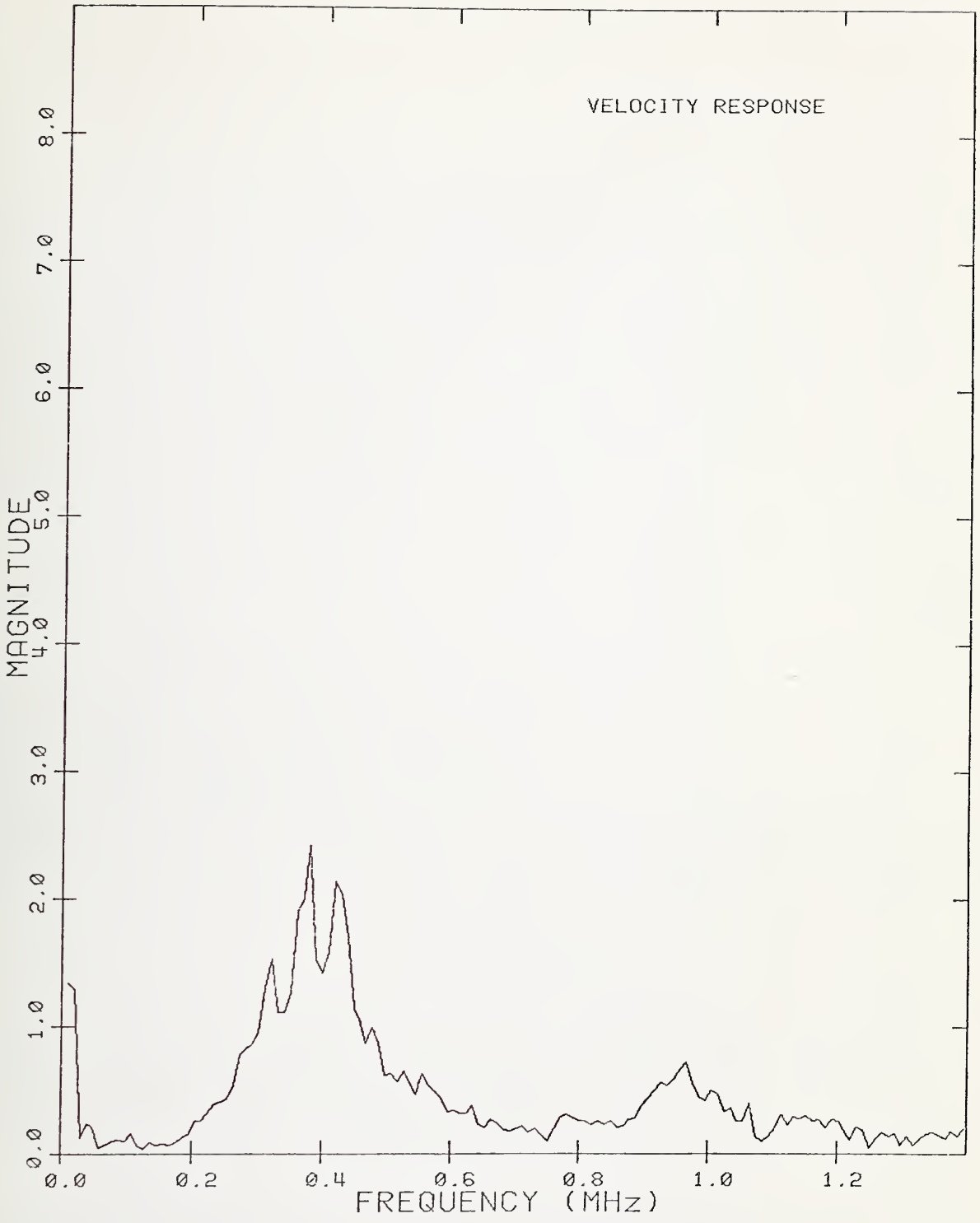

Figure 16. The frequency spectral response of a TO-100 acoustic-emission detector-preamplifier. (The PZT ceramic element used in this test was designed for a 5-MHz peak response.)

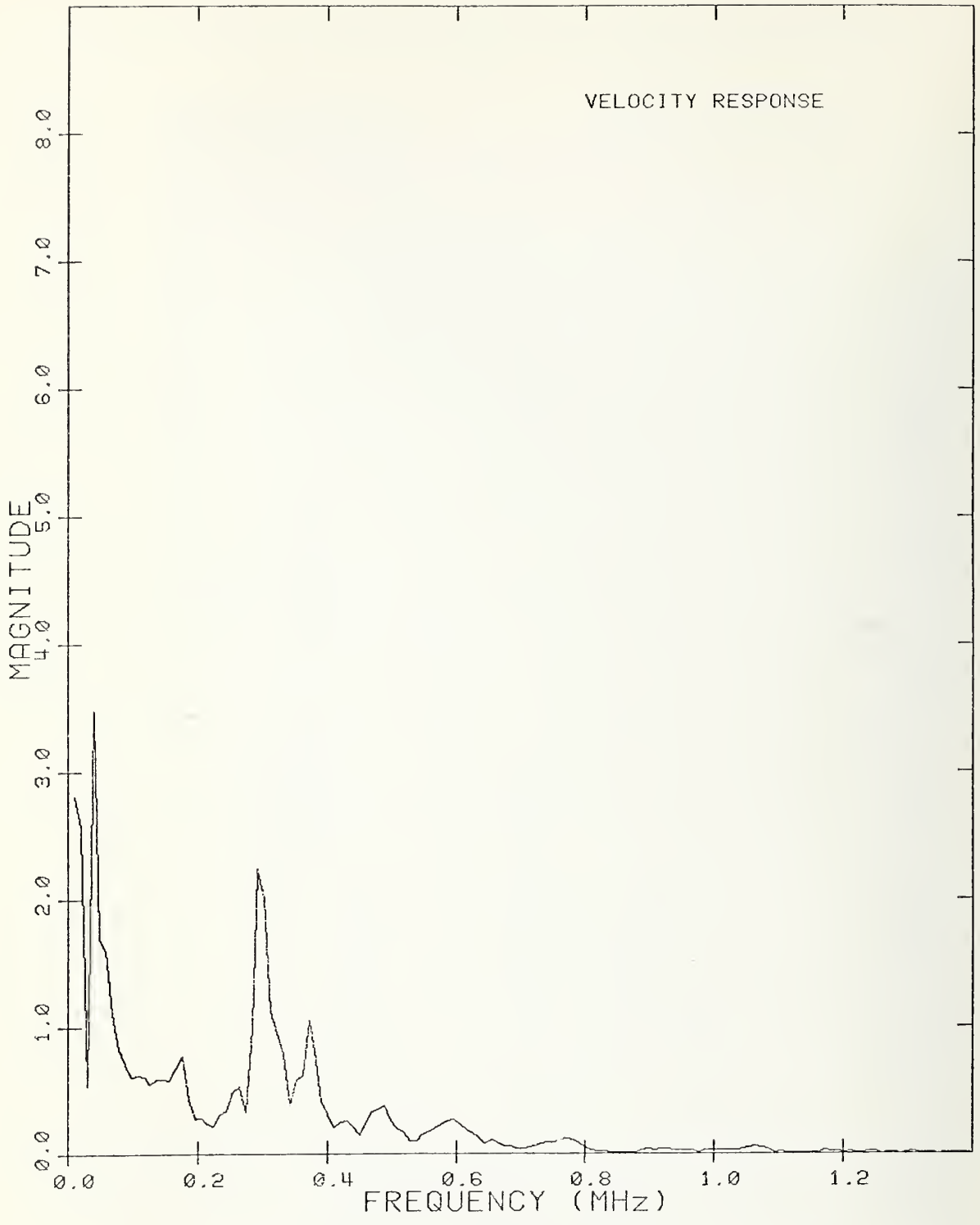

Figure 17. The frequency spectral response of a high-quality commercial AE detector. The sensitivity scales (amplification of measurement equipment) are different from those of figures 15 and 16; but for comparison, if the 0.2- to 0.4-MHz sensitivity peaks on this figure are multiplied by 1.35, the sensitivity of the ceramic detectors (void of the internal preamplifiers) can be directly compared.

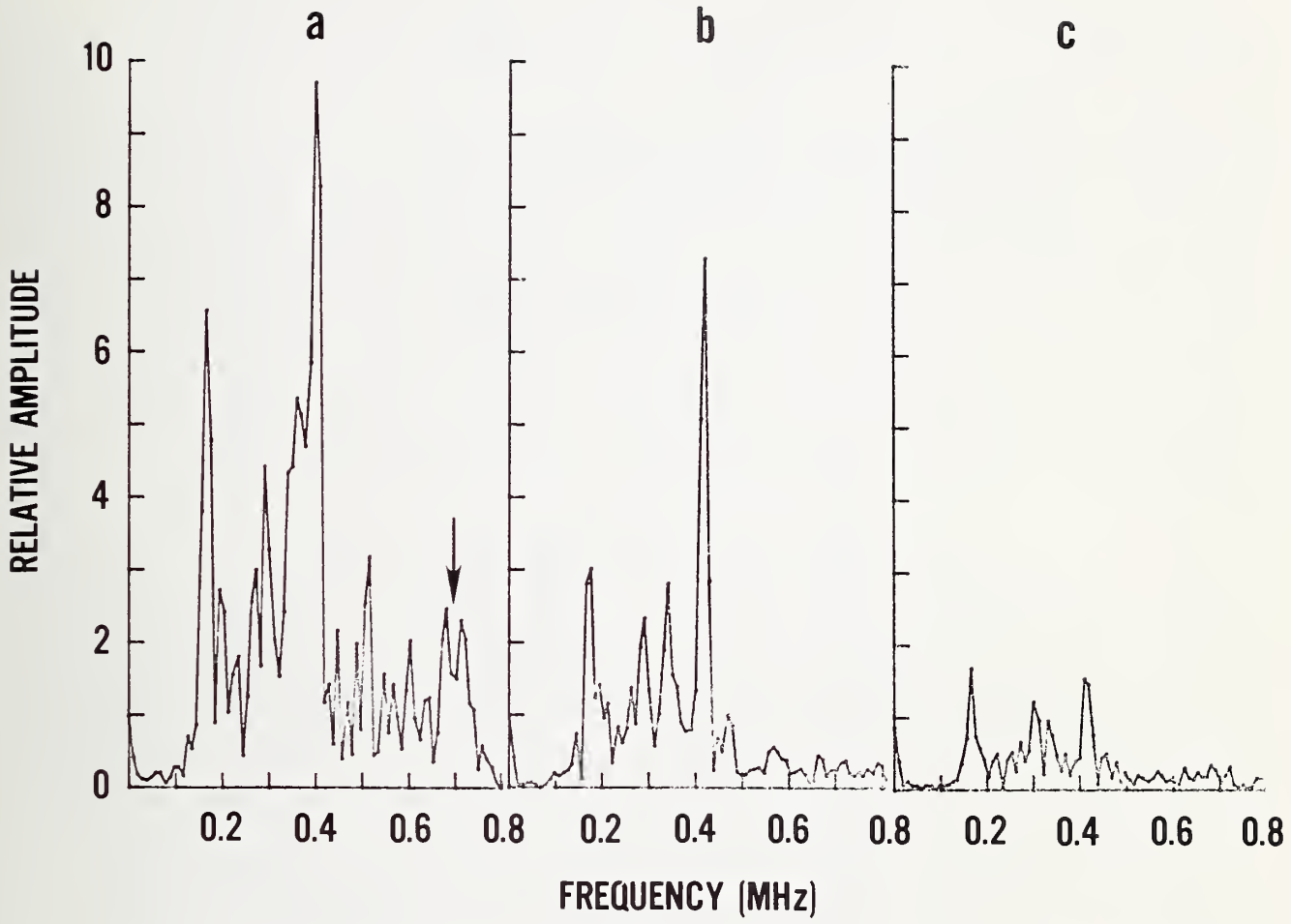

Figure 18. Fast Fourier transform (FFT) of an acoustic-emission waveform obtained by intentionally bending a lead on a hybrid until the glass seal cracked. The FFT was divided into three equal parts [(a) leading edge, (b) center, (c) trailing edge] to show any differences across the entire AE waveform. The arrow in (a) indicates the 700-kHz peaks that vanish after the first third of the AE burst.

Figure 18b shows the FFT of the middle third of the acoustic-emission burst. As with most AE bursts, the amplitude decreases with time across the burst. Therefore, the overall amplitude of this signal is somewhat lower than the first. One should note, however, that even though the amplitude is lower, the relative amplitude of the various peaks is significantly different. In this case the 0.2-MHz peak is relatively lower than the 0.4-MHz peak, and the 0.7-MHz peak has almost vanished. Figure 18c shows the last 1/3 of the FFT frequency spectrum. In this case, the overall amplitude is lower and there is no signal in the 0.7-MHz range. Also the relative amplitude has again changed between the two major peaks. They are now approximately equal.

Similar data to these were obtained with other glass cracks, and although the exact shape of the FFT peaks was different in each case, a shift to lower frequencies was observed from the leading edge to the center of the waveform. It had also previously been determined that the package metal-fatigue acoustic-emission signals did not produce the same high-frequency component in the leading edge, and in addition the overall amplitude was lower with more continuous AE rather than high bursts. Therefore, the triggering circuit that is used to activate the transient recorder was preceded by a filter that only passed the 0.7-MHz signal. Thus, by using the 0.7-MHz filter, it was possible to separate AE originating from lead fatigue from that produced by glass cracking. This separation had originally been thought to be a major problem since both fatigue and cracking produce acoustic emission.

A-3 Acoustic-Emission-Monitored Vibration Experiment

A-3.1 Equipment Setup

The first step in the AE-monitored vibration experiment was to establish a procedure to attach the TO-100 detectors to the hybrids. For this, it was necessary to determine the optimum material that would serve both as an AE couplant as well as a mechanical glue-like attachment for use in holding the detectors during vibration tests. Several thermoplastic materials typically used as AE couplants were rejected because of their brittleness, since any cracks that developed in the couplant due to the vibration could generate acoustic emission and this might be confused with signals emitted from cracking seals. A series of tests involving a dozen different materials determined that beeswax would adequately serve as both a mechanical and an AE couplant for vibrational purposes. The AE detector can be attached either by melting the beeswax (~70°C) or by solvent evaporation (the former is most desirable since it is quicker).

The AE equipment setup that was used to control and record the hybrid seal-cracking vibration experiments is given in figure 19. The output from the acoustic-emission detector can completely control the experiment. As seen in the figure, the shaker drive oscillator output was fed through an electronic trigger-controlled switch. This switch was triggered to the off-condition by a pulse from the acoustic-emission trigger unit. Thus, when an acoustic-emission burst was obtained, the sine wave drive to the shaker was removed within a few microseconds. Simultaneously, the acoustic-emission burst that initiated the trigger signal was recorded by the transient recorder, and the accelerometer output, which was plotted on an x-y recorder, displayed the

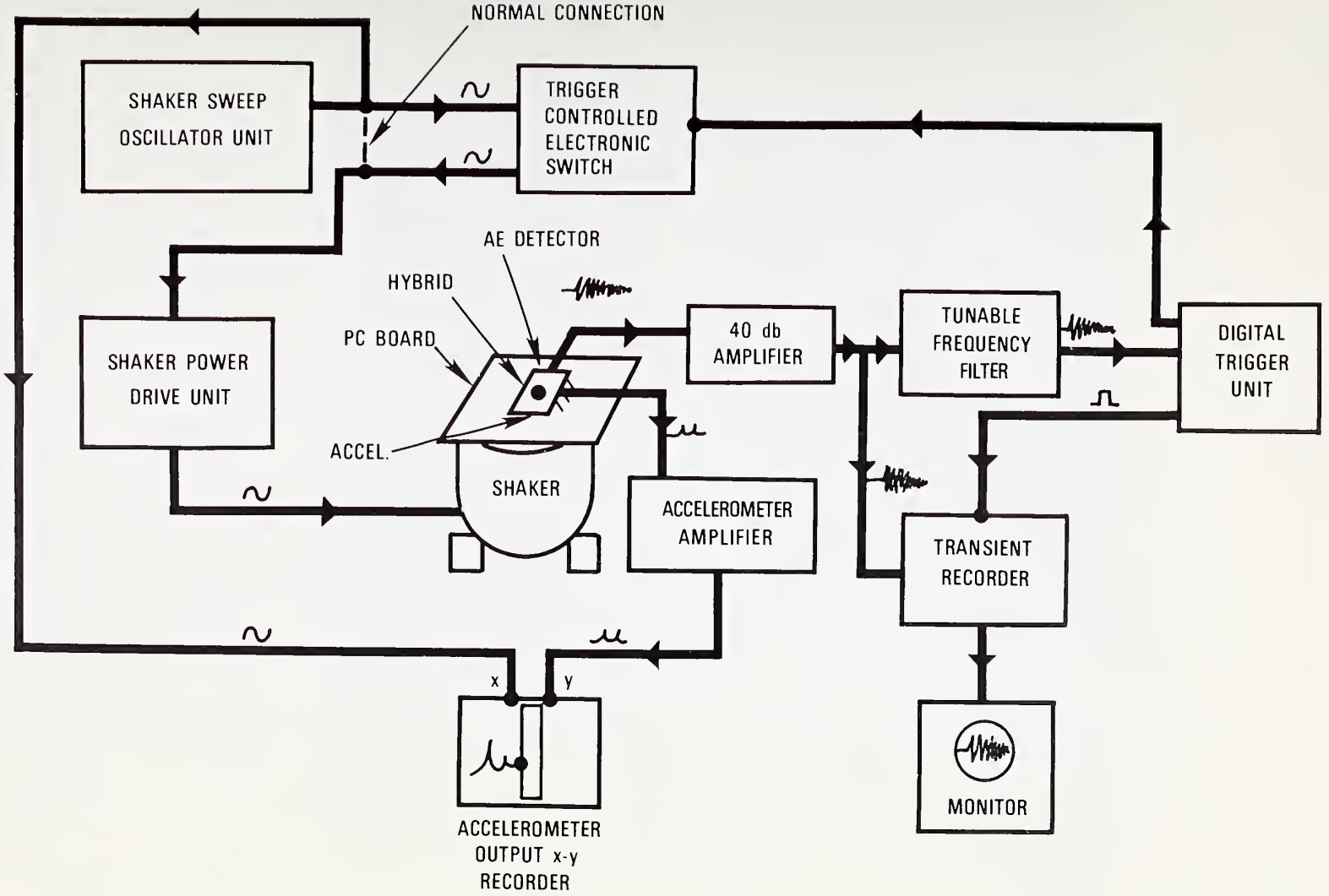

Figure 19. Block diagram of equipment setup for AE monitoring and control of the PC-board hybrid seal experiment.

acceleration that the package was undergoing. The AE burst was later photographed from the oscilloscope monitor and a complete record of the experiment was obtained.

The vibration equipment was described earlier and shown in figure 5, and figure 9 was a closeup of a PC board in the "fixed" vibration mount. Three flatpack hybrids were shown soldered on the printed circuit board. Figure 20 shows a comparable situation in which three plug-in-type packages are mounted on a printed circuit board. The acoustic-emission detector is attached to the hybrid on the left. The accelerometer is attached to an empty hybrid package in the center. An additional hybrid is on the right of the board. A closeup of the TO-100 detector mounted in a hybrid is given in figure 21. The general acceleration *versus* frequency data for this board configuration were given in figure 12.

New (unvibrated) flatpack-type hybrids were soldered into patterned printed circuit boards in order to assess seal damage in real time. Some of these hybrids had intentionally damaged glass seals that would have failed a visual inspection, although they passed leak tests at both low and high temperatures. Other hybrids that had almost perfect glass metal seals, both visually and in leak tests, were also mounted in order to assess correlation between initial visual characteristics and any hermetic damage resulting from the vibration.

Preliminary work (sec. A-1.7) had shown that high-quality plug-in-type packages that were soldered into PC boards remained undamaged (either by lead fatigue or hermetic leaks) when vibrated at high accelerations. Therefore, it was decided that all acoustic-emission experiments would be carried out on flatpack-type packages that were more subject to damage by vibration. The packages were split into two groups. In one group, there was essentially no glass cracking visually evident. The other had a significant amount of glass damage intentionally induced by moving the leads back and forth until large pieces of glass had cracked from the outside of the seal area. The packages were verified as being hermetic before soldering onto PC boards. Vibration tests were run separately for each package so that none would undergo acceleration when it was not being monitored by AE detectors.

Figure 22 is a composite of the x-y recorder curve tracing showing the acceleration experienced by an initially good package (no glass cracks by visual inspection) as it was scanned through its frequency spectrum until a glass crack occurred. The photographic insert shows the acoustic-emission burst that occurred at the peak acceleration. The acoustic-emission trigger removed the shaker drive, and the acoustic-emission burst was simultaneously recorded by the transient recorder (see fig. 19). After this first glass cracking occurred in the essentially perfect package, further runs produced AE bursts at lower accelerations, in the order of 1/3 to 1/2 that of the first run. Equivalent tests were also made with intentionally damaged packages. In no case during these experiments did the acceleration ever reach levels higher than 40 to 50 g before acoustic-emission bursts occurred. After the AE tests, all of the packages were tested on a helium leak tester, and even though glass cracking had occurred, there were no hermetic leakers.

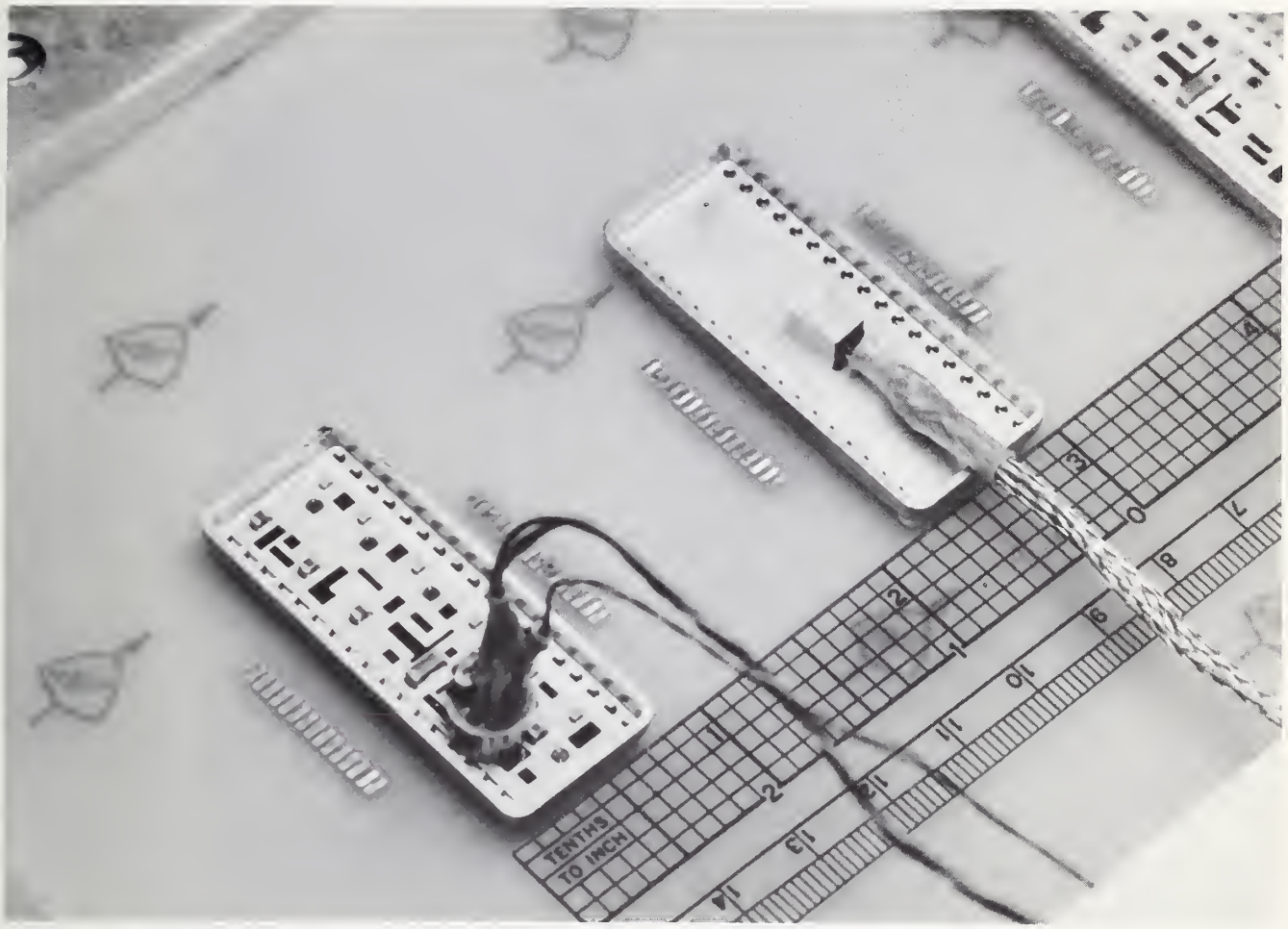

Figure 20. A printed circuit board with three plug-in-type hybrids soldered to it. The hybrid at the left has a TO-100 AE detector on it, and the center package has a small accelerometer on it. The board is in the "fixed" mount which is attached to the vibration shaker.

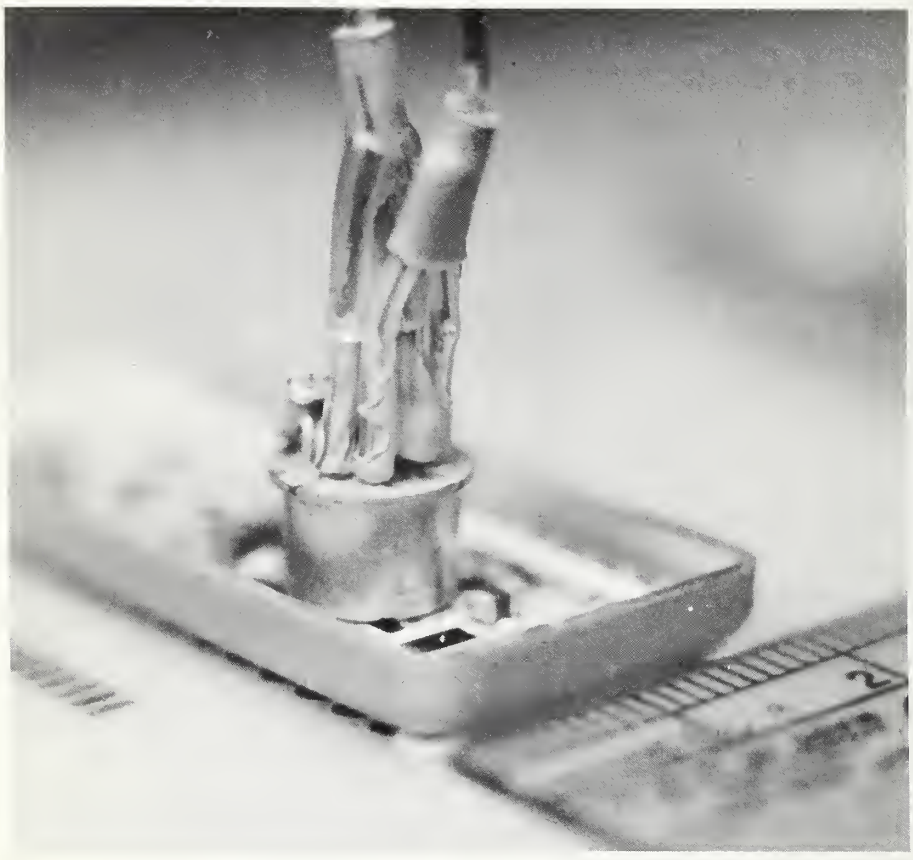

Figure 21. An enlargement of the leftmost hybrid in figure 20 showing more details of the TO-100 AE detector.

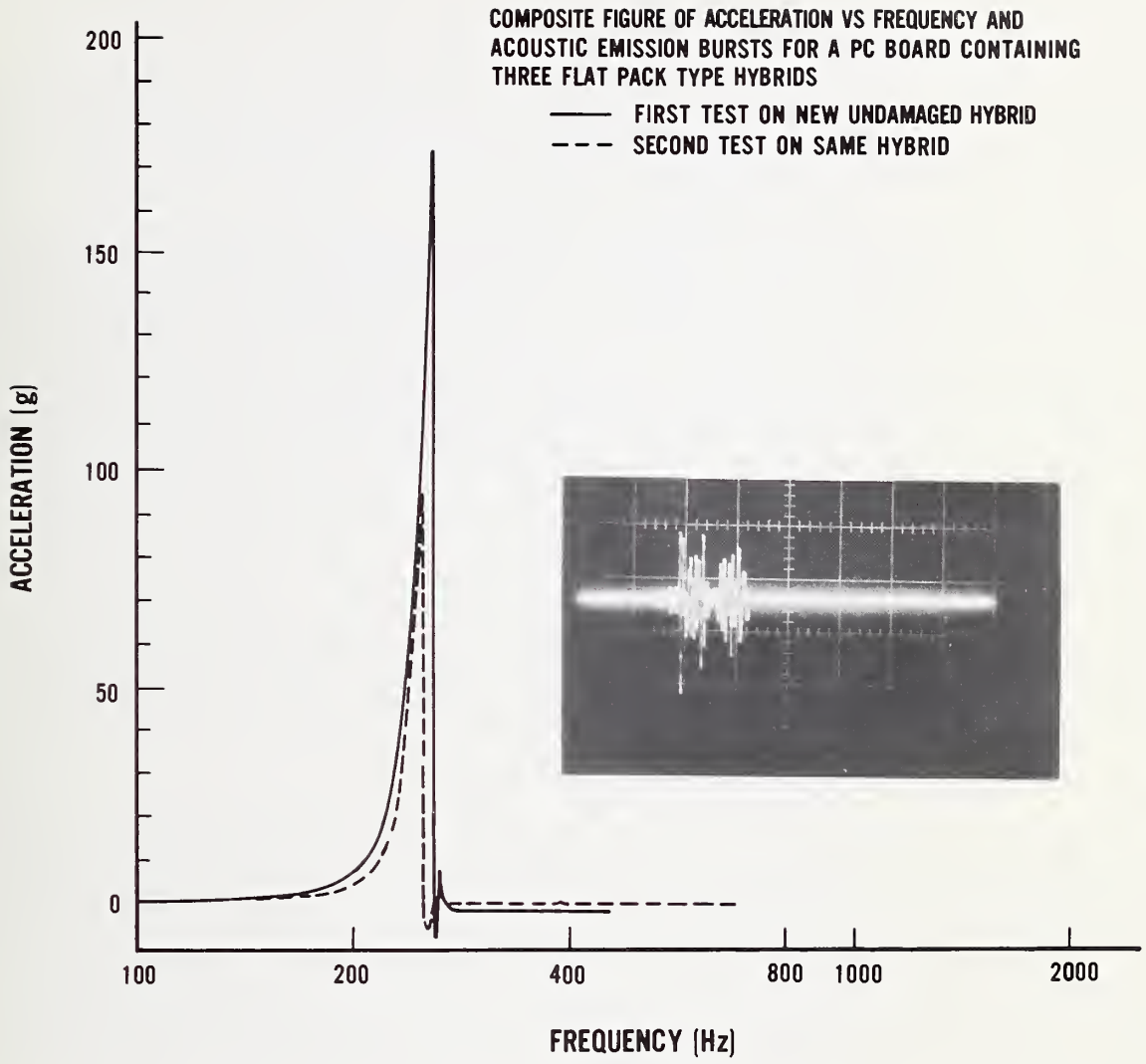

Figure 22. Composite of the acceleration experienced by a flatpack hybrid and the acoustic-emission burst emitted at the peak acceleration of the solid curve. The instrumentation turned off the vibration shaker drive when the burst was received, so the acceleration dropped to zero at that time.

In the above test using high-quality packages, it was found that glass cracking could occur under acceleration-type stresses. However, the objective of this study was to determine whether acceleration was capable of damaging the hermetic seals on PC-board-mounted hybrids. The normal way to determine whether such damage actually caused the seals to leak was to perform a helium-leak test. Such leak tests were run on all packages before and after vibration tests. Although some fatigue-damaged seals were observed to degrade slightly at 125°C after 25 thermal cycles from -55°C to 125°C, they would have still passed MIL-STD-883 hermeticity tests [36] for that size package. The above packages all came from lots that were considered excellent, and some selected packages from these lots had been shock tested from 350°C to liquid nitrogen temperature without loss of hermeticity.

The question still remained whether packages from reject lots that were screened as acceptable could undergo vibration and still maintain hermeticity. Lots rejected because of serious hermeticity problems are hard to obtain since the customer usually returns them to the manufacturer. However, samples from one such lot* called out in a GIDEP Alert (F3-A-80-01A) [38] were obtained and rescreened for leaks. Two of these packages from the lot were found to be hermetic. These were mounted on a PC board and vibrated for 1 h at 70 to 80 g. Some fatigue damage was observed and one or two leads fell off, but neither the lead damage nor visually evident glass seal cracking was in any way as severe as was observed on some of the high-quality packages described above. One of the two packages from the reject lot that were initially tested and found to be hermetic became a "gross" leaker after vibration. The sample size was small, but considering that no high-quality package became a leaker during vibration tests, it must be concluded that screened "good" packages from an otherwise "bad" lot appear to be more susceptible to vibration damage than do packages from initially "good" lots.

A-3.2 Conclusions of the Vibration Experiments

Hybrid packages that were soldered into PC boards were vibrated over a range of frequencies and accelerations. High-quality plug-in-type packages are essentially immune from vibration damage and appear to act as board stiffeners. Several of these packages sustained 450 g at 250 Hz for 30 min with no lead fatigue and no glass cracks or hermetic-seal damage. Normal conductors on PC boards would begin to fail at these accelerations. Therefore, high-quality plug-in-type packages soldered directly into plated-through holes in PC boards should be used where practical in equipment that may be subject to vibration.

The leads on flatpack-type packages are subject to vibration fatigue damage. The possibility of damage increases as lead lengths increase. However, the process of bending leads close to the glass seal may itself produce meniscus cracks. Care should be taken to design lead-bending jigs carefully in order to minimize this problem. If long leads are required, they should be protected by epoxy-bonding the cases to the board or by using appropriate board snubbers to dampen vibration.

---

* These flatpack samples were obtained from J. R. Beall, Martin Marietta Corporation, Denver, Colorado.

During flatpack vibration experiments, glass cracking (meniscus and other) starts at about 100 g for good packages and as low as 20 g on good packages with intentionally damaged glass seals, as revealed by real-time acoustic-emission measurements. When tests were run on good packages, there were no cases where the glass damage penetrated through the depth of the seal and caused hermetic leaks, even when leads were fatigued off rapidly and violently at 200- to 300-g levels.

Hermetic damage resulting from vibration was observed on one package out of two from a reject lot that had passed a hermetic test screen. This suggests that screening and then using the "passed" packages from a lot that had a high percentage of failures (a "bad lot") may lead to reliability problems.

No lead fatigue or glass-seal damage has been observed on high-quality PC-board-mounted flatpack-type packages from either resonant or nonresonant vibration at 10- to 15-g levels for extended periods (approximately 20 h).

A major conclusion of this work is that no correlation has been observed between visually obvious glass-seal damage in hybrid packages and hermetic leaks, as measured by a helium-leak detector, at room temperature and at 125°C.

PART B NONDESTRUCTIVE STRESS TESTS FOR HYBRID PACKAGE INTEGRITY

B-1 Leak Test Measurements and Procedures*

B-1.1 Development of a High-Temperature Open-Package Leak Test Procedure

It has been reported by Thomas [39] that some packages may leak at high temperatures or during rapidly changing temperatures, such as encountered in temperature-cycling tests, but are hermetic during normal room temperature leak tests. There are two reasons for this. The first is that the kovar-glass seal is in tension above ~125°C, but in compression at room temperature [40]. Thus, if there are defects in the seals, they may open at high temperature and result in temporary leaks, and then reseal at lower temperatures where leak tests are usually made. The second reason is that, during rapid temperature rise, nonequilibrium thermal conditions exist with the glass temperature lagging that of the better conducting kovar, putting any weak areas of the seal in significant tension, thus causing defects in the seal. Therefore, in order to fully evaluate seal damage and correlate this with acoustic-emission bursts, it was necessary to develop a high-temperature open-package leak test.

The normal open-package leak test, using neoprene rubber and a standard vacuum grease, is not useful at 125°C because the rubber can outgas and in addition becomes highly permeable to helium. The grease becomes mobile and moves out from under the package edges.

The first efforts to develop a high-temperature leak test were directed towards finding published data on the permeation of helium through various elastomers and greases at temperatures greater than 100°C. No such information was found. The next step was to obtain several different greases and very thin sections of different elastomers and greases, then leak testing known good packages and dummies at various temperatures, choosing the best combination. The present system uses thin Viton A elastomer and Fomblin grease. This combination is adequate for leak testing open hybrid packages to 10^{-7} atm•cm^3/s up to about 125°C. In addition, a temperature-controlled package heater was designed and constructed and is shown in figure 23.

Although a number of packages have been successfully tested by this method, new procedures and materials should be investigated in order to make utilization of the test more rapid and practical for monitoring large numbers of samples.

B-1.2 Preconditioning Procedure for Hybrid Packages Before Hermetic Testing

When leak testing, it is essential that packages be carefully prepared in order to remove any contaminants that can plug or otherwise clog possible leakage paths.

Two major interferences in the leakage testing of packages and package components are surface sorption and clogging. All device configurations consisting of glass, metal, and ceramic, or combinations thereof, including coatings

* The work in this section was done by Stanley Ruthberg.

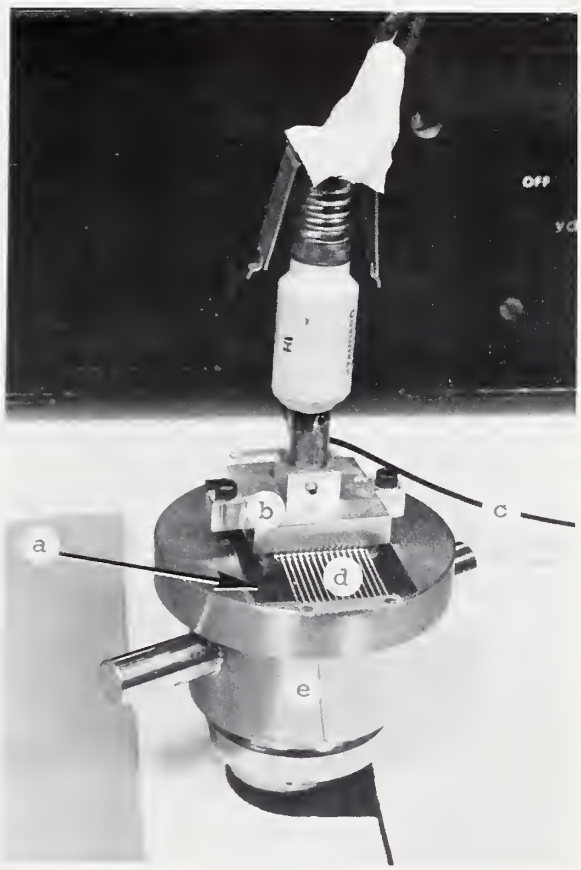

Figure 23. The high-temperature open package leak test apparatus. (a) Fluorocarbon elastomer gasket. (b) Platen used to conduct heat uniformly to the package. A thermocouple controls the temperature on the platen. (c) Heater element. (d) Hybrid package. (e) Leak detector port.

and external sealants, are subject to the adherence of tracer gases by adsorption on the surface and/or by absorption into the material. This effect can cause a high background indication which leads to reduced test sensitivity or in many instances can be great enough to cause spurious rejection as a leaking component. Fingerprint oils and other contaminants introduced by careless handling will cause the same effect. Thus, preliminary measurements should be made on representative specimens, and the dwell time between the pressurization of sealed packages and detection of helium or other tracer gasses should be lengthened until desorption has reduced the signal relative to the test reject level. A gas flush of the package with nitrogen or clean, dry air can accelerate desorption in some cases.

Very small holes that may give rise to appreciable leakage rates can be blocked by small solid particles or by condensed liquids. Test results may be negative; yet, such channels can reopen at a later time because the particles become dislodged or the liquid evaporated. Until leak tests have been made, the components should be kept out of contact with ambient or other vapors as well as particulates that could cause blockage. Test samples should not be held with bare hands!

In general, the retention of a condensed liquid within a microchannel is governed by surface tension. The differential pressure required to dislodge the liquid is equal to $2\sigma/r$, where σ is the surface tension and r is the channel radius. In the case of an air-water interface, σ is ~73 dyne/cm at 20°C and ~59 at 100°C, while the vapor pressure ranges from ~17 Torr at 20°C to one atm at 100°C. As an example, a meniscus in a channel of 1-μm radius requires ~1.4 atm pressure differential to dislodge the water at 20°C and ~1.1 atm pressure differential at 100°C. A channel of this radius and 1-μm length would give rise to a standard leak rate of $\sim 2 \times 10^{-6}$ atm•cm^3/s. Obviously, the 1-atm pressure differential normally encountered in a helium leak test of hybrid packages* is insufficient to dislodge the water in this instance. At 100°C, the 1-atm vapor pressure of water produces zero pressure differential within the channel when the component is in normal ambient, and the water could only be dissipated by the liquid diffusing out of the channel. This diffusion would occur at a rate approximately two orders of magnitude less than air would pass through this same leak size, considering the pressure increase inside the package due to gas expansion (~0.2 atm). However, were the component also placed in vacuum, the water would be eliminated at a rate faster than the standard leak rate since the internal pressure would add to the vacuum giving ~1.2 atm of driving force. In actuality, leaks are not uniform channels, but rather they are cracks and torturous passages much longer than in the example and require greater forces to dislodge any liquid.

Where surface contamination is suspected or where exposure to vapors and liquids has occurred, a preliminary solvent wash followed by a vacuum bake (filtered house vacuum is adequate) of two or more hours at 100°C or greater is necessary for both open or sealed package leak tests. Solvents should have relatively low surface tension and high vapor pressure. For example,

* MIL-STD-883 Method 1014.2 [36] specifies 30 ± 2 psig helium bombing for 4 h for most hybrid package sizes. The package is normally sealed at 1 atm (14.7 psig); thus the test is conducted at a 1-atm differential.

Freon TF has about 1/4 the surface tension of water at 20°C and ~4 atm of vapor pressure at 100°C. These characteristics provide a more appropriate driving force and dissipation rate under vacuum bake. Even with all of the above precautions, it is best that components be kept clean and that fine leak testing be carried out before any liquid contact. However, a bake at 150°C at normal atmospheric pressure or at 100°C in a vacuum is a satisfactory preparation for leak testing in order to remove water or fluorocarbon plugging.

B-2 Development of an AE-Monitored Thermal Shock Test for Open Hybrid Packages

B-2.1 Introduction

The published thermal expansion curves of kovar-glass seals [40] indicate that the outside perimeter of a hybrid package seal is in tension at ~150°C in the radial direction and either in compression or unstrained at room temperature. The center lead interface would be in compression at 150°C and in tension below room temperature.

The actual stresses in hybrid flatpack seals have never been characterized. The nearest configuration studied is the cylindrical seal [41]. The circular hole and rectangular lead configuration of the hybrid seals produces unknown stresses during temperature cycling and shock tests. Although such stresses could be calculated by finite element analysis, this has not been done. In addition, classical curves comparing the expansion coefficients of kovar (iron-nickel-cobalt alloy) and typical sealing glasses represent average rather than specific lot characteristics. Manufacturers' specifications for sealing glass permit expansion coefficient variations of $\pm 1.5 \times 10^{-7}$ m/m°C (from an average value of 5×10^{-6} m/m°C), and for kovar the ASTM specification (ASTM F 15-78) [42] allows $\pm 3 \times 10^{-7}$ m/m°C variations in the 30 to 400°C range (from an average value of 4.9×10^{-6} m/m°C). Worst case matching between the glass and metal can produce strained seals that may not tolerate temperature shock. Hybrid package manufacturers seldom ascertain the exact expansion coefficients of their raw materials, and thus, even if the kovar oxidation process is correctly controlled, a certain amount of luck is necessary in order to produce reliable seals. Furthermore, fillers and hardening additives are often mixed with the glass, and although these are generally considered to be benign, they have an unknown effect on the expansion coefficient as well as the "wetting" of the kovar oxide. To assure reliable glass-metal seals, it is essential that package manufacturers evaluate the residual strain of their specific kovar-glass combination. Methods such as that of ASTM Standard F 14-76 [42] offer simple, inexpensive means of obtaining such evaluation. It is fortunate, and perhaps essential to hybrid reliability, that the dimensions of the package seals are small, limiting the seal area and therefore the possibility of flaws.*

Considering the above facts, it is apparent that all hybrid package production lots should be screened by a sensitive, reliable test that will reveal reveal weak glass metal seals. McCormick and Zakraysek [43] described the effect of kovar oxide thickness on the reliability of glass-metal seals used

* Contributed by H. E. Hagy, Corning Glass Works, Corning, New York.

in hybrid packages. They concluded that a shock test (MIL-STD-883 Method 1011.2, Condition C) [36] was an adequate test for hybrid packages. However, inquiry revealed that many manufacturers routinely use only a hot plate shock test unless the MIL-STD-883 test is specifically called. Briefly, the hot plate test is performed as follows: a kovar flatpack containing glass-to-metal seals is placed (face up) on a hot plate that is heated to a temperature in the range of 350°C to 400°C. The package temperature is allowed to reach equilibrium. Following removal and cooling, the glass seals are examined and leak tested for damage. Because of the frequent use of the shock test as a screen, it would be desirable to instrument this test with AE-detection equipment to obtain rapid information on the seal integrity that may not be revealed in a visual inspection or even in a room temperature leak test. Such an AE-monitored test could save the time required for a leak test and may give other information related to reliability of the package.

B-2.2 Characterization of the Hot Stage Shock Test

An acoustic-emission-monitored hot plate shock test would require that the packages be put on the hot plate in a face-down configuration with the AE detector on top (attached to the normal bottom of the package). This face-down configuration is thermally different from the usual face-up hot plate test, so it was necessary to measure the thermal characteristics carefully for both situations. During these measurements, it became evident that this frequently used test is not well characterized and under various conditions could pass marginal packages because the temperature rise can be too slow to stress the package seals adequately.

The experimental apparatus consisted of a temperature-controlled hot stage with the package placed on it face-down (as shown later in fig. 25 but with the AE detector removed). The package temperature was monitored with a separate thermocouple. For this purpose, 0.003-in. diameter thermocouple wires were welded to the inside wall of a hybrid package adjacent to and at the same level as the lead-throughs. In order to be sure the actual wall temperature was monitored, the thermocouple was split and each wire separately welded, approximately 0.01 in. apart, to the package wall. Data were taken at five-second intervals using a digital read-out thermometer. Data from the first few runs showed poor reproducibility, so the hot plate surface was flattened and smoothed with a fine file. The package bottom was also lightly polished. Figure 24, curve (a), gives the average temperature-time curve of a package, open face up (the normal configuration), on the 400°C hot stage for a gold-plated package of 1.25 by 1.25 by 0.3 in. dimensions. Each point is the average of three runs. For comparison, curve (c) was taken under conditions identical to (a) except that two short pieces of 0.003-in. diameter alumel thermocouple wire were placed on the hot stage under one edge of the package. The wire was invisible except when viewed in oblique light. Curve (d) was taken similar to (c) except that a 0.05-in. long by 0.015- by 0.010-in. piece of kovar from a package lead was placed underneath and near one end of the package. The 0.015-in. dimension was parallel to the hot stage surface. From examination of the curves, it is apparent that the initial temperature rise at the glass seal can vary considerably, and much care should be exercised in carrying out the test. Factors leading to varying temperature rise at the seals are: package design (i.e., height of seals above bottom surface and size of package), surface plating material and its

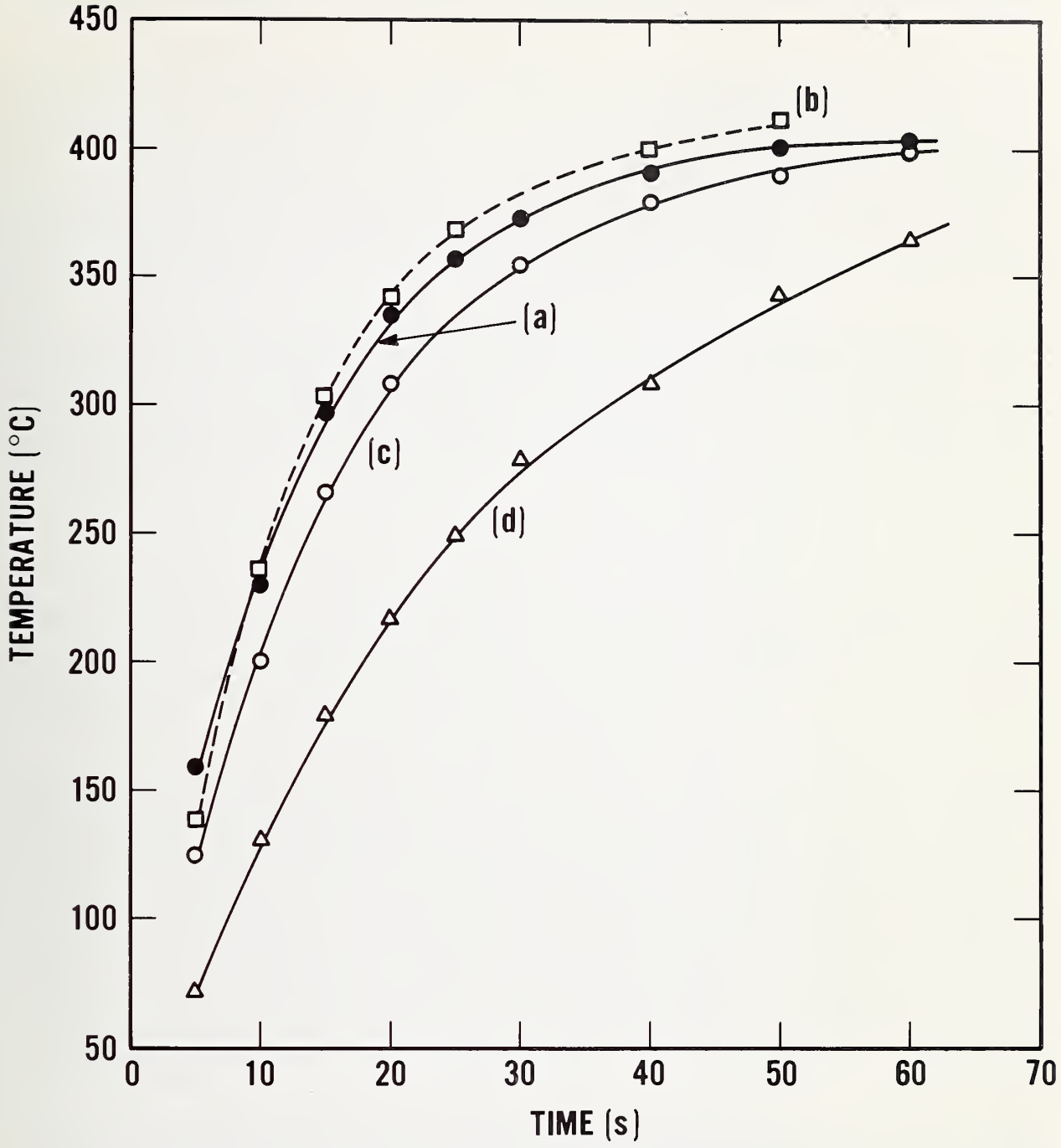

Figure 24. Temperature-rise curves for a hybrid package on the hot stage of figure 25. (a) Package face up, hot stage at 400°C (normal practice). (b) Package face down, hot stage at 425°C. (c) Section of 0.003-in. wire under face-up package (400°C). (d) Section of package lead under face-up package (400°C).

reflectivity, particles or other contaminants or irregularities on the surface of the hot stage, and possible ambient air motion (drafts) across its surface.

After characterizing the normal hot stage thermal shock test, it was necessary to obtain equivalent data on the package face-down with convection-radiation shields and a cooled detector on the bottom. After several runs, it was determined that the equivalent rate of temperature rise in the initial 20°C to 200°C range* was obtained with the stage temperature increased ~25°C to 425°C, as shown in figure 24, curve (b). However, because this temperature exceeds that normally employed, a maximum temperature of 400°C was set for further tests. This corresponds to a face-up shock temperature of about 375°C which is still in the range normally used.

Only a single hot stage and two types of packages have been characterized in these tests. Different organizations may use quite different hot stages, ranging from small substrate heaters to large hot plates, as well as a large variety of package types. Therefore, each particular setup should be characterized, and the surface of the stage smoothed and kept clean in order to obtain consistent results.

B-2.3 Acoustic-Emission-Monitored Shock Test

Most commercial hot plates generate AE during operation. For purposes of acoustic-emission-monitored tests, a "quiet" hot plate is required. It was found that units heated by insert "slug" type elements meet this requirement, whereas ones with wrapped coils, as are typical in commercial hot plates, are extremely noisy. One of the former designs was available from a heated stage of a bonding machine and therefore all AE-monitored shock tests described below used this type of hot stage.

The high temperatures of the hot stage required for this test presented dual problems for AE detectors. Rapid heating of these detectors can produce extraneous AE-like noise, and the most sensitive detectors have Curie point restrictions and/or mount constructional materials (i.e., epoxy) that can be damaged by the high temperatures. The first experiments to protect the detector used a stand-off acoustical waveguide made of Pyrex attached to an AE detector, the unattached end being acoustically coupled to the hot package with an indium-gallium liquid alloy. The detection efficiency of this method was very low because this waveguide extension had a low aperture for surface waves, and in addition the indium-gallium attacked gold plating on the package.

Next, a small water-cooled detector mount was designed and constructed. This adequately stabilized the detector temperature when the package was turned face down and a small sheet of insulation material, such as silica fiberglass, or woven ceramic, was interposed as a radiation-convection barrier between the hot plate and the bottom of the package (lying within the package cavity). A photograph of the cooled detector mount, hybrid package,

* This is the temperature range that produces maximum stress on the perimeter of glass-metal seals in the hybrid configuration [40].

and hot stage is shown in figure 25. This particular mount used a commercial AE detector. However, a similar mount was made for the TO-100 detectors.

Additional tests were made with a small thermocouple spot welded on the inside bottom of the package, directly under the detector. With the package side walls in equilibrium (>1 min on a 400°C hot stage), the detector temperature cycled (in synchronization with the hot stage cycling) from 50°C to 54°C. With higher water flow through the cooler, the detector cycled between 43°C and 45°C. Either temperature range is satisfactory and does not lead to spurious thermally induced signals. The water flow must be kept below the turbulent range since turbulence generates large AE signals which can mask the test results.

After temperature characteristics of the hot stage test and the cooling mount of the AE detector were determined, an acoustic-emission-monitored study of the thermal shock characteristics of various packages was carried out. A block diagram of the general AE equipment used in section B of this report is given in figure 26. Some tests may only use selected parts of the equipment. AE output during the shock tests was anticipated to extend over a period of up to 30 s, based upon the temperature-rise characteristics given in figure 24. Therefore, the apparatus capable of triggering on a single glass crack was not necessary. Instead, just the detector in its water-cooled mount, the totalizing system, and the printer portion of figure 26 was employed. Each AE cycle or pulse above a set threshold was recorded and the summation of these were printed each second. The plotted AE could then be compared with the temperature rise *versus* time curves (fig. 24) to determine the average temperature of the seal using the hot stage and AE detector apparatus of figure 25.

Initially, a control package was fabricated from stainless steel. However, because of residual machining strains as well as the high thermal expansion coefficient (compared to kovar), this package was noisy and emitted frequent AE bursts even after repeated tests on the 400°C hot stage. Similar tests on high-quality hybrid packages showed that they emitted essentially no AE during hot plate shock, so data from one of these were used as a control to define a good package. The accumulated acoustic-emission counts* *versus* time on the hot stage for the control sample are plotted as curve (a) in figure 27. The small, essentially linear increase in signal with time is due solely to the AE system noise above the set threshold and is not due to glass seal degradation. This package and others were tested for leaks at room temperature and at 125°C. The control sample leak rate was $<10^{-7}$ atm•cm^3/s at both temperatures.

Most of the 42 packages tested in this manner produced AE *versus* time curves similar to that of curve (a) of figure 27. However, a small lot of four packages from one manufacturer that had been thought to be of high quality showed large increases in AE when shock tested. Plots of the data from three of these are given as curve (b) in figure 27 and curves (a) and (b) in figure 28. These figures show a dramatic increase in AE when compared to the con-

* AE counts as used here are the number of cycles of signal having amplitudes above a set threshold. The threshold is usually set to minimize the noise.

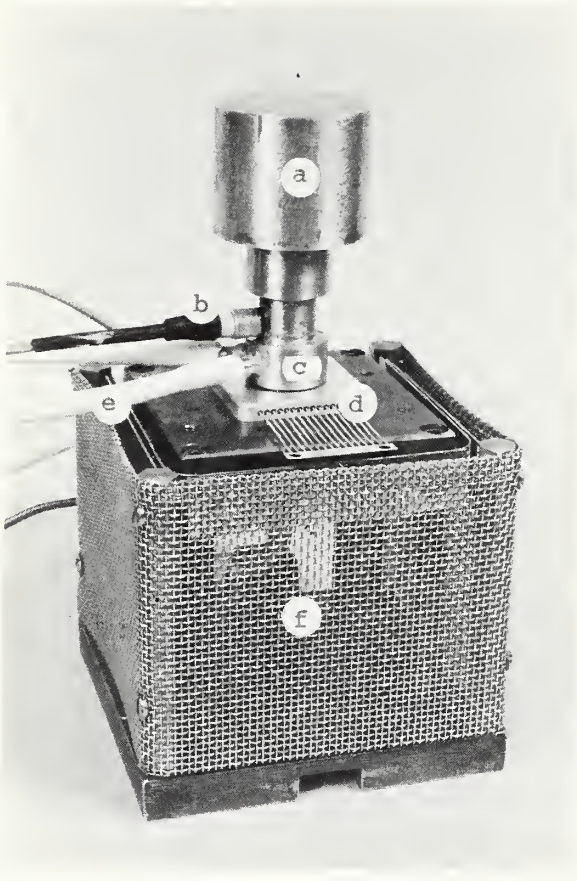

Figure 25. Thermal shock hot stage with a 1- by 1-in. hybrid package and a water-cooled AE detector on top. (a) Brass weight to hold the spring-loaded detector against the package. (b) Part of the lead and connector from the AE detector. (c) Water-cooling jacket around the AE detector. (d) Hybrid package shown face down on the hot stage. (e) Silicone rubber coolant tubing. (f) Hot stage surrounded by a protective screen.

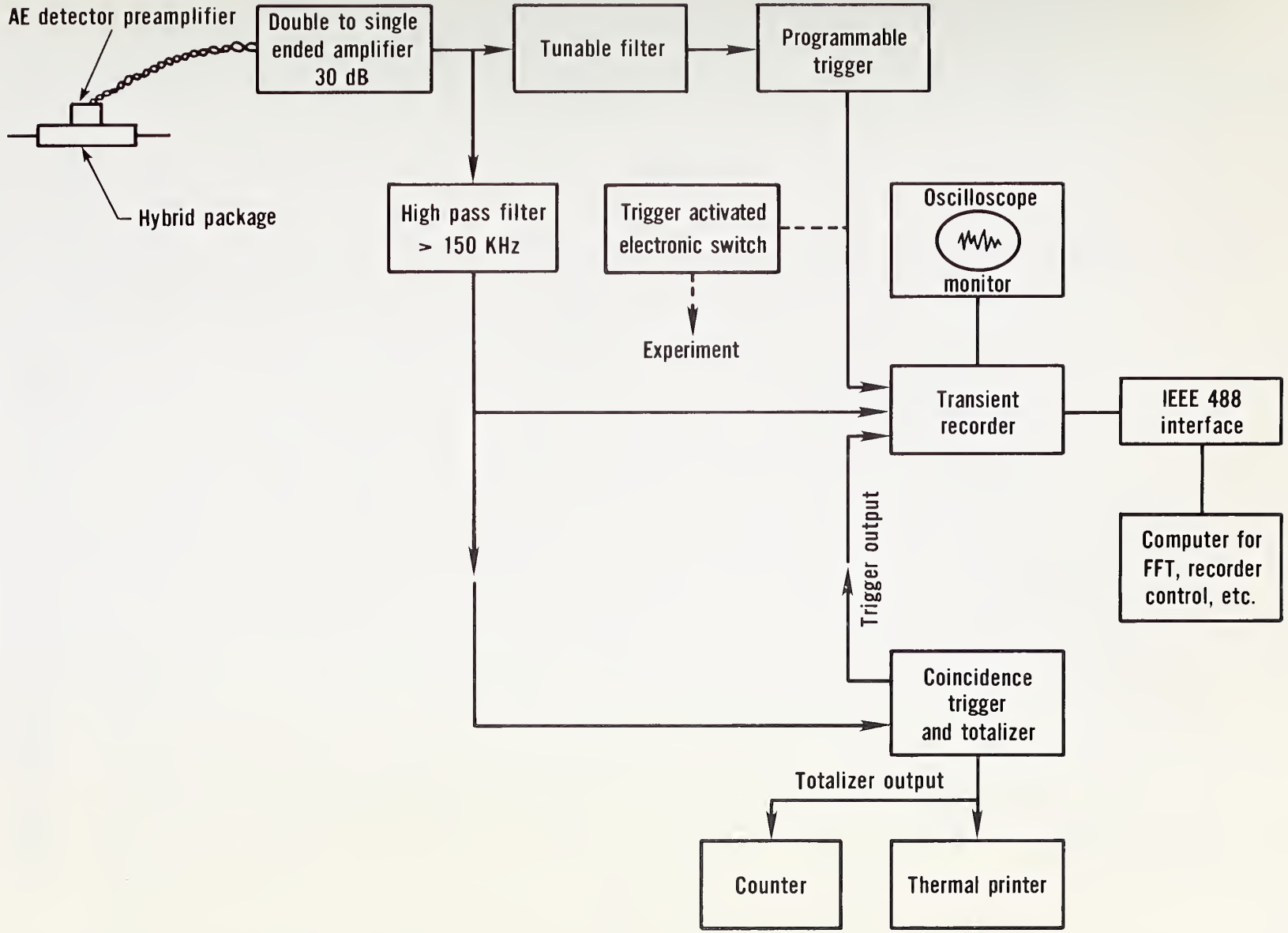

Figure 26. Block diagram of general circuitry used for acoustic-emission tests and data analysis. Various selected portions of the apparatus may be used for specific experiments.

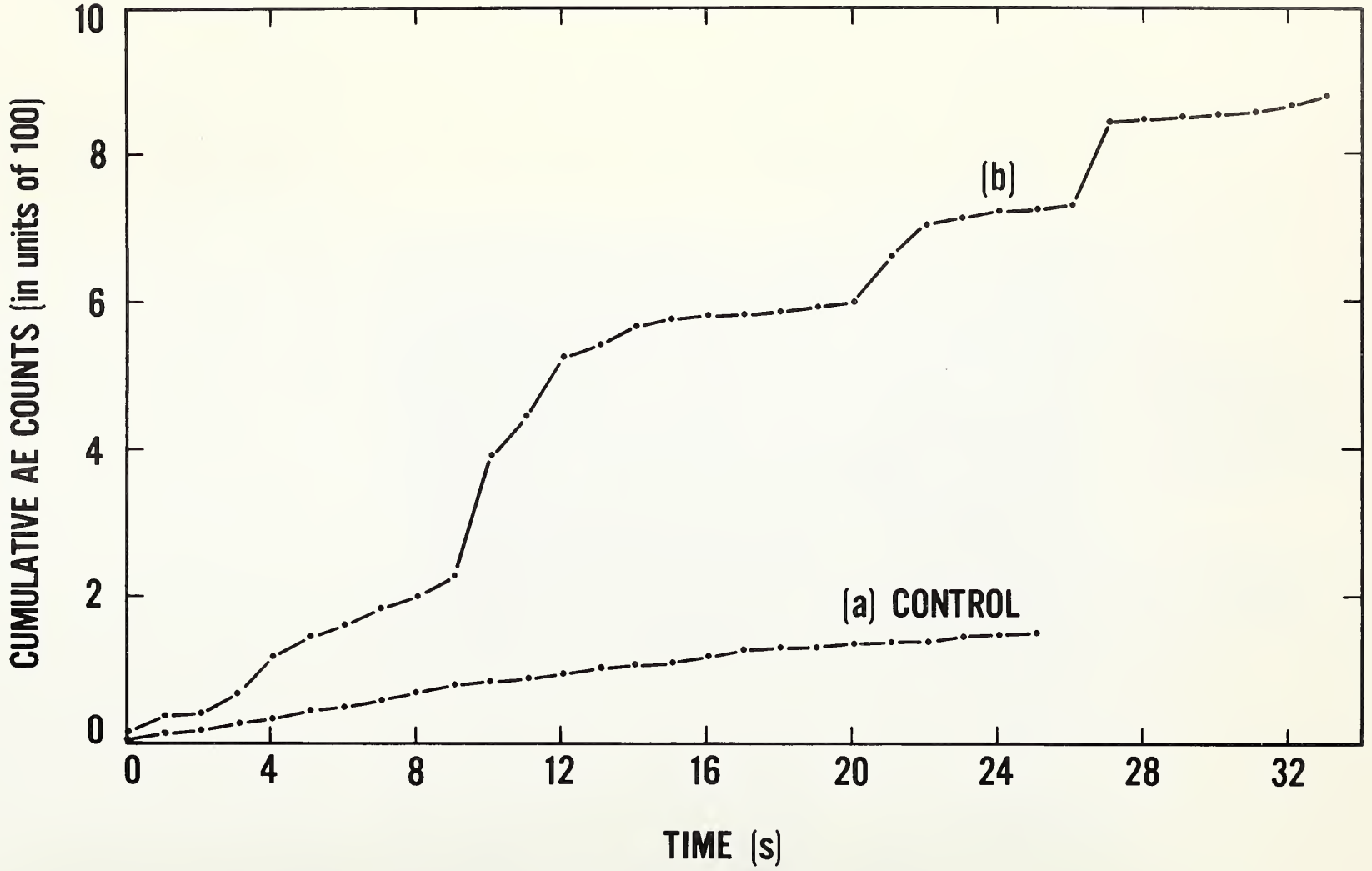

Figure 27. Cumulative acoustic-emission counts *versus* time for the AE-monitored hot stage shock test. (a) Data from a good control package. The curve represents cumulative noise counts (typical 6 to 8 per second). (b) Data from testing a package with weak seals.

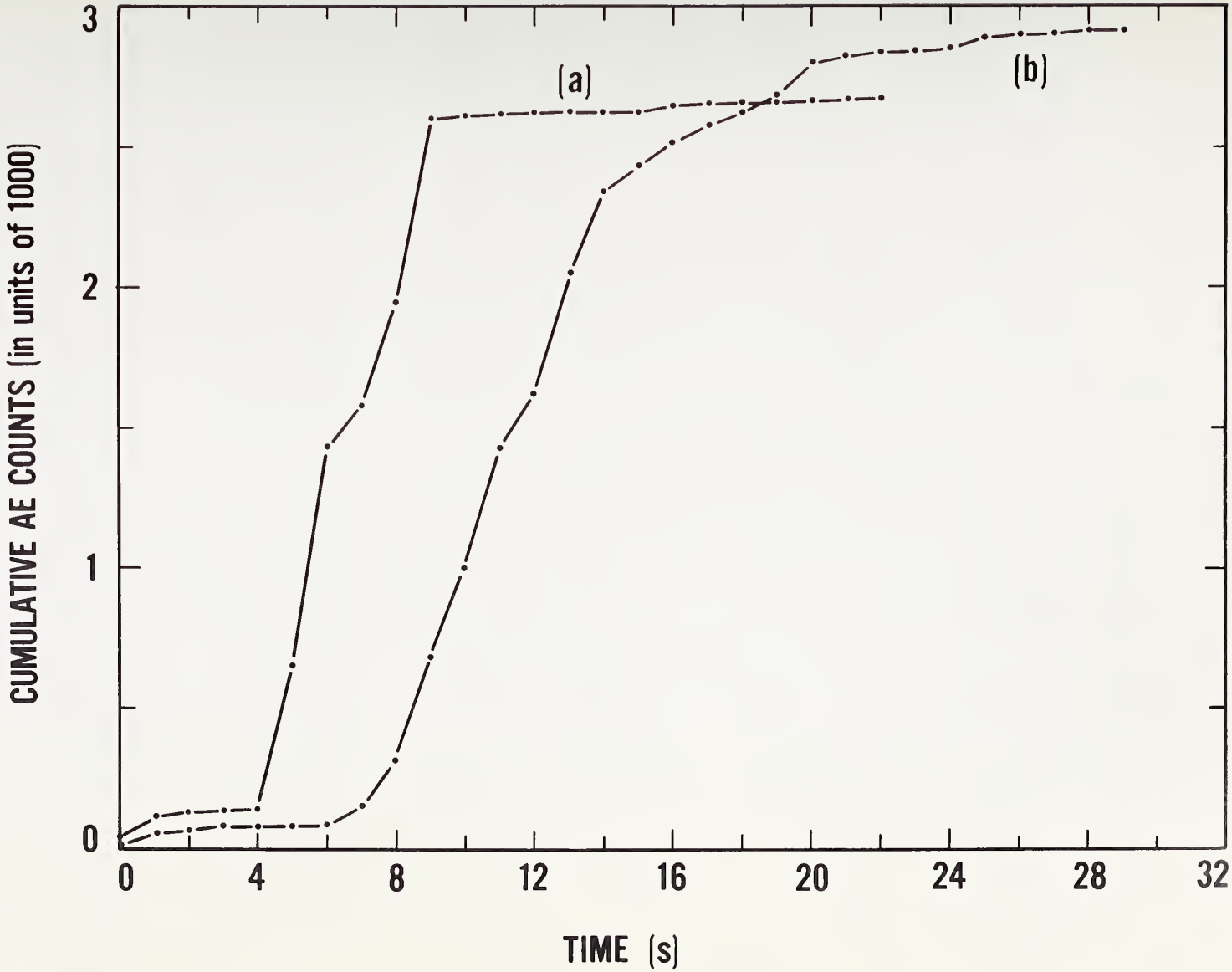

Figure 28. Cumulative acoustic-emission counts *versus* time for the AE-monitored hot stage shock test. (a) and (b) Typical data from testing packages with weak seals.

trol sample data of curve (a) in figure 27. The delay of AE for a few seconds after placing the packages on the hot stage was expected, since from the temperature rise curve (fig. 24) it takes several seconds to reach the 125° to 150°C required to place the seals in tension. A retest of the high AE-producing samples resulted in very low AE output, similar to and only slightly greater than that of the control sample. This "one-time-only" phenomenon is known as the Kaiser effect [2] in which little or no AE recurs until previously applied stress levels are exceeded. (Literally, a deformation or crack will only produce more AE if it is enlarged.)

Shock tests were also run on several of the "bad" packages that had been vibration tested in section A. These packages had undergone liquid-to-liquid shock, and many of the glass seals had previously become leakers. Very few of the leaking packages produced large AE signals. However, one of the unvibrated samples from the bad lot that was tested and found to be hermetic did produce large AE in the hot stage shock test similar to that shown in figure 28. The five packages that produced large AE signals were leak tested both at room temperature and at ~120°C. All of them were hermetic ($<10^{-8}$ atm•cm^3/s) at room temperature. However, two of these packages became leakers ($>10^{-6}$ atm•cm^3/s) at ~120°C, and the seals that leaked were identified by carefully spraying helium over the glass beads. There was no visual damage to identify the leaking seals. This temperature, 120°C, is about the minimum at which the forces in the perimeter of kovar glass seals change from compression to tension. The leak testing apparatus in its current configuration (see sec. B-1) cannot go to a higher temperature. However, since the AE test detected measurable seal damage in all five of these packages, it is speculated that the other three packages would also leak if the test temperature could have been raised somewhat higher. Even if the other three remained hermetic, a 40-percent detection rate for marginal packages is adequate to reveal seal problems on a lot basis. The total number of packages tested in this experiment was relatively small. Only 48 packages from three manufacturers involving six production lots were available for this particular study. It is recommended that a larger study, perhaps involving direct manufacturer participation, be undertaken to verify the results of the present work and to develop practical procedures for test implementation.

The AE shock test configuration used for flatpacks cannot be used for testing plug-in-style packages, and no such tests were performed on them in this work. The seals (and leads) in plug-in packages are on the bottom, significantly removed from the side walls that heat rapidly when the package is placed face down on a hot stage. A suggested configuration for AE-monitored shock testing of plug-in packages would incorporate a metal jig on the hot stage that would be similar in shape to a package socket but with larger lead pin holes to allow clearance of the glass beads. The AE detector could be attached to a normal package lid. The lid could be acoustically coupled to the package with a high-temperature vacuum grease, which would be cleaned off later. Because of the fast heat transfer to the glass leads in this configuration, the hot stage temperature might be lowered to perhaps 250°C and still match the 0°C to 150°C temperature rise given in the curves of figure 24.

If large-scale verification of the present results is obtained, AE shock tests can be effectively performed at the package manufacturer's plant on a

lot sample basis to assure delivery of only high-quality lots. The verified Kaiser effect for this test would render results obtained on incoming inspection at a user's facility somewhat less definitive unless the thermal shock history of the packages were known. Without such information, a high-temperature open-package leak test might be adequate, although the AE test could be used for added assurance.

The AE-monitored shock test can be performed more rapidly (about 10 to 15 s) and economically than a liquid-liquid shock test followed by a leak test. The ability of this test method to reveal marginal packages is unique and therefore warrants verification on a large scale. It would also be interesting to correlate AE tests with high temperature die penetrant tests. AE monitoring might also be used with shock tests at lower temperatures (~150°C) for hybrid component epoxy or solder bond integrity as well as to reveal substrate cracks.

B-2.4 The Possible Use of a Thermoelectric Temperature Cycler for Stressing Hybrid Packages in Conjunction with Acoustic-Emission Monitoring

A thermoelectric temperature-cycling system has been used in these studies to stress glass-to-metal seals in hybrid packages repeatedly from -55°C to 125°C. It had been expected that such a system would be acoustically "quiet" and that the packages could be monitored for acoustic emission during rapid cycling to supplement and extend the hot stage shock test. However, it became apparent that the thermoelectric modules themselves emitted large bursts of AE, especially when they were cooling. There were several possible explanations. One was that the polycrystalline bismuth-tellurium alloys, which make up the thermoelectric cooling elements, underwent crystallographic changes such as twinning. Others concerned possible twinning in the solder as well as crack propagation in the numerous interfaces between the solder and the Bi-Te segments or in the Bi-Te material itself. The latter possibilities might be curable by using different assembly procedures and materials. However, if the problem resulted from the Bi-Te material twinning, then thermoelectric temperature cyclers using Bi-Te elements could not be used for stressing packages that were being monitored with acoustic-emission sensors.

Slices from polycrystalline Bi-Te boules, of both n- and p-type, were obtained for test. Three experiments were performed: (1) slow increase in temperature as a hot stage heated up, (2) rapid surface heating by a concentrated infrared source, and (3) pressure. An acoustic-emission detector was coupled to the test samples at all times. Individual AE events were captured with a transient recorder and counts per second were recorded using the apparatus in figure 26.

The Bi-Te boule was placed on a "quiet" heat stage (shown in fig. 25) and further isolated from the stage with a ~1/16-in. thickness of silicone rubber. For the test, the temperature of the boule was increased at a rate of ~5°C per minute. Large acoustic-emission bursts were observed on both heating and cooling. The average number of AE counts recorded was in the range of 200 to 300 per second (the background was 3 to 5 counts per second). Next, the side of the boule was heated with a 500 W focused projector lamp placed 6 in. from the sample. This created a temperature-differential-induced strain near the surface similar to that of a thermoelectric cooling

element under power. Numerous large acoustic-emission bursts were observed within 1 s of turning the lamp on. AE counts of 3000 to 4000 per second were recorded for about 20 to 30 s until the average sample temperature had risen by about 30°C, then the count rate decreased to about 1000 per second. An example of an AE burst occurring during the rapid heating period is given in figure 29a.

Twinning and other crystallographic changes can often be induced by pressure in susceptible materials. Therefore, a simple pressure experiment was run. Force was applied by a "quiet" piece of tapered nylon with a contact surface area of 0.006 cm^2; AE bursts were usually observed to initiate in the 400- to 1000-gf range (64 to 160 kg/cm^2), although there were considerable variations over the surface of the sample and the number of bursts in a given pressure range was not uniform. Figure 29b is an AE burst obtained at 64 kg/cm^2. Bursts were also obtained during force unloading, sometimes at forces as low as 10 kg/cm^2.

In addition to acoustic-emission studies, several thermoelectric modules that had been cycled more than 1000 times and had become inefficient on the cooling cycle were visually examined around their Bi-Te element solder joints. Microcracks were observed in the solder. Also surface reconstruction of the solder was evident, indicating recrystallization had taken place, and finally some cracks in the Bi-Te elements themselves were observed.

All four possible sources of AE in thermoelectric modules have been verified to exist; therefore, it does not appear possible to use thermoelectric temperature-cycling equipment in electronics or other applications that require acoustic-emission monitoring.*

B-3 Determination of the Susceptibility of Kovar Glass Seals to Damage During Wire Bonding

B-3.1 Mechanical Characteristics of Kovar Leads in Hybrid Packages

There are a number of stresses that are applied to hybrid package seals during production that may damage those seals. Two obvious examples are lead forming (bending) and wire bonding to the internal package extension of the leads. This section describes work directed toward determining the levels of stress encountered during wire bonding that may damage the seals and, if found to be destructive, recommending procedural or other changes to retain seal integrity. The approach used was to determine mechanical characteristics by "beam bending" the lead extension inside the package, and any glass-seal cracking would be revealed by an AE sensor coupled to the package.

---

* It should be noted that most of the thermoelectric module degradation processes, such as cracks, are considered to result from the large range of temperature cycling (-55°C to 125°C). Thermoelectric modules are generally used only for cooling below room temperature; thus crack propagation and solder reconstruction would probably not be significant under normal usage. Twinning of the Bi-Te, which would occur during normal cooling, should not degrade the thermoelectric performance.

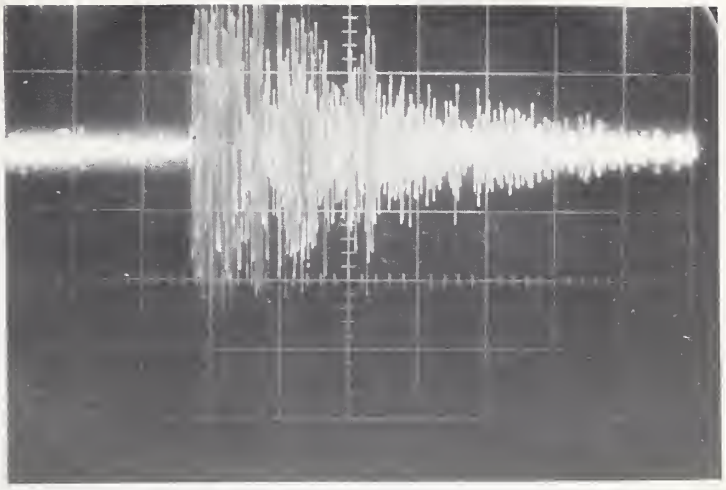

(a)

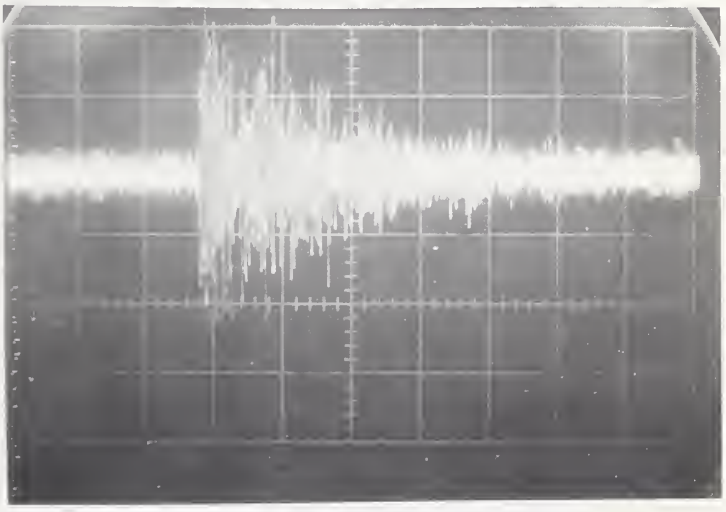

(b)

Figure 29. Acoustic-emission bursts resulting from stressing Bi-Te boules. (a) Burst obtained during rapid heating of a boule. The burst is attributed to twinning. (b) Burst resulting from the application of a force of 64 kg/cm^2 to the surface of a boule. The horizontal scale in (a) and (b) is 200 μs per major division.

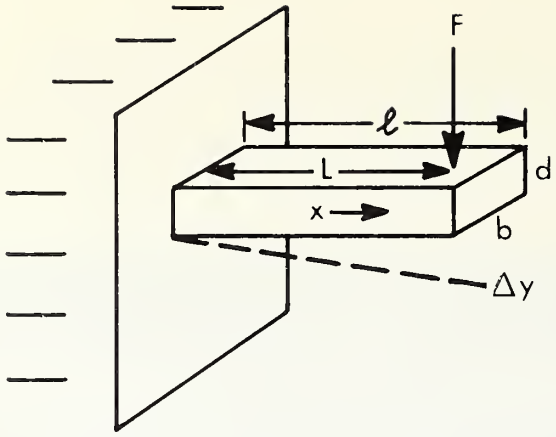

Figure 30. Sketch identifying beam-bending variables.

The simplified cantilever beam equation, in which the entire bending force is applied to one end while the other end is held fixed, is given in eq (3). The variables are identified in figure 30.

$$y = \frac{-F\ell^3}{3\ EI} = \frac{-4\ F\ell^3}{bd^3E}\ , \tag{3}$$

where:

F = applied force, lbs.;
ℓ = the beam length, in.;
I = 1/12 bd^3 = section moment of inertia; and
E = Young's modulus $\approx 19.8 \times 10^6$ psi for kovar [40].

The general equation of deflection at any point, x, along a cantilever beam with the force applied at any point, L [44], is:

$$y = \frac{FX^2}{2b^3\ E}(X - 3L) - \frac{FL^2}{3bd^3E}(x - L)Q \qquad \begin{array}{l}\text{when } x > L,\ Q = 1 \\ \text{when } x \leqslant L,\ Q = 0\end{array} \tag{4}$$

also X = x when $x \leqslant$ L, and X = L when $x >$ L; and
L = point of force application (in. from beam attachment).

It should be stressed that deflection is proportional to the cube of the lead length and inversely proportional to the cube of the lead thickness. Thus, it is important that the package manufacturer control these dimensions to minimize lead bending and any effect it can have on wire bonding, as well as for compliance with lead integrity tests (MIL-STD-883 Method 2004.2) [36].

The ISHM Hybrid Microelectronic Specification for Metal Packages (ISHM M-SP008, 1978) [45] and most manufacturers' catalogs allow a ±0.002-in. variation in lead thickness. This allowed variation can significantly affect bending under a given force as indicated in eqs (3) and (4). Therefore, lead thickness measurements were made on a number of the packages at hand in order to determine the typical range of lead thicknesses actually delivered. These 75 packages were predominantly from two manufacturers and included samples from many lots. The thicknesses measured are given in table 3.

Table 3. Measured Thicknesses of Hybrid Package Leads.

Specified Thickness, in.	0.005 in.		0.01 in.					
Measured Thickness, in.	0.0045	0.005	0.008	0.009	0.0095	0.010	0.0105	0.011
Number of Packages	6	2	1	3	14	38	10	1

In a few cases leads of the same package ranged in thickness from 0.009 to 0.011 in. (within tolerance) and in width from 0.011 to 0.016 in. (uncontrolled). Although the lead thicknesses were all within tolerance, there is an obvious skewing of the distribution towards the thin side where bending is easier. Packages from more manufacturers might show a larger spread.

The depth of lead extension into the package, where wire bonding takes place, is equally critical with lead thickness for bending under a given force. The packages studied showed interior lead lengths of from 0.025 to 0.054 in. Packages can be obtained from manufacturers with various internal lead extensions ranging from 0.025 in. to 0.110 in. $\frac{+0.01}{-0.005}$. Long leads will bend significantly even under the low forces of ultrasonic wedge bonding, presenting nonflat bonding surfaces which could result in relatively unreliable bonds. The bending of long leads would be severe under thermocompression (TC) or thermosonic (TS) bonding forces. If long leads (>0.05 in.) are encountered in a package, wire bonding should take place close to the glass bead rather than near the end of the lead as is the normal practice.

B-3.2 Characteristics of Kovar Leads under Simulated Wire Bonding Stresses

Tests were run to determine the characteristics of leads under thermocompression and thermosonic bonding forces. The apparatus used in these lead-bending experiments is shown in figure 31, with a closeup of the force probe, package, and AE detector shown in figure 32. Measurement of the deflection was made with a 120X binocular microscope having an eyepiece reticle which was calibrated with a precision stage micrometer. The force was applied by a special thin bonding tool and measured by the force gage.

Initial lead-bending tests were run on packages with relatively long leads in order to determine the mechanical characteristics of the kovar more easily. The leads of the packages selected were 0.010 in. thick by 0.014 in. wide and 0.10 in. long. The actual deflection was measured and then calculated using the published kovar modulus in the equation. The results of one such test are given in table 4.

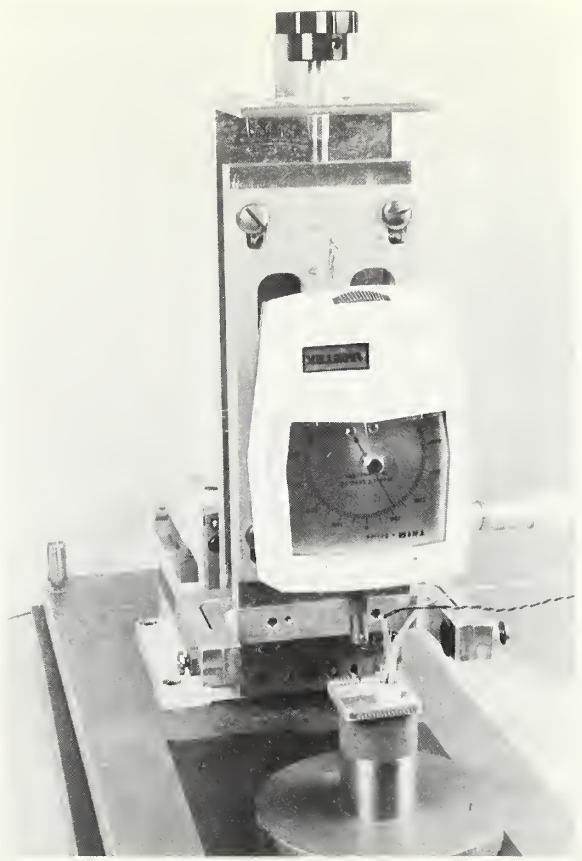

Figure 31. A force apparatus used to simulate bonding forces on hybrid leads.

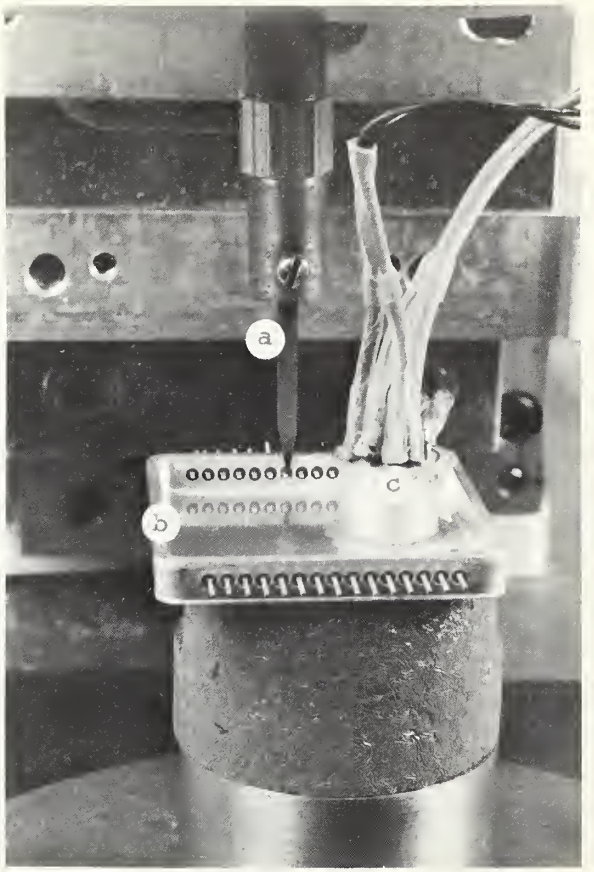

Figure 32. An expansion of the probe and sample portion of figure 31. (a) A closeup of the force probe (a bonding tool); (b) hybrid; and (c) TO-100 AE detector.

Table 4. Comparison Between Measured and Calculated Bending of Kovar Leads for Leads of 0.01 × 0.014 × 0.10 in.

Force (g)	Measured Deflect, in.	Calculated Deflect, in.	Ratio (meas/calc)
9	0.66×10^{-3}	0.28×10^{-3}	2.36
18	1.33	0.57	2.33
25.5	1.99	0.80	2.52
34	2.65	1.07	2.48
36	3.3*	1.13	2.92

* yielding observed.

The large differences (ratios) between experimental and calculated bending deflections have been verified on a number of different packages and with leads of different lengths and thicknesses, both with and without gold plating. The discrepancy cannot be attributed to yielding since the beam deflection returned to zero upon unloading for the first four force values in table 4, and the changes in the ratio (2.36 to 2.52) are within measurement error. However, the highest force was observed to bend the lead permanently. The only material constant in eq (4) is the modulus which is 19.8×10^6 psi for kovar. One would not expect any possible small compositional changes in the kovar to change the modulus enough to account for the discrepancy.

There may be a number of possible explanations for the discrepancy. However, the forces on the glass under the beam may be as high as 40,000 psi, and compression of the glass is possible.

An analysis of the contribution to lead bending resulting from the elasticity of the glass bead is based on the following equation for the slope of a beam attached to a compressible (nonrigid) support [46].

$$K = \frac{16.67\ M}{Ed^2} + \frac{(1 - \sigma)\ V}{Ed}\ , \qquad (5)$$

where the variables, not elsewhere defined, are:

K, the slope of the beam,
M, the bending moment (in.-lb./in.),
V, the shear force per unit width of beam at the support (lbs./in.),
E, the modulus for a typical kovar sealing glass, 8.2×10^6 psi,*
σ, Poisson's ratio for kovar sealing glass, 0.24.

The actual beam deflection due to compression of the elastic support is ℓK.

The deflection calculated from eq (5) and multiplied by ℓ is added to the deflection calculated from eq (4) to obtain the total deflection. Table 5 gives the corrected calculations and the ratio between calculated and measured deflection.

* Such as for Corning 7052 glass.

Table 5. Kovar Lead Bending Corrected for Glass Elasticity.

Force (g)	Measured Deflection (in.)	Calculated Deflect Eq (4) + (ℓK) (in.)	Ratio (meas./calc.)
9	0.66×10^{-3}	0.57×10^{-3}	1.15
18	1.33	1.14	1.16
25.5	1.99	1.62	1.23
34	2.65	2.16	1.23
36	3.3*	2.29	1.44*

* yielding observed.

Additional corrections for the glass meniscus and bending of the package kovar wall could lead to an even closer correlation between the measured and the calculated values. However, the results of table 5 bring the difference between the measured and calculated deflection within reasonable agreement and illustrate the importance of including all portions of the glass-metal seal when making a stress analysis of hybrid packages. In addition, these tests show that the often-made assumption that glass can be considered rigid in small seals is incorrect.

B-3.3 Acoustic-Emission-Monitored Tests to Determine Glass-Seal Damage During Bonding

B-3.3.1 Room-Temperature-Bonding Experiments

After determining the mechanical characteristics of kovar leads in sections B-3.1 and B-3.2, acoustic-emission-instrumented tests were begun in order to establish whether glass-seal cracking could be induced by the forces and temperatures of thermocompression and thermosonic bonding to the kovar leads and to establish whether any such cracking could be detected with the TO-100 acoustic-emission detector, which was waxed to the hybrid package, as was shown in the closeup of figure 32. (The block diagram of the AE circuit was given in fig. 26.) Both the transient recorder and the counts-per-second totalizer were used in this experiment.

Initial room temperature tests began on packages having relatively short lead extensions (~0.035 in.) inside the packages. The force was continuously monitored and recorded each time an AE burst occurred. The first observation was that the leads of certain packages produced numerous AE bursts in the relatively low force range, $\lesssim$50 gf. One such AE burst at a 45-gf load, shown in figure 33, was traced to a crack in the glass under the lead. Another larger burst that saturated the amplifier is shown in figure 34. In this case a sliver of glass under the lead cracked off at only a 35-gf load. One lead emitted bursts at 19, 39, and 60 gf. Packages that emitted bursts under low loads were observed to have glass wetting or "wicking" extending irregularly outward on the lead past the normal meniscus of the glass bead. This thin glass can crack off with minimal lead bending. There is no evidence thus far that such low-force-induced cracks affect the hermeticity

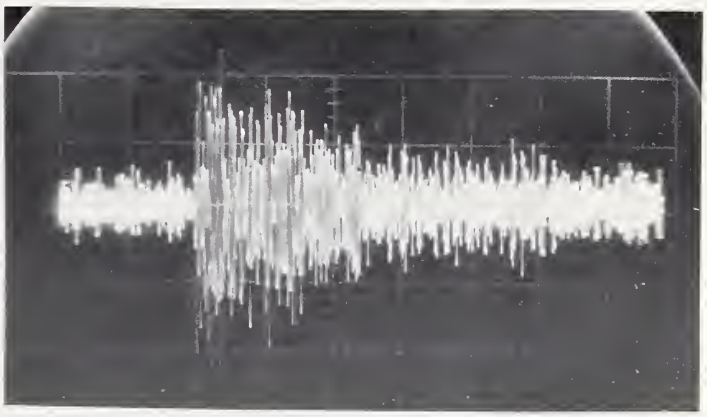

Figure 33. Acoustic-emission burst from glass cracking due to a force of 45 gf applied to the internal lead. The horizontal scale is 220 μs/div.

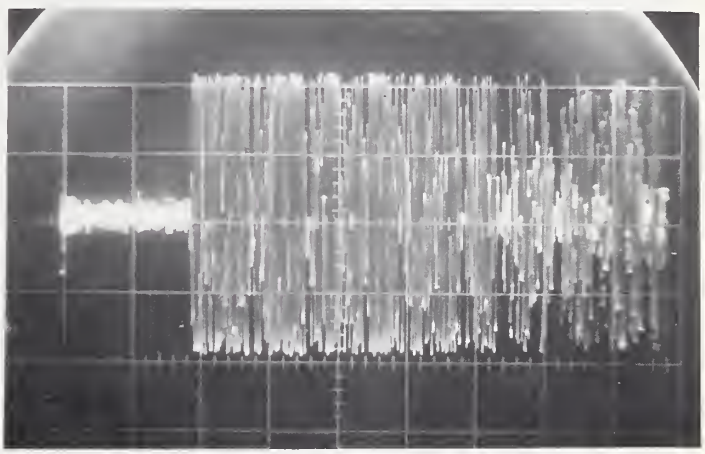

Figure 34. A large acoustic-emission burst (saturating the transient recorder) resulting from a small glass sliver cracking off from the bottom side of the lead and becoming a loose particle. The horizontal scale is 220 μs/div.

of the seal. However, glass slivers released (or cracked, but left loosely attached during the bending) could certainly act as loose particles if not removed before package sealing. The cracking and slivers generally occur in the package on the underside of the lead where it is difficult or impossible to observe. As a result, it is possible that such cracked or broken glass could be a significant source of nonmetallic loose particles in susceptible packages. Package specifications should require that the inside glass bead be either flat or have a small uniform meniscus shape.

An unusual form of protection against uneven miniscus glass cracking was observed. One step in the manufacture of packages, after fusing the glass beads and sealing the leads in the package, involves etch removal of the excess kovar oxide. If a package remains in the etch bath too long or is not completely cleaned, undercutting of the kovar below the glass may occur. Such undercutting is not normally considered desirable and if severe could lower the bending yield point of the lead. However, the combination of the slightly thinned kovar and the resulting clearance between the most extended part of the glass meniscus apparently serves as protection against glass cracking during slight bending of the lead. Therefore, even though the visual appearance of etch undercut leads is not ideal, such etching appears to protect the glass against cracking under relatively light-load bending. It should be pointed out, however, that when such etch undercut patterns appear on the outside of the packages, they could serve as stress risers or weak points and result in early fatigue damage in vibration environments (sec. A).

Several additional experiments were carried out using higher bending forces on the leads to determine the level required to produce significant glass-seal damage. The results indicate that, on the average, significant glass miniscus cracking occurs in packages with 0.010-in. thick leads extending inside the packages approximately 0.035 in., at forces between 150 gf and 200 gf. However, severe glass cracking was detected both by AE and visually on one seal with a very irregular meniscus at a force of 125 gf.

Other tests were carried out on seals that had been significantly cracked on the outside by intentionally bending the leads. These seals were subjected to probe forces on the lead extension inside the package as described above using the apparatus of figure 31. One such lead produced large AE bursts at 40, 95, 125, and 200 gf. These bursts were in the 200 to 500 count range and of sufficient amplitude to saturate the transient recorder input with no evidence of an inside sliver cracking off. Another seal that was less damaged than the above one produced several unusual double bursts when stressed, an example of which is shown in figure 35. Presumably, a small crack propagated into a larger one. The total AE count in this burst was 367 as registered by the totalizer. Apparently, in both of the above cases, the force was transmitted through the seal and resulted in propagating already formed cracks on the outside. It is reasonable to expect that force can be transmitted through a glass seal since the glass is compressible and has a relatively low modulus of 8.2×10^6 psi. This compressibility was discussed in section B-3.2.

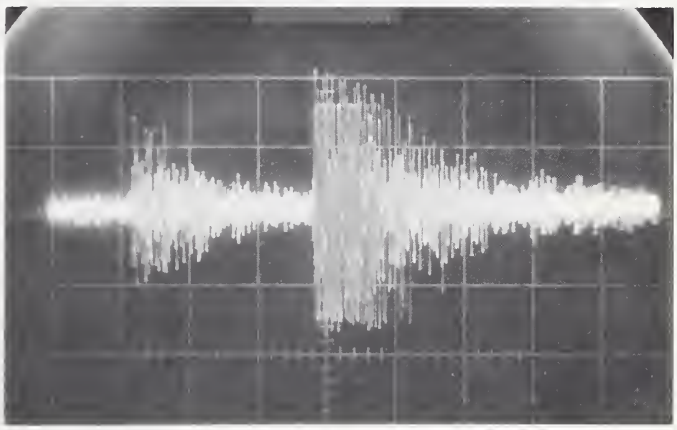

Figure 35. An AE burst at 25 gf applied to the lead from a seal that was damaged on the outside with no damage observed on the inner side of the seal. The double burst presumably resulted from a small glass crack propagating and causing a larger crack. Seals that are damaged on the outside appear to be susceptible to additional glass cracking under the stress of bonding forces. The horizontal scale is 220 μs/div.

B-3.4 AE-Monitored Package Lead Bending under Thermosonic Bonding Conditions

After the room-temperature bending characteristics of kovar leads were established on special laboratory equipment (fig. 31), the experiment was moved to a bonding machine with a heated stage, where any damage to the seals could be determined under bonding conditions. A photograph of the apparatus, including part of the bonding machine, is shown in figure 36. For convenience, the force was applied on the external lead extension at a fixed distance from the glass bead (usually 0.035 in.). The intent was to reproduce the experiments of section B-3.3 but at thermosonic bonding temperatures (~125°C to 150°C) and with the possibility of adding ultrasonic energy during the application of force. Interference between the 60-kHz ultrasonic bonding signal and possible acoustic emission was anticipated so the AE-detector output was passed through a 24-dB per octave tunable filter plus appropriate 18-dB per octave fixed frequency filters to minimize such interference. Actual wire bonding to the leads was performed to determine the frequency and bandwidth of the required filtering. To sharpen the response peak further, measurements were made at the sensitivity peaks of the TO-100 AE detector (see fig. 15). Because of the very large amplitude of the 60-kHz fundamental produced by the bonder as well as the numerous harmonics generated during bond formation, there was always too much interference to separate small glass cracking from the extraneous "noise." Only in the case of very large induced glass cracks could the AE signal be distinguished at all, and clear separation was not possible.

The result of this work revealed that there is an empirical relationship between various stages of bond formation and the AE-detector output and thus this technique might be useful as a bond monitor. Three waveforms are shown to illustrate the point. Figure 37 shows approximately the first 10 percent of a 50-ms bonding cycle. The individual "spikes" occur at the 60-kHz fundamental of the bonding machine. Figure 38 is a 5X expansion of the waveform starting at the arrow in figure 37. Figure 39 is the beginning of a second ultrasonic bonding pulse on the same (now mature) bond started in figure 37. The 60-kHz "spikes" are gone and the amplitude of the envelope varies along the bonding pulse. These three photographs were taken with the two AE-output filters placed in series and set for a bandpass of 650 to 800 kHz, and this response was further narrowed by the AE detector response. From this and the detector frequency response of figure 15, it is apparent that most of the signal was either the 11th or 12th harmonic of the 60-kHz ultrasonic bonding pulse. In any future studies of this phenomenon, it would be desirable to use a flat-response broad-band AE detector and perform an FFT on the signal in order to determine its usefulness as a bond monitor. One should also consider the possibility that the signal amplitude and frequency characteristics could be dependent upon the package geometry and the position of the AE detector.

Since it was impractical to monitor AE generated by hermetic seal cracks that occurred during ultrasonic or thermosonic bonding, the investigation was limited to studying glass cracking that resulted from the equivalent combination of temperature and force but without ultrasonic energy which might simulate thermocompression bonding. The equipment was as shown in figure 36, except that a thin, 60-deg bonding tool was used as the probe in order to

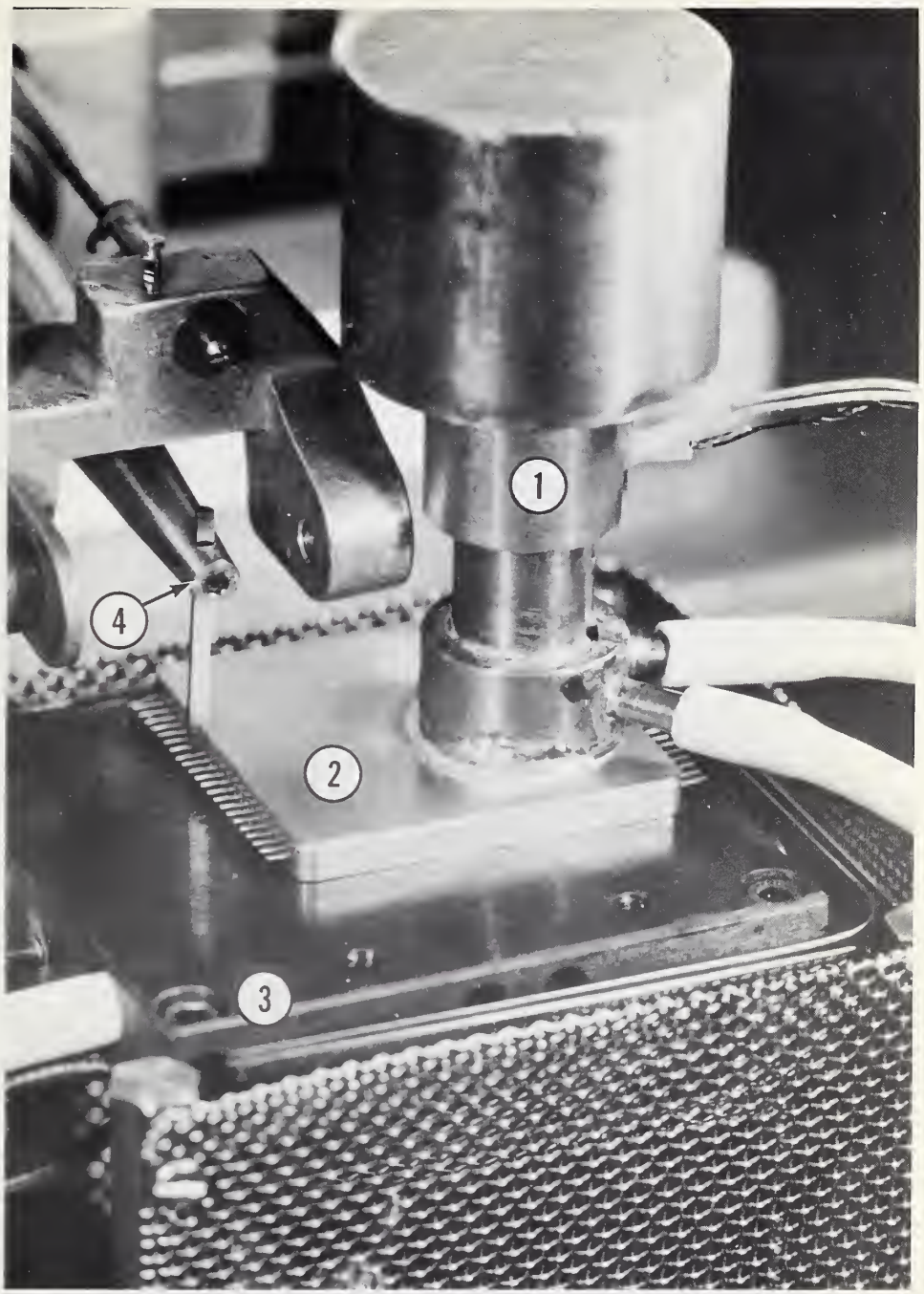

Figure 36. Apparatus to apply thermosonic-type forces and monitor any seal cracking in hybrid packages. (1) Acoustic-emission detector in a water-cooled mount. (2) Hybrid package face down with its external leads cut short. (3) Substrate heater to produce thermosonic bonding temperatures. (4) Bonding machine ultrasonic transducer and bonding tool.

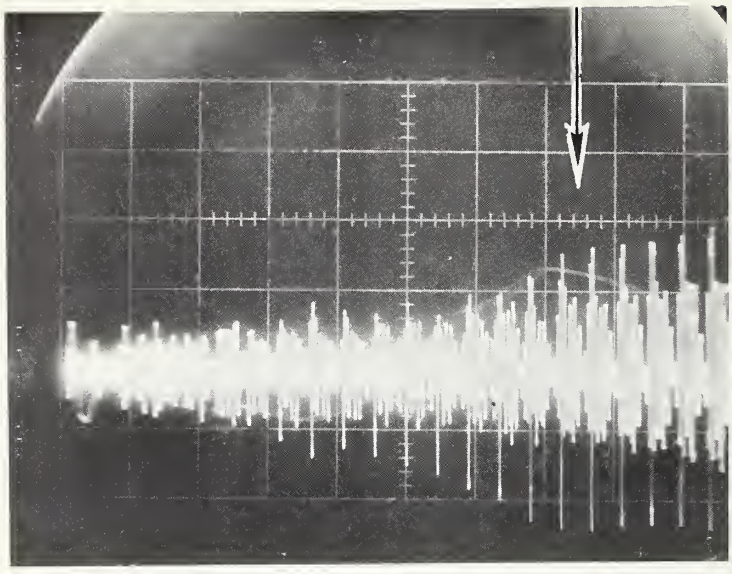

Figure 37. The first 10 percent of a 50-ms ultrasonic bonding pulse as detected by the AE detector in the equipment setup of figure 36. The "spikes" appear at 60-kHz time intervals. The substrate temperature was 125°C. This entire ultrasonic pulse resulted in bonding a 2-mil diameter aluminum wire to a hybrid package lead at approximately 0.03 in. from the glass seal. The horizontal scale is 36 μs per major division.

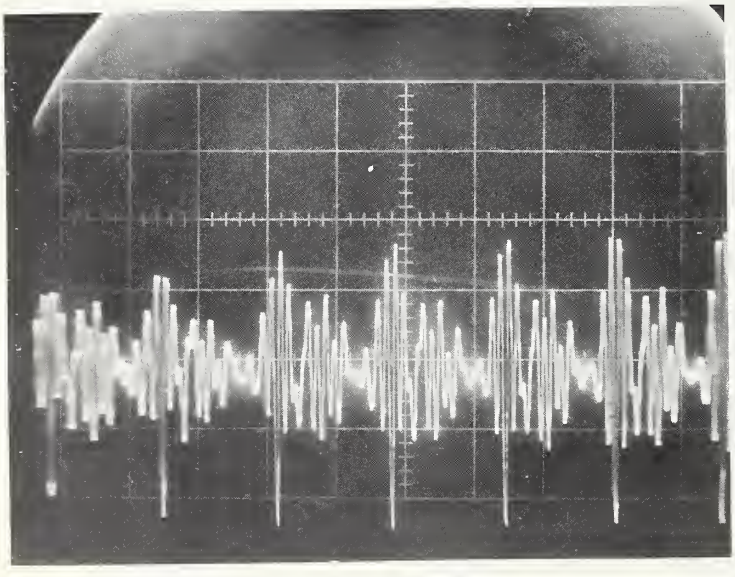

Figure 38. A 5X expansion of the waveform in figure 37 centered on the position of the arrow.

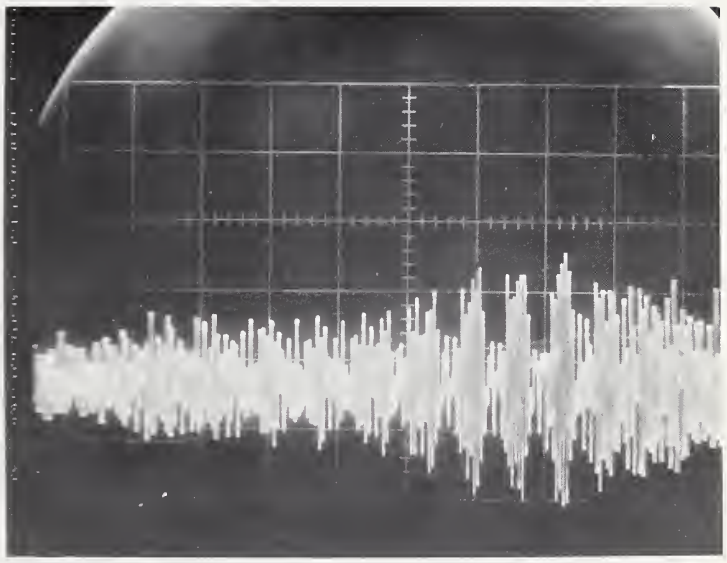

Figure 39. The initial 8 percent of a second 60-kHz bonding pulse applied to the same bond that was completely formed by the pulse shown in figure 37. This second pulse was applied immediately after the first, and the bonding tool remained in contact with the top of the bond. The 60-kHz "spikes" are gone, but the periodic bunching of the waveform is still in evidence. The horizontal scale is somewhat expanded from that of figure 36 (27 μs per major division).

apply force nearer the glass seal. The bonding machine was mechanically cycled in order to include the results of any impact loading. Substrate temperatures in various tests ranged from 100°C to 175°C and forces up to 200 gf. It was considered possible that the change in the glass-metal-seal internal forces from compression to tension at these temperatures might result in more damage than was observed during similar room temperature tests. The results of applying such stresses to 10 leads from each of 14 packages indicated that there is no significant difference between the force required to produce glass cracking at high or at room temperature. The high-temperature stressing appeared to result in a somewhat greater number of AE bursts (glass cracking), but the variations from package to package made the increases statistically insignificant. Most of the bursts were small, from 50 to 200 counts, and presumably resulted from tiny meniscus cracks that are of no significance as far as package integrity is concerned. The package hermeticity during these tests was affected in only one qualified case.* Even the breaking of glass slivers which produced large bursts of several hundred AE counts did not affect hermeticity. However, these slivers may result in loose particles, which could cause rejection or rework of expensive finished hybrids.

Most hybrid packages have relatively short lead extensions into the package. For 0.010- by 0.015-in. rectangular leads, this extension typically ranges from 0.030 to 0.048 in. No significant bending during bonding with normal forces, up to 125 gf, has been observed on such leads. However, forces on the order of 150 gf applied near the tip of all but the shortest leads will permanently bend them downward a significant amount and thus may result in weak bond formation. Such forces may be encountered if the bonding machine has a significant impact loading or when bonding with large wire (>0.001-in. diameter). The longer or thinner the lead, the lower the force required to bend it and, therefore, the greater the chance to produce a poorly welded bond.

B-3.5 Metallurgical Properties of Hybrid Package Leads†

Six flatpack hybrid packages with leads extending out of two sides were evaluated for the hardness and plating thickness of their leads. All came from the same manufacturer but were from three production lots made over a period of about a year. An evaluation was made of the hardness of the leads on each of the samples to determine if substantial variation existed in the lead strength of the three lots of kovar. The leads were approximately 0.01 in. thick and 0.015 in. wide with various thicknesses of gold and nickel plating.

---

* One package from the GIDEP Alert series [38] (see A-3.1) that initially had a fine leak did change to a gross leak after a number of its leads were bent at 200 gf. The AE bursts were similar to those from other packages subject to similar forces. It is not known whether this failure resulted from the mechanical unplugging of a gross leak or the creation of a new one. The package had previously been used in another test and may in some way have been partially damaged. No other "good" packages from reject lots were available to confirm this failure.

† These measurements were supplied by Dr. John H. Smith, NBS Fracture and Deformation Division.

Leads were cut from each of the six samples and mounted in metallographic mounting material. Vickers hardness readings [ASTM E 92-72 (1977)] [42] were made on the ends of the leads using a 500-g load. Hardness measurements were made on three leads from each end of the samples; that is, six leads were measured from each of the six samples. The results showed that all 36 hardness values were within the range of 144 to 150 on the Vickers scale (HV 0.5) using a 500-g load. This variation is not significant, so it is concluded that all six samples have the same hardness, and therefore, it is inferred that they all have the same strength.

Photomicrographs were taken of leads from each of the six samples evaluated. These photographs are shown in figure 40. Measurements of the thickness of the plating on each sample were made from these photomicrographs and are given in the figure captions.

Additional hardness measurements were made on the sides of the leads from samples shown in figures 40d and 40f. This was done to evaluate the possibility of using hardness measurements for inspection of incoming material. Hardness measurements were made using 500-, 1000-, and 2000-g loads on the Vickers hardness machine. The hardness results on the sample in figure 40d, which was unplated kovar, ranged from 148 to 158 HV. The hardness measurements taken on the sample in figure 40f, which was plated with both nickel and gold, showed wide variations due to the presence of the plating. The measured hardness varied from 130 to 176 HV with a 500-g load and from 370 to 850 HV with the 2000-g load. These results show that the plating interferes with the measurement and makes it impossible to determine the kovar hardness on plated specimens. The plating should be polished off before such a test could be useful. On the basis of this limited test of lead hardness on samples from one manufacturer, hardness testing does not appear to be a useful screen for kovar lead quality. No measurements were made on the package casing, which could be a more variable material.

B-4 Conclusions of Part B

Part B of this report concerned the development of several types of nondestructive tests to assess the integrity of hybrid packages.

A 125°C open package leak test method was developed along with the proper procedures for handling and preconditioning any type of hybrid package for hermeticity testing.

The hot plate thermal shock test often used by package manufacturers to assess the quality of glass-metal seals was characterized and various problems and pitfalls revealed. This quick, simple test, when monitored by acoustic-emission equipment, can reveal marginal seals that could only be detected by high-temperature leak tests. A thermoelectric temperature-cooling apparatus was evaluated for possible use as a "quiet" temperature-cycling system compatible with acoustic-emission monitoring of thermal-cycle-induced failures in hybrids. It was found that the thermoelectric modules themselves produced large amounts of acoustic emission which is fundamental to the materials and construction methods. No means of acoustic isolation that would still allow rapid heat transfer was found. Therefore, this means of temperature cycling cannot be used for acoustic-emission-monitored experiments.

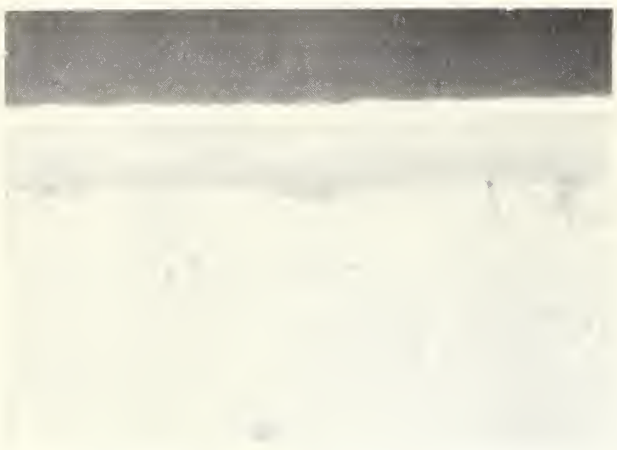

(a) 0.0004-in. nickel under 0.0001-in. gold coating.

(d) No coating.

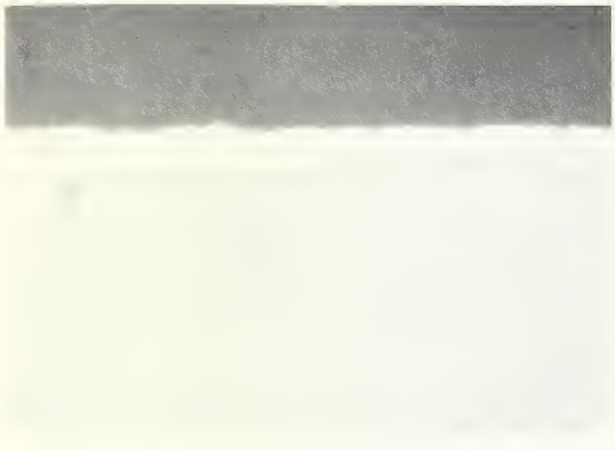

(b) 0.00025-in. gold coating.

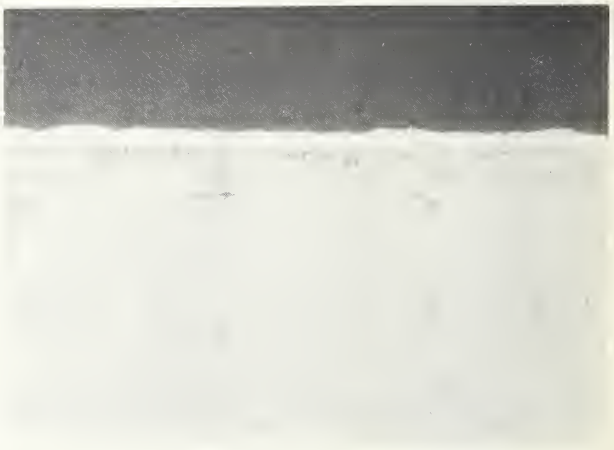

(e) 0.0001-in. gold coating.

(c) 0.0002-in. gold coating.

(f) 0.00015-in. nickel under 0.0003-in. gold coating.

Figure 40. Photomicrographs of kovar leads from six different hybrid packages. Each package had a different surface coating (plating). (Magnification, 750X - as polished)

A study was carried out to determine the susceptibility of the glass-metal seals in hybrids to damage during wire bonding. It was found that the amount of lead bending under bonding loads is significantly greater than predicted by theory, due to an extra component contributed by the compressibility of the glass. It was also found that the thickness of kovar leads tended to be skewed towards thinner-than-specified dimensions. This could result in increased bending and less reliable bonding. Under some bonding-force and glass-wetting conditions, glass slivers can be loosened or cracked off the kovar lead and could become loose particles after the package is sealed.

Acoustic-emission-monitored tests to assess possible seal damage during thermosonic bonding could not be successfully carried out because any acoustic emission due to glass cracking was masked by harmonics of the ultrasonic bonding pulse. The AE detector did sense signals that appear to be related to bond formation, and thus this technique may be useful as an in-process bond monitor. Measurements of glass-seal damage monitored by AE were made at thermosonic bonding temperatures of up to 175°C and forces to 200 g. Results revealed that the seals on high-quality packages are not significantly more susceptible to damage at these high temperatures than at room temperature. Forces on the order of 150 gf, applied to the ends of typical internal lead extensions, will cause significant bending which can result in poor bond formation.

The major problem in this study was to obtain packages from failure-prone lots that were still initially hermetic. Even with the generous cooperation of two package manufacturers and several user organizations, there were never enough "poor" packages to prove definitively the utility of all of the test methods. Future work should be preceded by an industry-wide appeal for appropriate specimens so that a statistically significant sample can be accumulated. The general conclusion of this work is that small meniscus glass cracks have no effect on the hermeticity of the package and that it is difficult to produce hermetic damage to the seals of high-quality packages. However, packages screened and found to be "good" from poor or reject lots (lots with a high percentage of failures) were found to be more susceptible to hermetic failure from all types of stress tests than packages from high-quality lots. An acoustic-emission-monitored shock test has been shown to separate "good" from "poor" package lots quickly. Additional verification of these results with a statistically significant number of packages is recommended.

Acknowledgments

K. A. Harmison, Naval Avionics Center, supplied some hybrid packages and printed circuit boards as well as information and cooperation essential to this work. The author would like to acknowledge valuable discussions with H. E. Hagy of Corning Glass. In addition, some special measurements in this report were performed by Drs. N. N. Hsu and F. R. Breckenridge, Mechanical Production Metrology Division, NBS. Stanley Ruthberg made all leak test measurements and contributed sections B-1 and B-2. Section B-3.5 was contributed by Dr. John H. Smith of the Fracture and Deformation Division, NBS. Cooperation from several hybrid package manufacturers, notably Tekform and Isotronics, is gratefully acknowledged. The manuscript was prepared by Mrs. Jane Walters.

REFERENCES

1. Harman, G. G., The Use of Acoustic Emission to Determine the Integrity of Large Hybrid Packages, NBSIR 80-2055 (June 1980).

2. Kaiser, J., Untersuchungen uber das Auftreten von Geraschen Beim Zugversuch, *Arkiv fur das Eisenhutterwesen* 24 (1/2), 43-45 (1953).

3. Spanner, J. C., *Acoustic Emission Techniques and Applications* (Society for Nondestructive Testing, Columbus, Ohio, 1974).

4. For a compilation of articles on AE, see Acoustic Emission, ASTM Technical Publication STP 505 (American Society of Testing and Materials, Philadelphia, Pennsylvania, 1972).

5. *The Western Electric Engineer* 23, 3-37 (1979). Includes four papers on AE testing.

6. Vahaviolos, S. J., Real Time Detection of Microcracks in Brittle Materials Using Stress Wave Emission, *IEEE Trans. Parts, Hybrids, and Packaging* PHP-10, 152-159 (1974).

7. Saifi, M. A., and Vahaviolos, S. J., Laser Spot Welding and Real-Time Evaluation, *IEEE J. Quantum Electronics* QE-12, 129-136 (1976).

8. Carlos, M. F., and Jon, M. C., Detection and Cracking During Rotational Soldering of a High Reliability and Voltage Ceramic Capacitor, *Proc. 28th IEEE Electronic Components Conference*, Anaheim, California, April 24-26, 1978, pp. 336-339.

9. Jon, M. C., Duncan, H. A., and Vahaviolos, S. J., Analysis of Stress Wave Emission in Resistance Welding of Tantalum Capacitor, *Materials Evaluation* 36, 40-44 (1978).

10. Jon, M. C., Keskimaki, C. A., and Vahaviolos, S. J., Testing Resistance Spot Welds Using Stress Wave Emission Techniques, *Materials Evaluation* 36, 41-51 (1978).

11. Knollman, G. C., and Weaver, J. L., Evaluation of an Acoustic Emission Monitor for On-Line Quality Control in Spotwelding of Electronic Components, *Proc. Third Acoustic Emission Symposium*, Tokyo, Japan, September 16-18, 1976, pp. 413-427.

12. Ikoma, T., Ogura, M., and Adachi, Y., Acoustic Emission from Single Crystals of Gallium Arsenide, *Ibid.*, pp. 329-341.

13. Harman, G. G., The Use of Acoustic Emission in a Test for Beam Lead, TAB, and Hybrid Chip Capacitor Bond Integrity, *Proc. 14th Annual IEEE Reliability Physics Symposium*, Las Vegas, Nevada, April 20-22, 1976, pp. 86-98.

14. Kumar, A., Failure Analysis of Electric Component Leads, *Proc. ATFA-1979*, Los Angeles, California, October 8-11, 1979, pp. 28-33.

15. Steinberg, D. S., *Vibration Analysis for Electronic Equipment* (John Wiley & Sons, New York, 1973).

16. Steinberg, D. S., Circuit Components vs. Random Vibration, *Electronic Packaging and Production*, 185-187 (July 1975).

17. Steinberg, D. S., Avoiding Vibration in Odd-Shaped Printed Circuit Boards, *Machine Design* 48, 116-119 (May 1976).

18. Steinberg, D. S., Preventing Vibration Damage in Electronic Assemblies, *Machine Design* 48, 74-77 (July 1976).

19. Steinberg, D. S., Avoid Failure of PC Board Components, *Electronic Design* 21, 68-70 (October 1976).

20. Steinberg, D. S., Snubbers Calm PC Board Vibration, *Machine Design* 49, 71-73 (March 1977).

21. Steinberg, D. S, Countering the Effects of Vibration on Chassis Systems, *Electronics* 50, 100-102 (August 1977).

22. Sevy, R. W., and Earls, D. L., The Prediction of Internal Vibration Levels of Flight Vehicle Equipment (Limited), Shock and Vibration Bulletin 38 (Supplement), 5-18 (1968).

23. Kohler, B. A., Resonant Beam High "G" Vibration Testing, Shock and Vibration Bulletin 39 (2), 171-176 (1969).

24. Isada, N. M., and Shear, J. C., Vibratory Response of Printed Circuit Boards, Shock and Vibration Bulletin 40 (3), 111-118 (1969).

25. Palmisano, R. R., and Neily, D. W., Particulate Silicone Rubber: An Effective, Removable Encapsulant for Electronic Packaging, Shock and Vibration Bulletin 46 (4), 277-283 (1976).

26. Blanks, H. S., Accelerated Fatigue Life Testing of Leads and Soldered Joints, *Microelectronics and Reliability* 15, 213-219 (1976).

27. Morse, P. M., *Vibration and Sound* (McGraw-Hill Book Co., Inc., New York, 1948).

28. Warburton, G. D., The Vibration of Rectangular Plates, *Proc. Instr. Mech. Engr.* 168, 371-380 (1954).

29. Hearmon, R. F. S., Communications on the Vibration of Rectangular Plates, *Proc. Instr. Mech. Engr.* 168, 381-384 (1954).

30. Hearmon, R. F. S., The Frequency of Vibration of Rectangular Isotopic Plates, *J. Appl. Mechanics ASME* 74, 402-415 (1952).

31. Rayleigh, Lord, *Theory of Sound*, Vol. 1 (MacMillan & Co., London, 1894).

32. Nelson, F. C., Damping PC Boards with Foam Plastic, *Circuits Manufacturing* 19, 50-53 (November 1979). (This paper gives several other references not included in the present study.)

33. Curtis, A. J., Tinling, N. G., and Abstein, H. T., Selection and Performance of Vibration Tests, The Shock and Vibration Information Center, SVM-8 (1971).

34. Fackler, W. C., Equivalence Techniques for Vibration Testing, The Shock and Vibration Information Center, SVM-9 (1972).

35. Zimmerman, D., Johns Hopkins Applied Physics Laboratory, private communication.

36. Information on Military Standards can be obtained from the Naval Publications and Forms Center, 5801 Tabor Avenue, Philadelphia, PA 19120.

37. Ebel, G., Singer Corporation, comments made at the Moisture Measurement Workshop, NBS, November 5-6, 1980.

38. GIDEP Alerts may be obtained from the Government-Industry Data Exchange Program, Corona, CA 91720.

39. Thomas, R. W., Moisture, Myths and Microcircuits, *IEEE Trans. Parts, Hybrids, and Packaging* PHP-12, 167-172 (September 1976).

40. See, for instance, Espe, W., *Materials of High Vacuum Technology,* Vol. 1-3 (Pergamon Press, New York, 1966).

41. Gulati, S. T., and Hagy, H. F., Expansion Measurement Using Short Cylindrical Seal: Theory and Experiment, *Thermal Expansion,* E. D. Peggs, Ed., Vol. 6 (Plenum Press, New York, 1978).

42. Information on ASTM Standards may be obtained from the American Society for Testing and Materials, 1916 Race Street, Philadelphia, PA 19103.

43. McCormick, J., and Zakraysek, L., A Metallographic Test for Glass-to-Metal Seal Quality, *17th Annual Proc. Reliability Physics,* San Francisco, California, April 24-26, 1979, pp. 44-50.

44. See, for instance, Griffel, W., *Handbook for Formulas for Stress and Strain* (Frederick Ungar Publishing Co., New York, 1967).

45. This and other ISHM publications are obtainable from the International Society for Hybrid Microelectronics, P.O. Box 3255, Montgomery, AL 36109.

46. Roark, R. J., and Young, W. C., *Formulas for Stress and Strain* (McGraw-Hill, New York, 1975).

☆ U.S. GOVERNMENT PRINTING OFFICE: 1982-360-997/2114

NBS-114A (REV. 2-8C)

U.S. DEPT. OF COMM. BIBLIOGRAPHIC DATA SHEET (See instructions)	1. PUBLICATION OR REPORT NO. NBS SP 400-70	2. Performing Organ. Report No.	3. Publication Date May 1982

4. TITLE AND SUBTITLE

Semiconductor Measurement Technology: The Use of Acoustic Emission to Determine the Integrity of Large Kovar Glass-Sealed Microelectronic Packages

5. AUTHOR(S)

G. G. Harman

6. PERFORMING ORGANIZATION (*If joint or other than NBS, see instructions*)

NATIONAL BUREAU OF STANDARDS
DEPARTMENT OF COMMERCE
WASHINGTON, D.C. 20234

7. Contract/Grant No.

P.O. N0016380MP0001

8. Type of Report & Period Covered

Final

9. SPONSORING ORGANIZATION NAME AND COMPLETE ADDRESS (Street, City, State, ZIP)

Naval Avionics Center
Indianapolis, IN 46218

10. SUPPLEMENTARY NOTES

Library of Congress Catalog Card Number: 82-600528

☐ Document describes a computer program; SF-185, FIPS Software Summary, is attached.

11. ABSTRACT (*A 200-word or less factual summary of most significant information. If document includes a significant bibliography or literature survey, mention it here*)

The general objective of this research was to develop tests to determine the integrity of large hybrid packages under various thermal and mechanical stresses that may be encountered during assembly, during installation in systems, or in operation. Several measurement techniques were investigated, but emphasis was placed on acoustic-emission test procedures. The accomplishments were: (1) The effects of avionics environmental vibration on the seals of hybrid packages mounted on printed-circuit (PC) boards were determined. A major conclusion of this section was that lead fatigue failure occurs before seal damage on packages from high quality lots. (2) A small acoustic-emission detector was developed that is sensitive to surface waves, but relatively insensitive to vibration induced cable noise. (3) A high-temperature (125°C) open-package helium leak test method was successfully developed to observe marginal seal damage. (4) An acoustic-emission test for inspection of hybrid packages during high-temperature thermal shock was developed. (5) A study of possible damage to seals during thermocompression and thermosonic bonding, during lead forming, and during other assembly operations was carried out. A general conclusion of this study is that the glass-metal seals in packages from known high quality lots are very reliable even when subjected to high stresses. However, the seals from packages "screened as good" from reject or poor quality lots are subject to hermetic failure under moderate stresses. There is little correlation between visual inspection failures of glass seals and their hermeticity.

12. KEY WORDS (*Six to twelve entries; alphabetical order; capitalize only proper names; and separate key words by semicolons*)

acoustic emission; hermeticity; hybrid microelectronics; hybrid packages; microelectronic packaging; thermal shock; vibration

13. AVAILABILITY

☒ Unlimited

☐ For Official Distribution. Do Not Release to NTIS

☐ Order From Superintendent of Documents, U.S. Government Printing Office, Washington, D.C. 20402.

☒ Order From National Technical Information Service (NTIS), Springfield, VA. 22161

14. NO. OF PRINTED PAGES 80

15. Price

NBS TECHNICAL PUBLICATIONS

PERIODICALS

JOURNAL OF RESEARCH—The Journal of Research of the National Bureau of Standards reports NBS research and development in those disciplines of the physical and engineering sciences in which the Bureau is active. These include physics, chemistry, engineering, mathematics, and computer sciences. Papers cover a broad range of subjects, with major emphasis on measurement methodology and the basic technology underlying standardization. Also included from time to time are survey articles on topics closely related to the Bureau's technical and scientific programs. As a special service to subscribers each issue contains complete citations to all recent Bureau publications in both NBS and non-NBS media. Issued six times a year. Annual subscription: domestic $18; foreign $22.50. Single copy, $4.25 domestic; $5.35 foreign.

NONPERIODICALS

Monographs—Major contributions to the technical literature on various subjects related to the Bureau's scientific and technical activities.

Handbooks—Recommended codes of engineering and industrial practice (including safety codes) developed in cooperation with interested industries, professional organizations, and regulatory bodies.

Special Publications—Include proceedings of conferences sponsored by NBS, NBS annual reports, and other special publications appropriate to this grouping such as wall charts, pocket cards, and bibliographies.

Applied Mathematics Series—Mathematical tables, manuals, and studies of special interest to physicists, engineers, chemists, biologists, mathematicians, computer programmers, and others engaged in scientific and technical work.

National Standard Reference Data Series—Provides quantitative data on the physical and chemical properties of materials, compiled from the world's literature and critically evaluated. Developed under a worldwide program coordinated by NBS under the authority of the National Standard Data Act (Public Law 90-396).

NOTE: The principal publication outlet for the foregoing data is the Journal of Physical and Chemical Reference Data (JPCRD) published quarterly for NBS by the American Chemical Society (ACS) and the American Institute of Physics (AIP). Subscriptions, reprints, and supplements available from ACS, 1155 Sixteenth St., NW, Washington, DC 20056.

Building Science Series—Disseminates technical information developed at the Bureau on building materials, components, systems, and whole structures. The series presents research results, test methods, and performance criteria related to the structural and environmental functions and the durability and safety characteristics of building elements and systems.

Technical Notes—Studies or reports which are complete in themselves but restrictive in their treatment of a subject. Analogous to monographs but not so comprehensive in scope or definitive in treatment of the subject area. Often serve as a vehicle for final reports of work performed at NBS under the sponsorship of other government agencies.

Voluntary Product Standards—Developed under procedures published by the Department of Commerce in Part 10, Title 15, of the Code of Federal Regulations. The standards establish nationally recognized requirements for products, and provide all concerned interests with a basis for common understanding of the characteristics of the products. NBS administers this program as a supplement to the activities of the private sector standardizing organizations.

Consumer Information Series—Practical information, based on NBS research and experience, covering areas of interest to the consumer. Easily understandable language and illustrations provide useful background knowledge for shopping in today's technological marketplace.

Order the **above** *NBS publications from: Superintendent of Documents, Government Printing Office, Washington, DC 20402.*

Order the **following** *NBS publications—FIPS and NBSIR's—from the National Technical Information Services, Springfield, VA 22161.*

Federal Information Processing Standards Publications (FIPS PUB)—Publications in this series collectively constitute the Federal Information Processing Standards Register. The Register serves as the official source of information in the Federal Government regarding standards issued by NBS pursuant to the Federal Property and Administrative Services Act of 1949 as amended, Public Law 89-306 (79 Stat. 1127), and as implemented by Executive Order 11717 (38 FR 12315, dated May 11, 1973) and Part 6 of Title 15 CFR (Code of Federal Regulations).

NBS Interagency Reports (NBSIR)—A special series of interim or final reports on work performed by NBS for outside sponsors (both government and non-government). In general, initial distribution is handled by the sponsor; public distribution is by the National Technical Information Services, Springfield, VA 22161, in paper copy or microfiche form.

U.S. DEPARTMENT OF COMMERCE
National Bureau of Standards
Washington, DC 20234

OFFICIAL BUSINESS

Penalty for Private Use, $300

POSTAGE AND FEES PAID
U.S DEPARTMENT OF COMMERCE
COM—215

THIRD CLASS